ปฏิกิริยาไฮโดรจิเนชันแบบเลือกเกิดของอะเซทิลีนบนตัวเร่งปฏิกิริยา นิเกิล-สังกะสี-ฟอสฟอรัส บนตัวรองรับพอลิยูรีเทนโฟม

นางสาวซารา อะหมะดี พีรซะหีด

วิทยานิพนธ์นี้เป็นส่วนหนึ่งของการศึกษาตามหลักสูตรปริญญาวิศวกรรมศาสตรมหาบัณฑิต
สาขาวิชาวิศวกรรมเคมี ภาควิชาวิศวกรรมเคมี
คณะวิศวกรรมศาสตร์ จุฬาลงกรณ์มหาวิทยาลัย
ปีการศึกษา 2554

SELECTIVE HYDROGENATION OF ACETYLENE OVER Ni-Zn-P CATALYSTS SUPPORTED ON POLYURETHANE FOAM

Miss Sara Ahmadi Pirshahid

A Thesis Submitted in Partial Fulfillment of the Requirements
for the Degree of Master of Engineering Program in Chemical Engineering
Department of Chemical Engineering
Faculty of Engineering
Chulalongkorn University
Academic Year 2011

Thesis Title	SELECTIVE HYDROGENATION OF ACETYLENE OVER Ni-Zn-P CATALYSTS SUPPORTED ON POLYURETHANE FOAM
By	Miss Sara Ahmadi Pirshahid
Field of Study	Chemical Engineering
Thesis Advisor	Associate Professor Joongjai Panpranot, Ph.D.
Thesis Co-advisor	Yuttanant Boonyongmaneerat, Ph.D.

Accepted by the Faculty of Engineering, Chulalongkorn University in Partial Fulfillment of the Requirements for the Master's Degree

……. Dean of the Faculty of Engineering
(Associate Professor Boonsom Lerdhirunwong, Dr.Ing.)

THESIS COMMITTEE

……. Chairman

(Associate Professor Artiwan Shotipruk, Ph.D)

……. Thesis Advisor

(Associate Professor Joongjai Panpranot, Ph.D.)

…….Thesis Co-advisor

(Yuttanant Boonyongmaneerat, Ph.D.)

…….Examiner

(Assistant Professor Suphot Phatanasri, Ph.D.)

……. External Examiner

(Assistant Professor Okorn Mekasuwandamrong, Ph.D.)

ซารา อะหมะดี พีรซะหีด : ปฏิกิริยาไฮโดรจิเนชันแบบเลือกเกิดของอะเซทิลีนบน ตัวเร่งปฏิกิริยานิเกิล-สังกะสี-ฟอสฟอรัส บนตัวรองรับพอลิยูรีเทนโฟม (SELECTIVE HYDROGENATION OF ACETYLENE OVER Ni-Zn-P CATALYSTS SUPPORTED ON POLYURETHANE FOAM) อ. ที่ปรึกษาวิทยานิพนธ์หลัก : รศ.ดร.จูงใจ ปั้นประณต, อ. ที่ปรึกษาวิทยานิพนธ์ร่วม : อ.ดร. ยุทธนันท์ บุญยงมณีรัตน์, 91 หน้า.

งานวิจัยนี้ศึกษาการใช้โลหะที่มีราคาถูกเป็นตัวเร่งปฏิกิริยาในกระบวนการไฮโดรจิเนชันแบบเลือกเกิดของอะเซทิลีน โดยเตรียมตัวเร่งปฏิกิริยา นิเกิล -สังกะสี-ฟอสฟอรัส โดยวิธีการชุบแบบไม่ใช้ไฟฟ้าบนตัวรองรับพอลิยูรีเทนโฟมที่ปริมาณสังกะสีในน้ำยาชุบต่างกัน ($ZnSO_4.7H_2O$ 6-24 กรัมต่อลิตร) โดยให้ปริมาณของนิเกิลและฟอสฟอรัสคงที่ $NiSO_4.6H_2O$ 42 กรัมต่อลิตร และ NaH_2PO_2 24 กรัมต่อลิตร ผลการวิเคราะห์อัตราการพอกพูนของโลหะ การทดสอบแรงกด SEM และ EDX ชี้ให้เห็นว่าปริมาณสังกะสีที่เพิ่มขึ้นส่งผลให้ปริมาณและอัตราการพอกพูนของโลหะมีค่าลดลง อย่างไรก็ตามตัวเร่งปฏิกิริยาที่เตรียมโดยมีปริมาณสังกะสี 18 กรัมต่อลิตรมีการกระจายตัวของโลหะที่ดีที่สุดบนผิวของพอลิยูรีเทนโฟมและมีอัตราส่วนของสังกะสีต่อนิเกิลมากที่สุดอีกด้วย โดยปริมาณสังกะสีสูงที่สุดของตัวเร่งปฏิกิริยามีค่าร้อยละ 17 โดยน้ำหนัก โดยมีปริมาณนิเกิลและฟอสฟอรัสร้อยละ 65.2 และ 7.5 โดยน้ำหนักตามลำดับ เมื่อทำการทดสอบในปฏิกิริยาไฮโดรจิเนชันแบบเลือกเกิดของอะเซทิลีนพบว่าตัวเร่งปฏิกิริยาที่เตรียมโดยมีปริมาณสังกะสี 18 กรัมต่อลิตร ให้ค่าการเปลี่ยนของอะเซทิลีนและค่าการเลือกเกิดเป็นเอทิลีนสูงที่สุด อย่างไรก็ตาม ประสิทธิภาพของตัวเร่งปฏิกิริยานิเกิล -สังกะสี-ฟอสฟอรัสที่เตรียมโดยวิธีการพอกพูนโดยไม่ใช้ไฟฟ้าเพิ่มขึ้นเมื่อใช้ ตัวรองรับเป็นอะลูมินา แบบเม็ดและอะลูมินา แบบผง ตามลำดับดังนี้ นิเกิล-สังกะสี-ฟอสฟอรัส/อะลูมินา แบบเม็ด > นิเกิล-สังกะสี-ฟอสฟอรัส/อะลูมินา แบบผง > นิเกิล-สังกะสี-ฟอสฟอรัส/พอลิยูรีเทนโฟม โดยคาดว่าเป็นผลของพื้นที่ผิวที่มากขึ้น

ภาควิชา วิศวกรรมเคมี ลายมือชื่อนิสิต.....

สาขาวิชา วิศวกรรมเคมี ลายมือชื่อ อ.ที่ปรึกษาวิทยานิพนธ์หลัก.....

ปีการศึกษา 2554 ลายมือชื่อ อ.ที่ปรึกษาวิทยานิพนธ์ร่วม.....

5370423021 : MAJOR CHEMICAL ENGINEERING
KEYWORDS : Ni-Zn-P CATALYST / ELECTROLESS / POLYURETHANE FOAM / SELECTIVE ACETYLENE HYDROGENATION / COMPOSITES

SARA AHMADI PIRSHAHID : SELECTIVE HYDROGENATION OF ACETYLENE OVER Ni-Zn-P CATALYSTS SUPPORTED ON POLYURETHANE FOAM. ADVISOR : ASSOC. PROF. JOONGJAI PANPRANOT, Ph.D., CO-ADVISOR: YUTTANANT BOONYONGMANEERAT, Ph.D., 91 pp.

In the present work, cheap metals were studied as alternative catalysts in the selective hydrogenation of acetylene. The Ni-Zn-P catalysts supported by polyurethane foam were prepared by electroless deposition method with various zinc salt contents in the deposition bath (6-24 g/l $ZnSO_4.7H_2O$). The amounts of Ni and P in the bath were fixed at 42 g/l $NiSO_4.6H_2O$ and 24 g/l NaH_2PO_2, respectively. From the deposition rate, compression test, SEM and EDX results, increasing amount of Zn in the bath resulted in lower rate of metal deposition. The catalyst prepared with amount of Zn 18 g/l showed the best dispersion on PU foam as well as the highest Zn/Ni ratio and the highest amount of Zn obtained in the final catalysts at 27.3 wt% with Ni and P 65.2 and 7.5 wt%, respectively. Such catalyst also exhibited the best catalyst performances in terms of acetylene conversion and ethylene selectivity. Further improvement of the Ni-Zn-P catalysts can be obtained using the Al_2O_3 supports in the order: Ni-Zn-P/γ-Al_2O_3 pellet > Ni-Zn-P/γ-Al2O_3 powder > Ni-Zn-P/PU foam (Zn 18 g/l).

Department Chemical Engineering	Student's Signature .....
Field of Study Chemical Engineering	Advisor's Signature .....
Academic Year 2011	Co-advisor's Signature .....

ACKNOWLEDGEMENTS

The author would like to express my greatest sincere and deepest appreciation to Associate Professor Joongjai Panpranot, and co-advisor, Dr. Yuttanant Boonyongmaneerat from Metallurgy and Materials Science Research Institute, Chulalongkorn University, for their invaluable suggestions, support, guidance, and useful discussion throughout this thesis.

The author would also be grateful to thank to Associate Professor Dr. Artiwan Shotipruk, as a chairman, and Assistant Professor Dr. Suphot Phatanasri, Assistant Professor Dr. Okorn Mekasuwandamrong, as the members of the thesis committee for their kind cooperation.

Most of all, the author would like to thank all members of the Center of Excellence on Catalysis and Catalytic Reaction Engineering, Department of Chemical Engineering, Faculty of Engineering, Chulalongkorn University for their assistance and friendly support.

Moreover, the author wishes to thank the members of the Metallurgy and Materials Science Research Institute, Chulalongkorn University for friendship and their kind assistance.

Finally, the author would like to express my highest gratitude to my parents who always pay attention for all times and encouragement. The most success of graduation is devoted to my parents.

CONTENTS

Page

Page

LIST OF TABLES

LIST OF FIGURES

Figure **Page**

Figure **Page**

CHAPTER I

INTRODUCTION

Polyethylene (PE) is a member of the important family of polyolefin resins. It is the most widely used plastic in the world. Polyethylene is created through polymerization of the monomer of ethylene with the chemical formula $C_{2n}H_{4n+2}$; where n is the degree of polymerization. Polyethylene is made into products ranging from clear food wrap and shopping bags to detergent bottles and automobile fuel tanks. It can also be slit or spun into synthetic fibres or modified to take on the elastic properties of a rubber. The ethylene feedstock is generally produced by thermal or catalytic cracking of higher hydrocarbons, which also generates impurities, such as acetylene, that must be removed to a level of less than 5 ppm because it can poison the traditional ethylene polymerization catalysts [1,2]. Presence of acetylene in ethylene steam leads to low ethylene selectivity at high acetylene conversion and low quality of the polyethylene production.

Purification of acetylene stream can be done via various routes, depending on acetylene content. There are basically two main paths to extract the acetylene from the C2-stream and recover it as a product, or to convert the acetylene into useful product which is ethylene. Each paths involved different unit operations and it affects the overall process sequences [2]. The removal of acetylene in ethylene steam by solvent extraction adsorption is costly and difficult so that the selective acetylene hydrogenation is more popular for industrial application [3].

Many precious catalysts are used in the selective hydrogenation of acetylene such as Au [4], Ag [5], Mo [6], and Pd [3,7-36]. The commonly used supports from preparation of the selective acetylene hydrogenation catalysts are SiO_2 [5,8,10,11,17-19,23,31] Al_2O_3 [12-14,20,25-33,37,38] and TiO_2[5,10,15,16]. Different promoters including Zn [14], Si [10,21,22], Cu [8,12,39], Ti [3,10,15,16,23], Nb [3,40], Ce [3] have been studied in order to increase the selectivity of ethylene as well as the catalyst life time. Since precious metal is very costly, the use of cheaper non-precious

metal catalyst is interested. In acetylene hydrogenation, non-precious catalyst such as Ni/SiO2 [41] had been investigated with or without metal promoters or modifiers with the objective of replacing much more expensive noble metals. In addition the, Ni-Zn bimetallic catalysts have been used in the selective acetylene hydrogenation reaction. Incorporation of Zn^{2+} in the solid structure of Ni-Zn resulted in significant improvement in the catalytic properties in the selective hydrogenation of acetylene [43,43].

The commonly used methods for preparing supported metal catalysts include incipient wetness impregnation, precipitation, sol-gel, and vapor deposition. These methods, however, usually take long time for each step during preparation such as drying and calcination steps. Electroless plating is a chemical reduction process which depends upon the catalytic reduction process in an aqueous solution (containing a chemical reducing agent) without the use of electrical energy of metallic and non-metallic substrates. It is known to be one of the most frequently adopted methods to deposit metallic film on either conductive or nonconductive substrates because of its low cost, easy control, simplicity of processing, and applicability to complicated-shaped materials[44]. Recently, electroless deposition has been employed for preparation of supported metal catalysts such as Au-Pd/SiO_2 [7], Ag-Pd/SiO_2, Cu-Pd/SiO_2 [8], and Co-Ni-P [45], and studied in many catalytic reactions.

In this study, Ni-Zn-P catalysts supported on polyurethane (PU) foams were prepared by electroless deposition method with different Ni/Zn ratios. The PU foams are porous materials with a special structure made of a skeleton of more or less regular open or closed cells. The unique properties of PU foams lie in their high surface area, lightness, and relatively low price [44,46,47,48]. The catalytic properties of Ni-Zn-P/PU foam were evaluated in the gas-phase acetylene hydrogenation as non-precious metals catalysts to replace the high cost Pd-based ones and compared with Ni-Zn-P/γAl_2O_3 pellet, Ni-Zn-P/γAl_2O_3 powder, 0.82%Pd/PU foam, 1.37%Pd/PU foam and Pd-Ag/γ-Al_2O_3 (commercial).

1.2 Objectives

The objectives of this research are to synthesize and investigate the characteristics and catalytic properties of Ni-Zn-P catalysts supported on polyurethane foam in the selective hydrogenation of acetylene compared with Ni-Zn-P/γAl_2O_3 pellet, Ni-Zn-P/γAl_2O_3 powder, 0.82%Pd/PU foam, 1.37%Pd/PU foam and Pd-Ag/γ-Al_2O_3 (commercial).

1.3 Scope of work

1. Determination of the optimum conditions (pH and deposition time) for electroless deposition of Ni-Zn-P on a polyurethane foam.

2. Preparation of nickel, zinc, phosphorus on polyurethane foam with various amounts of zinc sulfate ($ZnSO_4 \cdot 7H_2O$) (6, 12, 18, 24 g/l), $NiSO_4$ 42 g/l, NaH_2PO_2 24 g/l.

3. Preparation of Ni-Zn-P/γAl_2O_3 pellet, Ni-Zn-P/γAl_2O_3 powder, 0.82%Pd/PU foam, 1.37%Pd/PU foam.

4. Catalyst characterization by s*canning electron microscopy* and energy dispersive X-ray spectrometer (SEM-EDX), and X-ray photoelectron spectroscopy (XPS*),* 1 X-ray diffraction (XRD) analysis and Universal testing machine.

5. Evaluation of the catalytic performance of Ni-Zn-P supported on PU foam, Ni-Zn-P/γAl_2O_3 pellet, Ni-Zn-P/γAl_2O_3 powder, 0.82%Pd/PU foam, 1.37%Pd/PU foam and Pd-Ag/γ-Al_2O_3 (commercial) catalysts in the selective hydrogenation of acetylene to ethylene. The catalyst was reduced in situ with hydrogen by heating from room temperature to 90°C at a heating rate of 10°C/min. Then the reactor was purged with argon and cooled down to the reaction temperature (50, 60, 70, 80 ^oC). The reaction was carried out using a feed composition of 1.5% C_2H_2, 1.7% H_2, and balanced C_2H_4 .

CHAPTER II

THEORIES

2.1 Selective hydrogenation of acetylene

2.1.1 Overview[2]

Ethylene is one of the most widely produced petrochemicals in the world. More recently, ethylene has taken the place of acetylene in virtually all large-scale chemical syntheses. However, acetylene itself is a byproduct of modern ethylene production processes, and the removal of this contaminant will be considered. To begin, the formation of acetylene in ethylene product streams will be examined. More than 97% of ethylene around the world is produced by pyrolysis of hydrocarbons. To begin, the formation of acetylene in ethylene product streams will be examined.

More than 97% of ethylene around the world is produced by pyrolysis of hydrocarbons, which is the thermal cracking of petrochemicals in the presence of steam. This process can be described as the heating of a mixture of steam and hydrocarbon to the necessary cracking temperature, which can range from 260°C to 340°C depending on the hydrocarbon used. This mixture is then fed to a fired reactor or furnace and heated to between 400°C and 470°C. As a result, the original saturated hydrocarbon "cracks" into smaller unsaturated molecules. This process is extremely endothermic, and the product must be cooled back to the original feed temperature upon leaving the reactor in order to minimize secondary reactions. Possible alkane feedstocks for pyrolysis include ethane, propane, n-butane, polymerize, naphtha, kerosene, and various gas oils. In the U.S., ethane and natural gas liquids (often a mixture of ethane and propane) are most commonly used in ethylene production. Incidentally, using an ethane feedstock produces the smallest amount of acetylene byproduct, which averages about 0.26% by weight of the product stream. For other feeds, this quantity can become as large as 0.95% by weight. Ethylene to be used for polymerization processes has to be 99.90% pure. This is known as polymer-grade ethylene and the maximum allowable limit of acetylene should not be higher than 5 ppm.

2.1.2 Industrial acetylene hydrogenation

2.1.2.1 Reaction[4,10,49]

Industrially, ethylene is usually formed by the pyrolysis of hydrocarbons in the presence of steam. Acetylene is a byproduct of this process, which subsequently acts as a poison for the catalyst used for the synthesis of polyethylene from ethylene. Because acetylene adsorbs at the active sites of ethylene and blocks the polymerization process, that must be removed to a level of less than 5 ppm.

The following reactions proceeding in an acetylene hydrogenation:

$$C_2H_2 + H_2 \xrightarrow{k_1} C_2H_4 \qquad \Delta H = -42{,}000 \text{ kg-cal/kg-mol} \qquad (1)$$

$$C_2H_4 + H_2 \xrightarrow{k_2} C_2H_6 \qquad \Delta H = -32{,}900 \text{ kg-cal/kg-mol} \qquad (2)$$

$$nC_2H_2 + \tfrac{1}{2}n\,H_2 \xrightarrow{k_3} (C_2H_3)n \qquad (3)$$

The first reaction, hydrogenation of ethylene to ethane (1) is the desired reaction and the second reaction, hydrogenation of ethylene to ethane (2) is undesired side reaction. And the third reaction, dimerisation and oligomerisation (n = 2, 3, 4, ..) (3) occurring during normal operation which the main product is 1,3- butadiene which can be hydrogenated to so-called C_4 hydrocarbons 1-butene, n-butane, cis- and trans-butene. C_6- hydrocarbons commonly called green oil which is a higher hydrocarbons are formed in small quantities.

The acetylene hydrogenation reaction has two parameters to desired reaction can be assigned. First is the reaction temperature, which relation directly with the kinetics (k_1, k_2, k_3) of this reaction. The second parameter is the ratio of Hydrogen and acetylene ($H:C_2H_2$). Actually, the ratio of $H:C_2H_2$ would be 1:1 to make the conversion of acetylene to be completed so hydrogen would not remain for the side reaction, But in practice the catalyst is not 100% selectivity and the ratio of $H:C_2H_2$ is usually higher than 1:1 to get the conversion of acetylene completed. Increasing $H:C_2H_2$ ratio can help offset the decline in catalyst activity and higher $H:C_2H_2$ ratio

can have a cost in selectivity which lead to ethylene lost. Generally, the ratio of $H:C_2H_2$ is between 1.1 to 2.5.

2.1.2.2 Basic requirements for acetylene hydrogenation units[2]

- Safe operation.
- The maximum allowable limit of acetylene should not be higher than 5 ppm; however, acetylene may be expected to be maintained below 1 ppm; perhaps, below 0.5 ppm. in ethylene customers.
- Operating with a net gain of ethylene.
- Do not be the cause of interruptions to continuous operation of the ethylene plant.
- Ethylene plant, project execution, feedstocks, energy, etc. must have "low investment cost".
- Good catalyst life and reasonable catalyst cost.

2.1.2.3 Reactor of acetylene hydrogenation reaction

The reactor of acetylene hydrogenation is a fixed bed catalytic reactor, normally operated adiabatically. There are also operated in isothermal tubular reactors commercially. There are three major reactor configurations

1) The cracked gas train
2) The back-end reactor
3) The front-end reactor

Commercial front-end and tail-end processes

There are two basic methods of selective hydrogenation of acetylene in ethylene-rich streams, the so-called front-end (Fig 2.1) and tail-end (Fig 2.2) processes [50].

Ethylene hydrogenation reactor

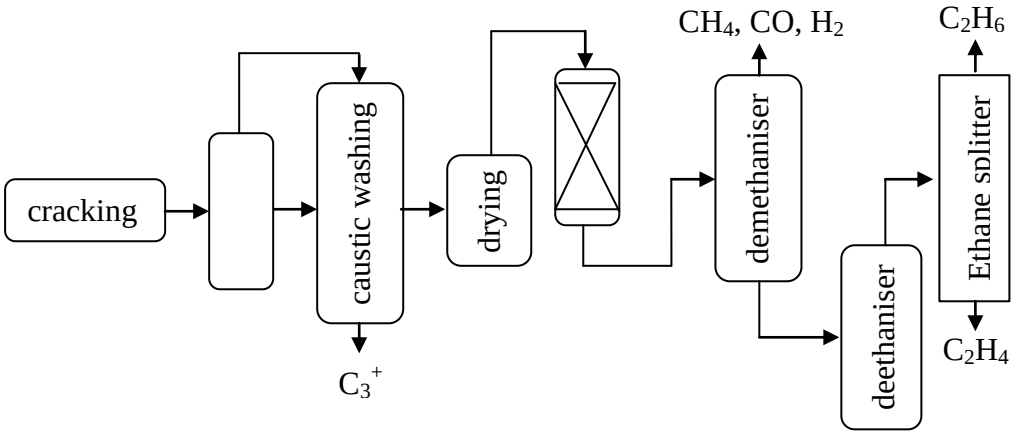

Figure 2.1 Location of front-end acetylene hydrogenation reactors in a simplified scheme of downstream treatment of steam cracker effluents.
(Redrawn from Ref[50])

Ethyne hydrogenation reactor

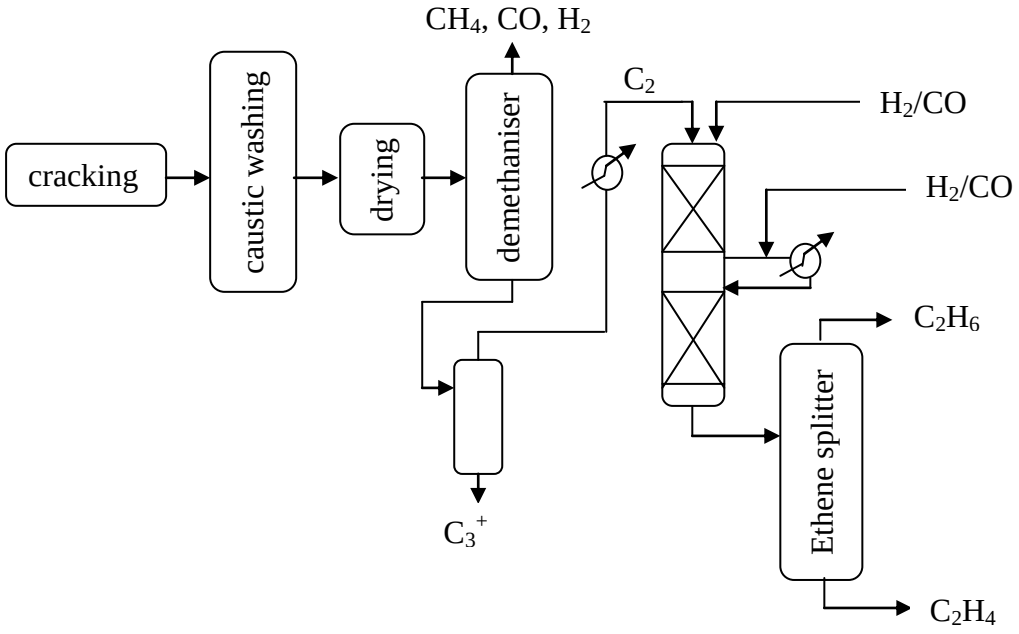

Figure 2.2 Location of tail- and acetylene-hydrogenation reactors in a simplified scheme of downstream treatment of steam cracker effluents.
(Redrawn from Ref [50])

The feed compositions as the function of reactor location are shown in Table 2.1 [16,51**]**. Basically, acetylenes (inclusive of methyl acetylene and acetylene) in a naphtha cracker is higher than an ethane cracker.

Table 2.1 Typical acetylene concentration in the feed gas and conversion rate [51].

	Feedstock	Concentration (vol %)			Conversion Rate (%)		
		C_2H_2	C_3H_4	C_4H_6	C_2H_2	C_3H_4	C_4H_6
Back-end Hydrogenation	Naphtha	1.3	-	-	100	-	-
Front-end Hydrogenation (deethanizer)	Naphtha	0.61	-	-	100	-	-
Front-end Hydrogenation (depropanizer)	Naphtha	0.53	0.067	-	100	>60	-
Raw Gas Hydrogenation	Ethane/ propane	0.3	0.13	0.85	100	>60	>90

2.1.3 The mechanism of acetylene hydrogenation [52]

In the partial catalytic hydrogenation of acetylene compounds, the triple bond has to be converted into a double bond. In doing so, there arise the following problems of selectivity:

(a) The double bond which is formed can be further hydrogenated.
(b) The double bond which is formed can be displaced (position isomerism).
(c) The double bond which is formed can have cis, trans configuration (geometriciso merism).

Since acetylene only have two carbon atoms, the problems stated in (c) is not applicable. To achieve high selectivity, the catalyst must not further hydrogenate the partially hydrogenated product. This can be affected by two factors, the kinetics and the thermodynamic factors. Kinetic and thermodynamic effects are frequently combined, and they cannot readily be distinguished. Further, not only the catalyst but also the chemical structure can have an influence on the selectivity. In case of the

subsequent reactions (undesired reaction) proceeding much more slowly than the partial hydrogenation (desired reaction); the selectivity is then based on a mechanistic (kinetic) factor. Besides, the partially hydrogenated product can also be protected from subsequent reactions by being rapidly desorbed from the catalyst surface and then not being re-adsorbed again. This thermodynamically dependent selectivity is based on the triple bond being more strongly adsorbed than the corresponding double bond, because it is more electrophilic character. Even relatively small differences in the adsorption energy are sufficient for the acetylenic compound to immediately displace the primary resulting hydrogenation product from the catalyst surface and accordingly act as a "poison" for the subsequent reactions. The poisoning action is naturally only effective as long as the acetylenic compound is still present.

Acetylene itself is a good example of thermodynamically controlled selectivity. This can be proven from the effluence of a fixed bed palladium catalyst reactor, where the resulting ethylene only contains 1-5% ethane although this catalyst have 10 to 100 times greater activity for the hydrogenation of ethylene than for the hydrogenation of acetylene.

A general mechanism shown in Table 2.2 suggested that selectivity is controlled by the equilibrium between the two forms of adsorbed C_2H_3 (step 3 and step 4). The hydropolymerisation (formation of oligomer or "green oil") is consider to be a polymerization of adsorbed acetylene, in which the free radical is the initiator.

Table 2.2 General mechanism of catalytic acetylene hydrogenation [53].

Step 1 : Adsorption	Acetylene is associatively adsorbed on the longer lattice spacing of the transition group Metal , and that it reacts with a H_2 molecule (there being no independently adsorbed hydrogen on Ni) or	$HC^{\cdot}=CH^{\cdot} + H_2 \longrightarrow HC^{\cdot}=CH_2 + H^{\cdot}$
	With an adsorbed H atom (on Pd or Pt)	$HC^{\cdot}=CH^{\cdot} + H^{\cdot} \longrightarrow HC^{\cdot}=CH_2$
Step 2 : Isomerisation	The adsorb vinyl radical is thought to isomerise in part into a free radical from	$-HC^{\cdot}-CH_2$
Step 3 : Hydrogenation to ethylene	The vinyl from hydrogenation to give ethylene which leaves the surface	$HC^{\cdot}=CH_2 + H^{\cdot} \longrightarrow CH_2=CH_2$
Step 4 : Hydrogenation to ethane	The free radical from gives an adsorbed ethylene which can react with more hydrogen	$-HC^{\cdot}-CH_2 + H^{\cdot} \longrightarrow CH_2-CH_2$ $CH_2-CH_2^{\cdot} + H^{\cdot} \longrightarrow CH_2-CH_3$

The asterisks indicate adsorption links.

2.2 Electroless deposition method [54]

Electroless plating, also known as chemical or auto-catalytic plating, is a non-galvanic type of plating method that involves several simultaneous reactions in an aqueous solution, which occur without the use of external electrical power. Electroless deposition is the process of depositing a coating with the aid of a chemical reducing agent in solution, normally sodium hypophosphite (Note: the hydrogen leaves as a hydride ion), and oxidized thus producing a negative charge on the surface of the part. This reaction is the process without the application of external electrical power. It is therefore applicable to non-conducting substrates, and has been used extensively for metallizing printed wiring boards (PWB). Though electroless metal deposition rates are typically lower than those of *electrolytic deposition* rates, as dimensions of circuit lines continue to get smaller, electroless deposition will continue to be attractive for next generation PWB products which have much finer and thinner lines than traditional PWB products. More recently,

selective electroless deposition has been found to yield encouraging results in the case of the self-aligned cobalt-tungsten-phosphorus alloy capping, or barrier, layer on back-end-of-line (BEOL) copper interconnects, for example, in tests aimed at high performance logic chips at the CMOS 45 nm node and below.

2.2.1 Application of electroless deposition [54-55]

Electroless deposition as we know today has many applications, for examples, in corrosion prevention and electronics. Although it yields a limited number of metal and alloy deposits compared to electrodeposition, materials with unique properties, such as nickel-phosphorus (corrosion resistance) and cobalt-phosphorus (magnetic properties) based alloys, are readily obtained by electroless deposition. In principle, it is easier to obtain coatings of uniform thickness and composition using the electroless process, since one does not have the current density uniformity problem of electrodeposition. Electroless deposition is experiencing increased interest in microelectronics, in part due to its *selectivity* of deposition. The most common electroless plating method is electroless nickel plating, although silver, gold and copper layers can also be applied in this manner, as in the technique of Angel gilding.

2.2.2 Advantages and disadvantages of electroless deposition method [56-57]

In the electroless plating process, the driving force for the reduction of metal ions and their deposition is supplied by a chemical reducing agent in solution. This driving potential is essentially constant at all points of the surface of the component, provided the agitation is sufficient to ensure a uniform concentration of metal ions and reducing agents. Electroless deposits are therefore very uniform in thickness all over the part's shape and size. This process offers distinct advantages when plating irregularly shaped objects, holes, recesses, internal surfaces, valves or threaded parts.

The advantages of electroless plating method are [56-57]:

- High corrosion resistance in the as-deposited condition.
- Maintains better uniform thickness and surface finish.
- Can plate small diameters.
- Deep bores and intricate shapes.
- No electricity is required.
- Nonconductive materials can be plated by this process such as plastics, nylon or rubber.
- Simple process requiring simple equipment.
- Uniformity of the deposits, even on complex shapes.
- Deposits are often less porous and thus provide better barrier corrosion protection to steel substrates, much superior to that of electroplated nickel and hard chrome.
- Deposits can be plated with zero or compressive stress.
- Deposits have inherent lubricity and non-galling characteristics, unlike electrolytic nickel.
- Deposits have good wet ability for oils.
- In general low phosphorus and especially electroless nickel boron are considered solderable. Mid and high phosphorus electroless's are far worse for solderability.

The disadvantages of electroless plating method are[56-57]:

- Environmentally responsible waste treatment can add significant costs to the electroless plating process.
- Generally concerning the chemicals used both in pretreatment and the plating bath itself.
- It’s not necessary to monitor an electric current and keep the bath heated and agitated.

- It is necessary to monitor the level of alloy ions in the bath and replenish them as they decline.
- Lifespan of chemicals is limited.
- Requires high standards of quality control of surface preparation and plating solution.
- It is difficult to control with regards to film thickness and uniformity.

2.2.3 The electroless deposition solution

An electroless solution typically consists of [55]:

- A source of metal ions.
- A reducing agent, or reductant, such as formaldehyde for copper deposition and hypophosphite for nickel deposition.
- A complexant for the metal ions to keep these dissolved ions in solution, and to minimize homogenous reaction between the metal ions and the reducing agent.
- Most likely a pH adjustment buffer.
- Often a few ppm of a catalytic poison, such as lead ions, to stop unwanted plating on the walls of the tank, hoses, pumps, miscellaneous particles in the solution, and on inert regions of the sample undergoing electroless deposition.
- oxygen gas dissolved in solution, which is invariably present, may also undergo reduction, and which can influence deposition uniformity due to non-planardiffusion.

2.2.4 Electroless deposition pretreatment process

The pretreatment process is a necessary step in electroless plating for kind of polymer with low chemical activity, they must be pretreated before electroless plating [58]. The goal of the pretreatment process is to remove unwanted contaminants that may hinder the bonding process and result in low-quality or unusable results.

Depending on the substrate being used, this can be a time - consuming process that requires several steps.

In general, the pretreatment process requires the substrate to be cleaned with a series of base or acid chemicals. In between each chemical treatment, the substrate must be rinsed with water to sufficiently remove residual chemical adhesion. Degreasing can remove contaminant oils and further acid cleaning can remove scaling [59].

Metallization techniques based on electroless plating are widely used to coat polymer meterials in a large variety of technological applications. Traditionally, dilute tin chloride ($SnCl_2$) and palladium chloride ($PdCl_2$) solutions in HCl are used to render the surface of such non-conductive substrates catalytically active towards metal deposition in the electroless plating solution [60].

There are many methods for making the non-conductive surfaces catalytically active *in* Fig. 2.3a represents a schematic diagram of the surface preparation processes which are conventionally method [60]. After substrate cleaning with the solvents to remove surface contaminants and chemical treatment to obtain a micro roughened oxidized surface, the activation processes can be classified into two systems. The first system involves the use of a sensitization step followed by an activation step. The second system, the most widely employed system in practice today, involves the use of a direct activation step an acceleration operation. These two systems are often referred to as the two-step and one step procedures, respectively. In other respects, Fig. 2.3b represents the routes which were, at first, explored in our laboratory and which have led to the development of new and simplified electroless plating methods. The latter make use of plasma or UV-laser-induced conditioning procedures instead of chemical etching processes used in the conventional methods [60].

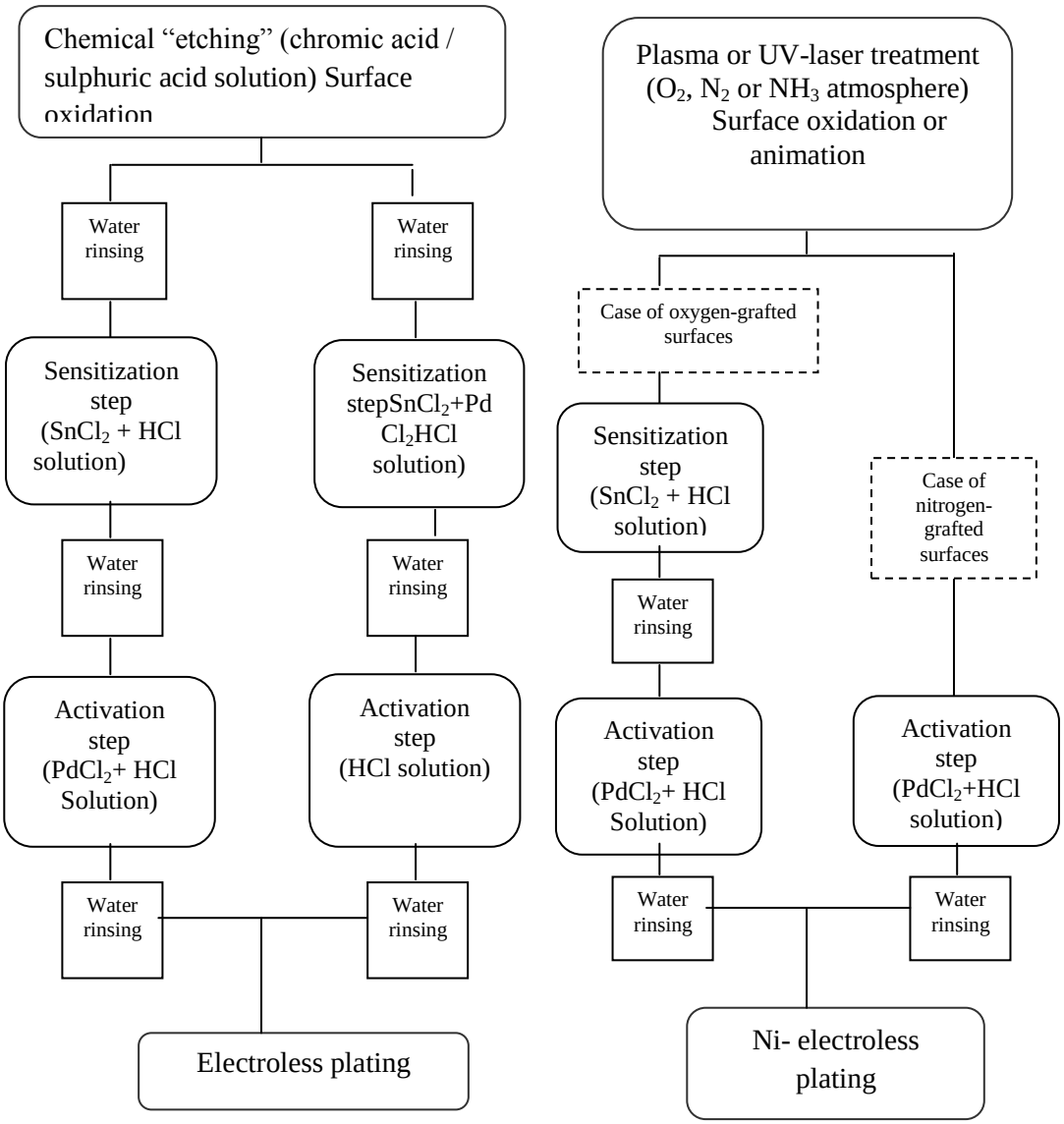

Figure 2.3 Schematic diagram of the conventional electroless plating processes **a.)** using a chemical etching pretreatment and the two-step sensitization/activation or one-step activation–acceleration procedures leading to the surface attachment of the catalyst (Sn/Pd ‘‘compound’’). **b.)** using a plasma or UV-laser pretreatment in O_2, N_2 or NH_3 atmosphere, and the two-step sensitization/activation (case of oxygen-grafted surfaces) or one-step direct activation (case of nitrogen-grafted surfaces) procedures leading to the surface attachment of the catalyst (Sn/Pd ‘‘compound’’ or Pd(+2) species, respectively) (Redrawn from Ref [60]).

2.3 Polyurethane (PU) foam

A polyurethane is polymer composed of a chain of organicunits joined by urethane links. Polyurethane polymers are formed by combining two bi- or higher functional monomers. One contains two or more isocyanate functional groups) and the other contains two or more hydroxyl groups. More complicated monomers are also used. The alcohol and the isocyanate groups combine to form a urethane linkage:

ROH + R'NCO → ROC(O)N(H)R' (R and R' are alkyl or aryl groups) [61]

Foaming of PU occurs when a small amount of blowing agent and water was added in polymerization. Water was reacts with isocyanate groups giving carbamic acids, which spontaneously lose CO_2, thus generating the foam bubbles. The blowing catalyst composition provides the resulting polyurethane foam with improved breathability [62-63]. The unique properties of PU foam are lie in their high energy absorption capacity, particularly useful for shock applications, acoustic and thermal insulating properties, filtering applications [64]. And the PU foams are porous materials with a special structure made of a skeleton of more or less regular open or closed cells with non-conductive surfaces, high surface area, lightness, and relatively low price [44,46,47].

CHAPTER III

LITERATURE REVIEWS

3.1 Catalysts for selective hydrogenation of acetylene

There are many types of catalyst which is suitable for the selective hydrogenation of acetylene reaction. For high performance, the catalyst should exhibit these characteristics [65]:

1. High activity sustained over long operating periods, high space velocity, and consequently a low-catalyst inventory.
2. High selectivity over a relatively wide temperature range to avoid losses of ethylene and to prevent polymer and carbon formation. These latter products result from temperature variations within the catalyst bed due to the exothermic nature of the reactions.
3. Resistance to poisoning by CO and traces of sulfur compounds.
4. Rugged structure to permit periodic regeneration of catalyst pallets.

Although in the absence of acetylene, ethylene often hydrogenates more rapidly than acetylene over the same catalyst, acetylene hydrogenates much faster than ethylene when both are present. There are several metals and metallic oxides can act as catalysts in the selective hydrogenation of acetylene reaction.

3.1.1 Pd-based catalysts

Supported Pd-based catalysts have been proven to be the best catalysts so far for the selective hydrogenation of acetylene especially in the industrial production of polyethylene. Various factors have been found to affect the performance of Pd-base catalysts in the selective hydrogenation of acetylene such as particle size, promoters, and the method of pretreatment.

3.1.1.1 Effect of Pd dispersion

The effect of Pd dispersion obtained on different supports, for examples, silica [3,10,11,15,18,19,23,31,40,41], alumina [1,14,20,24-34,38,66,67], mesoporous and microporous materials [34], on their catalytic properties in the selective hydrogenation of acetylene has been reported. In these previous studies, they suggest that high metal dispersion yields a structure sensitivity reaction and/or Pd particle size effect on the acetylene hydrogenation [35-36]. For examples, the specific activity decreases one order of magnitude while the dispersion increases [35].

3.1.1.2 Effect of additives/promoters

The role of the additives, or selectivity promoters, is generally considered to be derived from two factors: geometric and electronic, to improve the activity and selectivity of acetylene hydrogenation reaction. There are many kind of metals that have been employed as the promoter for this process such as Ti [3,10,15,16,23], Ag [5,11,24-29,66-68], Au [17,18], Si [21,22], Nb [3,40], and Zn [14].

Jung *et al*., (2000) [3] studied Pd/SiO_2 catalysts promoted with transition-metal Ti, Nb and Ce oxides. The results showed that metal oxides spread on and modified both geometrically and electronically the Pd surface after the catalyst was reduced at 500^oC. The ethylene selectivity of the Pd catalysts was improved significantly by the oxide addition. And among the three metal oxides examined in this study, Ti oxide showed the most promotional effect. Woo Jae Kim, *et al*. (2002) [15] studied selective hydrogenation of acetylene by addition of TiO_2 to Pd catalysts. They compared the TiO_2-added Pd catalyst reduced at 500◦C, Pd–Ti/SiO_2/500°C, with the case of Pd/SiO_2/300°C, or Pd/TiO_2/500°C. TiO_2 was selected as a candidate promoter because it was well known that it interacts strongly with Pd, particularly after reduction at high temperatures. They found that ethylene adsorption was suppressed in two ways. The ethylene decomposition was inhibited because the multiple Pd sites were blocked by Ti species, and the adsorption of ethylene were weakened presumably because the Pd was electronically modified by the Ti species and small Pd crystallites on the Pd/SiO_2 catalyst were preserved even after TiO_2

addition and reduction at 500°C. The Pd surface was decorated with Ti species to different extents depending on the reduction temperatures. The Pd–Ti/SiO_2/500°C showed an improved selectivity for ethylene production in acetylene hydrogenation. Woo Jae Kim, *et al*. (2004) [10] also studied TiO_2-added Pd catalyst and showed that the addition of TiO_2 suppressed the formation of green oil and improved the lifetime of the catalyst. TiO_2 also suppressed Pd sintering in the regeneration step by reducing the mobility of Pd crystallites and deactivated at slower rates than the Pd-only catalyst. Kontapakdee *et al*,.(2006) [16] reported that the used of pure anatase TiO_2 (either micron- or nano-sized) as supports for Pd catalysts produced high ethylene selectivities In contrast, the used of pure rutile TiO_2 supported ones resulted in ethylene loss due to over hydrogenation of ethylene to ethane. The differences in ethylene selectivity of the various Pd/TiO_2 were due mainly to the presence/absence of the Ti^{3+} defective sites on the TiO_2 support, rather than the difference in the crystallite sizes of the TiO_2 support.

Ahn *et al*., (2006) [40] studied Pd catalysts promoted by La_2O_3 and Nb_2O_5, which were selected among metal oxides showing a strong metal-support interaction (SMSI).La_2O_3-added catalysts that were reduced at 500°C showed the highest ethylene selectivity at a reaction temperature of 60°C. On the other hand, Nb_2O_5-added catalysts showed higher acetylene conversions as well as both improved ethylene selectivity and catalyst lifetime when compared with the Pd-only catalyst. In this case, the improved selectivity attained by reducing the catalyst at 500°C was significant when the reaction was conducted at low temperatures, i.e. 40°C and 50°C instead of 60°C. The La_2O_3-added catalyst was deactivated more slowly than the TiO_2-added catalyst.

Ahn *et al*,. (2009) [11] studied Ag-promoted Pd/SiO_2 catalysts. The results show that addition of Ag geometrically blocked multi-coordinated large ensembles of the Pd surface and also modified Pd electronically to facilitate the desorption of 1,3-butadiene from the Pd surface. Consequently, the green oil that formed on the Pd-0.5Ag/SiO_2 became more volatile and mobile than that formed on Pd/SiO_2. Zhao *et al*., (2011) [23] studied the catalytic performance of a Ti added Pd/SiO_2 catalyst that were prepared by the incipient wetness impregnation. The results showed that the titanium oxide in Pd–Ti/SiO_2 catalyst was amorphous and the addition of Ti reduced

the particle size of Pd significantly. Comparing to the Pd/SiO_2 catalysts, the ethylene yield increased from 64.1% to 88.3% under $Pd–Ti/SiO_2$ catalytic system. Huang *et al.,* (2007) [1] showed that Pd–Ag bimetallic catalysts exhibited higher selectivity for acetylene hydrogenation in the presence of ethylene than either Pd or Ag monometallic catalysts. The Na+-*β*-zeolite-supported catalysts exhibited higher selectivity than their γ -Al_2O_3 counterparts. Sárkány *et al*., (2002) [17] investigated two series of Pd and $Pd-Au/SiO_2$ catalysts. Gold was deposited via ionization of pre-adsorbed hydrogen over pre-reduced Pd/SiO_2 in order to ensure selective poisoning of the Pd surface. Presence of Au decreased the carbon coverage and improved the ethene selectivity. Decoration of Pd by Au and the morphology of particles explain the ethene selectivity improvement. Sárkány *et al*., (2008) [18] synthesized Pd/Au shell/core particles supported on SiO_2. The Pd shell thicknesses was varied in the range of 0.12–1.5 nm by depositing 15, 30, 45, 65 and 80 at% Pd on preformed Au particles of 5 nm. The results showed that the hydrogenation activity of the Pd/Au shell/core particles supported on SiO_2 appeared decreased with the increasing thickness of the Pd shell. $Pd(80)–Au/SiO_2$ showed better activity and selectivity performance than the Pd shell of 1.5 nm thickness. Shin *et al*., (2002) [21] studied supported Pd catalyst modified with Si. The results showed that the hydrocarbon species deposited on the Si-modified catalyst have a shorter chain length than those produced on the Pd-only catalyst as well as the facilitated desorption of ethylene, reduced amounts of chemisorbed hydrogen, and suppressed C_2 polymerization. Kim *et al*., (2003) [22] studied the deactivation behavior of Si-modified Pd catalysts. They reported that Si modification retard not only the sintering of Pd crystallites during catalyst regeneration but also the deactivation rates of the catalyst during the hydrogenation process after the regeneration. Chinayon *et al*., (2008) [14] studied the catalytic performance of Pd catalysts supported on nanocrystalline α-Al_2O_3 and Zn-modified α-Al_2O_3 prepared by sol–gel and solvothermal. Both of acetylene conversions and ethylene selectivities were improved in the order: Pd/Zn-modified α-Al_2O_3-sol–gel > Pd/Zn-modified α-Al_2O_3-solvothermal > Pd/α-Al_2O_3-sol–gel ≈ Pd/α-Al_2O_3-solvothermal >> Pd/α-Al_2O_3-commerical. Zn-modified α-Al_2O_3 also showed less deactivation by coke formation.

From previous studies, it can be concluded that addition of promoter resulted in the improvement of ethylene selectivity in acetylene hydrogenation by retarding the sintering of Pd crystallites, decreasing the carbon coverage, modification geometrically and/or electronically. In addition, the promoted catalysts also showed the slower rates of catalyst deactivation [10,11,14,22,40].

3.1.1.3 Effect of pretreatment

The effect of pretreatment on catalytic behavior for selective hydrogenation of acetylene has been investigated by many authors. Praserthdam et *al.,* (2000) [68] studied the activation of acetylene selective hydrogenation catalysts using oxygen containing compounds on the Pd–Ag catalyst at 60^{o}C with a space velocity of 2000 h^{-1}. It was found that an enhancement in the performance of Pd–Ag catalyst can be obtained by pretreatment with N_2O. It is suggested that a certain amount of N_2O added to the catalyst before will augments the sites associated with ethylene production from acetylene and depletes the sites responsible for direct ethane formation. Ngamsom *et al.,* (2002) [24] studied the catalytic performance of Pd-Ag/α-Al_2O_3 pretreated with oxygen and/or oxygen-containing compounds, i.e. O_2, NO, N_2O, CO and CO_2. The enhancement of catalytic performances by the pretreatment was a consequence of an increase in accessible Pd sites responsible for acetylene hydrogenation to ethylene. Furthermore, the sites involving direct ethane formation from acetylene could be suppressed. Lamb *et al.,* (2004) [66] studied the effects of pretreatment on the surface of alumina-supported Pd–Ag catalysts with oxygen or oxygen-containing compounds (NO, N_2O, CO and CO_2). Analysis of the surface after reduction shows evidence of a Pd–Ag alloy. The binding energy of the Pd 3d is not affected by pretreatment, whereas a significant shift of the Ag 3d is revealed after NO and N_2O pretreatment. The surface after reaction shows no state change of either Pd or Ag compared to those measured prior to reaction, which was in agreement with the reactivity test; therefore surface modification occurs after pretreatment and retained even after 8 h on stream. No carbonaceous deposits were formed after 8 h on stream. Ethylene gain enhancement by NO and N_2O pretreatment was a result of strong

adsorption on the surface which may block the sites responsible for ethylene hydrogenation without facilitating carbonaceous deposits for hydrogen spillover. On the other hand, pretreatment with O_2, CO or CO_2 increases the Pd active sites, which increases acetylene hydrogenation activity as well as the rate of H_2 spillover onto the support. And ethylene gain increases with time on stream for all pretreatments. Ngamsom *et al*., (2004) [67] reported that pretreatment with NO and N_2O resulted in the blockage of the Pd sites responsible for direct ethane formation, thereby increasing ethylene gain. Overall, there are many kind of pretreatment that affect the catalytic performance of Pd-based catalysts. Pretreatment resulted in an increase of accessible catalyst sites which gave higher ethylene gains because the number of sites for direct ethane formation was lessened [24,66-68].

3.1.2 Non-precious metal catalyst

In order to replace the expensive Pd-based catalysts, non-precious catalysts have been studied in the selective hydrogenation of acetylene such as Ni/SiO_2[69], Ni/Al_2O_3[69], Ni/Al_2O_3[43], $Ni\text{-}Zn/Al_2O_3$[43], Ni–Al–Cr[42], $Ni/NiAl_2O_4$[70], $Ni\text{-}Zn/MgAl_2O_4$[71] and Cu[8,39,71-73]. Guimon *et al*., (2003) [69] studied Ni–Si–Al mixed oxides catalysts prepared by sol–gel technique with different supports (silica and silica-alumina). Catalyst activation (reduction) was carried out in situ at 500°C for 2.5 h using H_2 (vol. 50%)/N_2 mixture. The feed composition consisted of $H_2/C_2H_2/N_2$ (60/15/25) and the temperature was kept at 175 °C. The results show that silica had very weak interactions with the metal. The pre-reduction induced a non-negligible sintering for the samples with high Ni content, and thus the formation of large size crystallites. The addition of alumina to silica led to the existence of two types of Ni^{2+} crystallites, one presenting strong interactions with the support, the other with very weak interactions (or none). The amount of the latter increased with the Ni content. This addition had a positive effect on the formation of coke, which was mainly related to the hydrogenolytic (naked) metallic sites corresponding to the metal without interaction with the support. Three types of coke had been detected which were, ordering them according to their oxidability, filamentous carbon, amorphous coke, and strongly adsorbed hydrogenated carbons. The production of coke was relatively

high, particularly in the case of Ni/SiO_2. It did not alter (or only slightly in this series) the desired selectivity (hydrogenation of acetylene to ethylene). On the contrary, for Ni/SiO_2-Al_2O_3 catalysts with high Ni contents, it improved the initial selectivity because the coke deactivated the hydrogenolytic sites which were active for the side reactions.

Rodr´ıguez *et al.*, (1997) [43] studied the influence of zinc addition on the catalytic performance and physicochemical properties of a Ni-based catalyst in acetylene hydrogenation. The catalysts used in this work were prepared by the coprecipitation method. In this work, they varied amounts of Zn in the catalysts. They reported that coke formation and the initial coking rate diminished as the Ni/Zn ratio was decreased, which mean that nickel was also responsible for coke formation. Furthermore, zinc inclusion into the matrix structure seemed to reduce coke deposition considerably. The activity and selectivity of Ni-based catalysts, used in the selective hydrogenation of acetylene, can be improved by incorporating Zn^{2+} in the solid structure. The zinc-modified catalysts produce smaller amounts of coke and methane in comparison with those not containing zinc. Furthermore, coke deposited on ternary Ni/Zn/Al catalysts had a strong effect on ethylene production. Their high dispersion reduced the concentration of neighbour nickel atoms and thus also methane and coke yields.

Rives *et al.,* (1998) [42] studied acetylene hydrogenation on Ni–Al–Cr oxide catalysts and the role of added Zn**.** The feed composition contained $H_2/C_2H_2/N_2$ mixture (volumetric composition: 60/15/25) and the temperature was kept at 448 K. In this process, methane and coke were byproducts. In this work they suggested that decreasing in the amount of coke deposited is due to the formation of Zn into the oxide structure. It was also found that the sample without Ni, formation of coke is also observed, indicating that, in addition to the role of Ni, the acidity of the support plays a role in coke formation. The largest selectivity to methane being found for the catalysts with the maximum Ni/Zn ratio and the selectivity to ethylene increased as the Ni/Zn ratio decreased. The highest selectivity to ethylene was achieved for Zn/Ni $\approx$ 4 (molar ratio).

Pe˜na *et al.,* (1996) [70] studied $Ni/NiAl_2O_4$ catalyst used for the hydrogenation of acetylene at temperatures between 423 and 493 K. The results

showed that the catalytic activity increases with time on stream (activation period), until a point is reached in which catalyst deactivation predominated (deactivation period). Catalyst aging in this system was found to reduce coke formation and increase the hydrogenation activity.

Studt *et al,* (2008) [71] synthesized a series of Ni-Zn alloy catalysts on $MgAl_2O_4$ spinel supports that had a Zn content between 45 and 75% and tested their selectivity in the hydrogenation of acetylene in a gas mixture of 1.33% ethylene, 0.0667% acetylene, and 0.67% hydrogen. The results showed that a highly selective catalyst had very low ethane production, even at high conversion, where the amount of acetylene in the reactants was small. They also suggested that pure Ni has rather poor selectivity, on the other hand, showed a very good selectivity under high conversion. The selectivity increased substantially as the amount of Zn was increased. The Ni-Zn catalyst with the highest Zn content had an even greater selectivity than the best Pd-Ag catalyst that they tested. The Ni-Zn catalysts that they studied appeared to be more stable than has been reported for Cu.

As mentioned above, the catalysts with high Ni achieved the positive effect on the formation of coke contents which improved the initial selectivity because coke deactivated the hydrogenolytic sites which are active for the side reactions[43,69]. The zinc-modified Ni-based catalysts can produce smaller amounts of coke and methane as well as increasing the selectivity to ethylene in the selective acetylene hydrogenation [42,43,71].

3.2 Electroless deposition on polyurethane foam

Polyurethanes are polymers which contain urethane linkages and are produced by reacting diisocyanates with polyols and some supplementary chemicals and catalysts[62]. The PU foams are porous materials with a special structure made of a skeleton of more or less regular open or closed cells. The unique properties of PU foams lie in their high surface area, lightweight, and relatively low price [44,46,47,62].

PU foam is non-conductive materials, the pretreatment process is a necessary step in electroless plating for this kind of polymer with low chemical activity [58].

The method for pretreatment has been studied by Yang *et al*., (2008) [58] on the magnetic Ni–P plating that was coated on surface of polyurethane foam. The pretreatment process of : PU foams involved cleaning, degreasing, and polishing with ethanol (C_2H_5OH) and 1 mol/L sodium hydroxide (NaOH) solution (at 60 ^oC for 5 min), and then sensitizing in 77.5 g/L stannum chloride ($SnCl_2$), 7 g/L sodium stannate (Na_2SnO_3) and 1 mol/L hydrochloric acid solution for 3 min and activating in 1 g/L palladium chloride ($PdCl_2$) and 1 mol/L hydrochloric acid solution for 10 min at room temperature. After that, PU foams were washed fully with distilled water. The results of deposition showed that the Ni–P plating was composed of particles with diameters in the range of 1–2 mm. The plated PU foams are magnetic and can be used in some special applications. Tian *et al,*. (2010) [9] studied electroless plating method of copper on the surface of polyurethane and optimization the conditions of electroless deposition method. The electroless plating was carried out by multi-step processes which included degreasing, rinsing, roughening, rinsing, sensitization, rinsing, activation and electroless copper plating. For the pretreatment process, the specimens were cleaned, degreased and polished with ethanol (C_2H_5OH) for 1 min, and then scoured in solution (35 g/L NaOH, 25 g/L Na_2CO_3, 10 g/L Na_3PO_4) at 70 ^oC for 5 min to remove the dirt and release agent on the surface of polyurethane foam. The samples were rinsed then in distilled water and etched in a mixture of 1 g/L $KMnO_4$ and 0.5 mL/L H_2SO_4 solution at 45 ^oC for 5 min. The surface sensitization was conducted by immersion of the samples into an aqueous solution containing 50 g/L $SnCl_2$ and 1 mol/L HCl at 30 ^oC for 5 min. The specimens were then rinsed in distilled water and immersed in an activator containing 0.5 g/L $PdCl_2$ and 1 mol/L HCl at 40 ^oC for 5 min. The specimens were then rinsed in a large volume of deionized water for more than 5 min to prevent contamination of the plating bath .The results showed that the deposition rate increased with increasing temperature to 40-50 ^oC and pH value of 12.5-13.0. The optimum conditions were $CuSO_4$ 16 g/L, HCHO 5 mL/L, $NaKC_4H_4O_6$ 30 g/L, Na_2EDTA 20 g/L, $K_4Fe(CN)_6$ 25 mg/L. The deposition rate increased with increasing concentrations of $CuSO_4$ and HCHO, and decreased with increasing concentration of $NaKC_4H_4O_6$ and Na_2EDTA. And the addition of $K_4Fe(CN)_4$ to the bath can reduce the deposition rate and make the deposits more compact. Adding ultrasonic on the process can elevate the deposition rate of copper

by 20%-30%. The foam metal material with a porosity of 92.2% and a three-dimensional network structure was fabricated by electro-deposition after the electroless copper plating.

3.3 Electroless Ni-Zn deposition

Veeraraghavan *et al*., (2004) [74] studied the optimization of electroless Ni–Zn–P deposition process both experimentally and mathematically. A mathematical model based on mixed potential theory was developed which was used to optimize a non-anomalous Ni–Zn–P electroless deposition process. The model was developed by assuming an adsorption step in addition to the electrochemical steps. The concentrations of the Zn and Ni complex were estimated by solving the material balances in addition to the electroneutrality condition and the equilibrium relations. The composition of the coating was estimated from the partial current densities of all charge transfer reactions, which occur at the electrode–electrolyte interface. The model results showed that the adsorption plays a significant role in the alloy deposition process. From the model results, it was seen that the addition of Zn ions to the bath inhibited the deposition rate by changing the surface coverage of the adsorbed electroactive species on the electrode surface. The zinc surface coverage decreased while the alloy deposition rate increased with an increase of the pH of the bath. The model results fit well with the experimental data. Sharif *et al*., (2007) [75] studied the interfacial reactions of electrolytic Ni and electroless Ni(P) metallization of the ball-grid-array (BGA) substrate with the molten Sn–9Zn (wt.%) eutectic solder alloy, focusing on the shear strengths and the identification of the intermetallic compound (IMC) phases at various reflow periods. Zn-containing Pb-free solder alloys were kept in molten condition (240 °C) on the bond pads for different durations ranging from 1 to 60 min to render the ultimate interfacial reaction and to observe the consecutive shear strength. The results show that electroless Ni(P) metallization gave better results in terms of shear strength on liquid state annealing than electrolytic Ni metallization with Sn–Zn solder. Less than 0.5 μm of the electroless Ni layer was consumed by the Sn–Zn solder with 60 min molten reaction at 240 ◦C. However, more than 1.4μm thick electrolytic Ni layer was consumed by the same solder within

the same reported period. With the increase of reaction time, the thick Ni–Zn compound layer created the weakest link with original electrolytic Ni layer. Neither P-rich Ni layer, nor Ni–Zn compound was observed at the interface of the Sn–Zn solder/Ni(P) system even after a long time molten reaction. Sn–9Zn solder and electroless Ni(P) metallization was identified as a good combination in soldering technology.

Takács *et al*., (2007) [76] studied the effects of pre-treatments on the corrosion properties of electroless Ni–P layers deposited on $AlMg_2$ alloy. They reported that both the corrosion properties and deposition rates of the electroless Ni layers were affected by the proper pre-treatments. From the measured polarization resistances of amorphous Ni–P layers with an average of 13 μm thickness and 9 wt.% phosphorus content, it was found that the nickel pre-coating and the hypophosphite adlayer formed by suitable immersion pre-treatments improved the corrosion resistance of the samples immersed in aerated sodium sulphate solution of pH 3. The decrease of the corrosion rate was mainly attributable both to the lower microporosity and smoother morphology of the nickel–phosphorus coatings. While both the zinc and the immersion nickel pre-coatings decreased the deposition rate, the hypophosphite adsorption layer did not decrease it. In case of electroless nickel plating on aluminium base alloys a pre-treatment bath containing hypophosphite with lactic acid can be used with the major advantage of the improved corrosion resistance of the electroless Ni layer without any decrease in the deposition rate. Ther found that electroless Ni–P deposition systems the decrease of corrosion rate could mainly be attributed to the lower microporosity and smoother morphology of the nickel–phosphorus coatings.

Ranganatha *et al*., (2010) [77] studied the properties of electroless Ni–Zn–P/nano-TiO_2 composite coatings. In this study TiO_2 was synthesized by a sol–gel method. Electroless plating were performed under constant stirring of 500 rpm for 3.5 h at the temperature of 80±5 ◦C and pH of the bath was 9. They found that after heat treatment the surface morphology of both pure and composite coated specimens were changed and the composite coatings exhibited higher microhardness than pure alloy. The electrochemical measurements showed that the annealed Ni–Zn–P–TiO_2 coatings have good corrosion resistance in 3.5 wt% NaCl solution compared to Ni–Zn–P coatings.

From these previous studies it can be summarized that for the Ni-Zn deposition the addition of Zn ions to the bath inhibited the deposition rate by changing the surface coverage. The zinc surface coverage decreased while the alloy deposition rate increased with an increase of the pH of the bath[74,75]. In addition, the deposition rates of the deposit layers were affected by the proper pre-treatments[74-77].

CHAPTER IV

EXPERIMENTAL

This chapter consists of experimental systems and the experimental produce in this work

4.1 Chemicals

The chemicals used in this work for preparation Ni-Zn-P catalysts with various amounts of $ZnSO_4$ supported on polyurethane foam are specified in Table 4.1

Table 4.1 Details of chemicals used in the experiments

Chemicals	Formula	Supplier
Nickel sulfate	$NiSO_4 \cdot 6H_2O$	Carlo Erba
Zinc sulfate	$ZnSO_4 \cdot 7H_2O$	Carlo Erba
Sodium citrate	$C_6H_8O_7Na_3\ 2H_2O$	Carlo Erba
Ammonium chloride	NH_4Cl	Carlo Erba
Sodium hypophosphite	NaH_2PO_2	Carlo Erba
Sodium hydroxide	NaOH	Carlo Erba
Palladium chloride	$PdCl_2$	Aldrich
Stannous chloride	$SnCl_2$	Fluka
Ammonia hydroxide 28%	NH_4OH	Aldrich
Hydrochloric acid 37%	HCl	Carlo Erba

4.2 Catalyst preparation

4.2.1 Pretreatment of polyurethane foam support

In this work, a polyurethane foam was used as the support for preparation of supported Ni-Zn-P, Pd catalysts. The surface PU foam (0.06 g) was pretreated by dipping in 30% sodium hydroxide (NaOH) at 60^{o}C for 10 min. and washed with distilled water at room temperature. Then, it was dipped into 1g/l palladium chloride ($PdCl_2$), 50g/l stannous chloride ($SnCl_2$) and 1 mol/L hydrochloric acid solution at room temperature for 10 min. The PU foams were repeatedly washed with distilled water and dried with a blower.

4.2.2 Preparation of Ni-Zn-P/PU foam catalysts

The Ni-Zn-P composites were prepared from the electroless bath of the following compositions: 42 g/l nickel sulfate ($NiSO_4 \cdot 6H_2O$), 102 g/l sodium citrate ($C_6H_8O_7Na_3\ 2H_2O$), 60g/l ammonium chloride (NH_4Cl), 24 g/l sodium hypophosphite (NaH_2PO_2), thiourea 0.01% with the amounts of zinc sulfate ($ZnSO_4 \cdot 7H_2O$) varying from 6, 12, 18, 24 g/l in bath and then added into 250 ml distilled water. These experiments were performed at temperature of 85± 2^{o}C. The pH in bath was adjusted to 8-11 using sodium hydroxide (NaOH). The deposition conditions are summarized in Table 4.2. and polyurethane foam which was pretreated was dipped in the electroless solution for 30-120 min.

4.2.3 Preparation of Ni-Zn-P/γ-Al_2O_3 catalysts

The pretreatment and activation step of γ-Al_2O_3 powder and pellet support are similar to PU foam. First, γ-Al_2O_3 powder and pellet was pretreated by putting in 30% sodium hydroxide (NaOH) at 60^{o}C for 10 min. Then the sample was washed with distilled water at room temperature. Then, it was put into 1g/l palladium chloride ($PdCl_2$), 50g/l stannous chloride ($SnCl_2$) and 1 mol/L hydrochloric acid solution at room temperature for 10 min. After that repeatedly washed with distilled water and then dried at 110 ^{o}C for 24 hr.

The solution of Ni-Zn-P on γ-Al_2O_3 powder and pellet support are also same as Ni-Zn-P/PU foam in Table 4.2 with the amounts of zinc sulfate ($ZnSO_4 \cdot 7H_2O$)18 g/l. Support γ-Al_2O_3 powder and pellet was put in the electroless solution for 1 and 60 min respectively . The catalyst was cleaned with distilled water and then dried at 110 ^oC for 24 hr.

Table 4.2 Experimental conditions for electroless deposition

Composition of electrolyte	
$NiSO_4 \cdot 6H_2O$ (g/l)	42
$ZnSO_4 \cdot 7H_2O$ (g/l)	6, 12, 18, 24
$C_6H_8O_7Na_3$ $2H_2O$ (g/l)	102
NH_4Cl (g/l)	60
NaH_2PO_2 (g/l)	24
Thiourea 0.01% (ml/l)	4.8
Operating conditions	
pH	8-11
Temperature (^oC)	85
Time (min)	30-120

4.2.4 Preparation of Pd/PU foam catalysts

The Pd composites were prepared from the electroless bath of the following compositions: palladium chloride ($PdCl_2$) 0.009 and 2 g/l, Hydrochloric acid 37% (HCl) 4 ml/l, Ammonium hydroxide (NH_4OH) 27 g/l then added into 100 ml distilled water. After that sodium hypophosphite (NaH_2PO_2) 10 g/l was added**.** These

experiments were performed at temperature of at 60 ^{o}C for 20 and 60 min, respectively with ultrasonic vibration.

4.3 Reaction study

The catalytic performance for the selective hydrogenation of acetylene was measured at different temperatures. Materials, apparatus and operating procedures are detailed as below:

4.3.1 Materials

Feed composition of the selective acetylene hydrogenation reaction was composed of 1.5%C_2H_2, 1.7%H_2, and balanced C_2H_4. Ultra high purity hydrogen was used for reduction and pretreatment processes and ultra high purity argon was used for cooling down the processes. All of the gases were supplied by Thai Industrial Gas Limited (TIG).

4.3.2 Apparatus

Selective acetylene hydrogenation was performed in a pyrex tubular reactor, an electrical furnace and an automation temperature controller. The instruments used in this system are shown as follows:

4.3.2.1 Reactor

The reaction was performed in a conventional pyrex tubular reactor (inside diameter = 10.1 mm), at atmospheric pressure.

4.3.2.2 Automation temperature controller

This unit consisted of a magnetic switch connected to a variable transformer and a thermal overload relay (HITACHI, TR1 2B-1E, AC 600 V) linked to a

temperature controller (Shinks, ECS, 220-R/E) in which connected to a thermocouple attached to the catalyst bed in a reactor. A dial setting established a set point at any temperature within the range between 0 and 999°C. The accuracy was of ±2°C.

4.3.2.3 Electrical furnace

The furnace supplied the required temperature to the reactor which could be operated from room temperature up to 500°C at maximum voltage of 220 volts.

4.3.2.4 Gas controlling system

Reactant, hydrogen and carrier gas for the system was each equipped with a pressure regulator and on-off valve and the gas flow rates were adjusted by using mass flow controller (AALBORG, GFC).

4.2.2.5 Gas chromatograph

The products and feeds were analyzed by a gas chromatograph equipped with a FID detector (SHIMADZU FID GC 8APF, carbosieve column S-II) for separating CH_4, C_2H_2, C_2H_4 and C_2H_6. H_2 was analyzed by a gas chromatograph equipped with a TCD detector (SHIMADZU TCD GC 8APT, molecular sieve 5A). The operating conditions for each instrument are summarized in Table 4.3.

Table 4.3 Operating conditions of gas chromatographs.

Gas chromatograph	SHIMADZU GC-8APF	SHIMADZU GC-8APT
Detector	FID	TCD
Packed column	Carbosieve column S-II	Molecular sieve 5 A
Carrier gas	Ultrahigh purity N_2	Ultrahigh purity Ar
Carrier gas flow rate (ml/min)	40-60	40-60
Injector temperature (°C)	180	80
Initial column temperature (°C)	100	50
Programmed rate (°C/min)	10	-
Final column temperature (°C)	160	50
Current (mA)	-	70
Analyzed gas	CH_4, C_2H_2, C_2H_4, C_2H_6	H_2

4.3.3 Procedures

The catalytic activity was evaluated in the gas-phase selective hydrogenation of acetylene. The catalyst was packed in a pyrex tube reactor (i.d. 10.1 mm) by setting up catalyst bed length was about 1.3 mm. The reactor was placed into the furnace. Prior to start of each experimental run, the reactor was purge with argon in order to remove remaining air. After that the catalyst was pretreated *in situ* in hydrogen flow by heating from room temperature to 90^{o}C for 1 h. with a heating rate of 10^{o}C/min. Then the reactor was purged with argon and cooled down to the reaction temperature 50°C

The reaction was carried out using a feed composition of 1.5%C_2H_2, 1.7%H_2, and balanced C_2H_4. In addition to various temperatures such as 50, 60, 70 and 80°C, 1 atm, and flow rate of 10 ml/min were used to test the catalytic performance. The sampling was taken when the steady state of the system was reached, which was approximately within 1 h. The products and feeds were analyzed by a two gas chromatographs equipped with a FID detector (SHIMADZU FID GC 9A, carbosieve

column S-2) and TCD detector (SHIMADZU TCD GC 8A, molecular sieve-5A). System of selective acetylene hydrogenation is shown in Figure 4.1

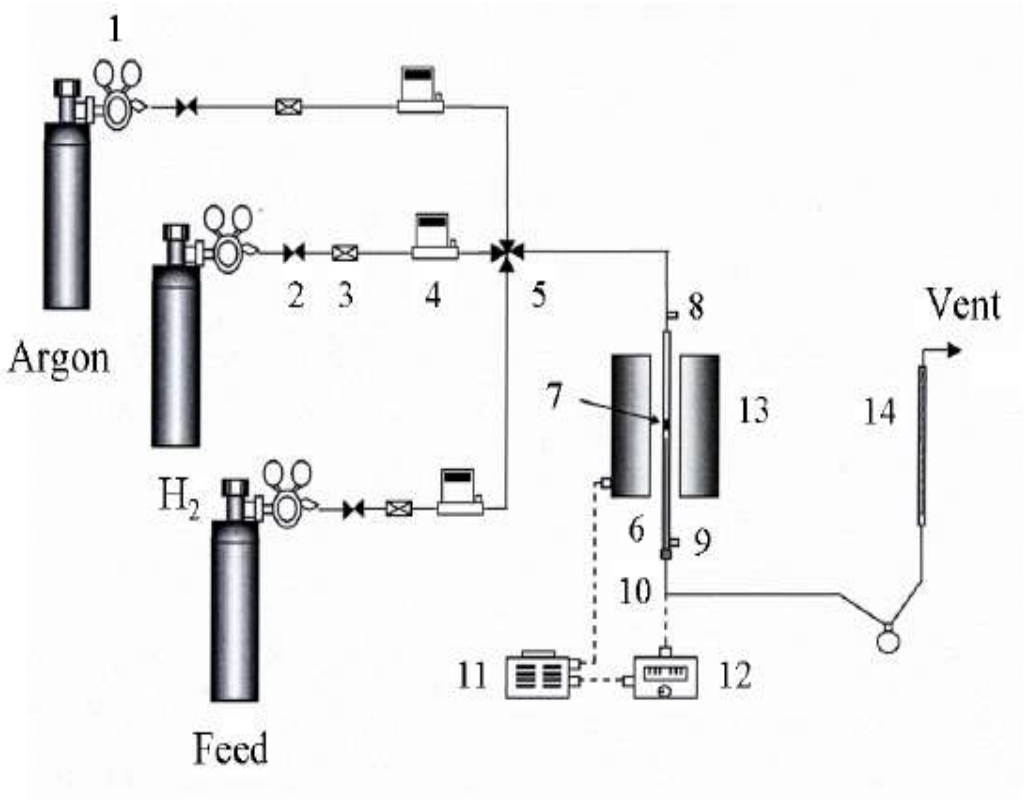

1. Pressure regulator
2. On-off valve
3. Filter
4. Mass flow controller
5. 4-ways fitting
6. Reactor
7. Catalyst bed
8. Sampling point (feed)
9. Sampling point (product)
10. Thermocouple
11. Variable voltage transformer
12. Temperature controller
13. Electric furnace
14. Bubble flow meter

Figure 4.1 Flow diagram of the selective hydrogenation of acetylene.

4.4 Catalyst characterization

Various characterization techniques were used in this work in order to clarify the catalyst structure, the morphology as well as the surface composition. The effect of $ZnSO_4$ on the behavior catalysts was characterized by using the following techniques.

4.4.1 X-ray diffraction (XRD) analysis

X-ray diffraction data provides information on the structures of crystalline solids to determine the bulk phase of catalyst. XRD patterns were carried out using *ex situ* employing an X-ray diffractometer, SIEMENS XRD D5000. X-ray diffractometer connected to a personal computer with diffract AT version 3.3 program for fully control of the XRD analyzer at Center of Excellence on Catalysis and Catalytic Reaction Engineering, Chulalongkorn University. The observations will be proceeded by using Cu Kα radiation with a Ni filter in the 2θ range of 20-80 degrees resolution 0.04°.

4.4.2 X-ray photoelectron spectroscopy (XPS) analysis

X-ray photoelectron spectroscopy (XPS) is a quantitative spectroscopic technique that measures the elemental composition. The XPS analysis was performed using an AMICUS photoelectron spectrometer equipped with an Mg K〈 X-ray as primary excitation and KRATOS VISION2 software. XPS elemental spectra were acquired with 0.1 eV energy step at a pass energy of 75 kV. The C 1s line was taken as an internal standard at 285.0 eV.

The presence of peaks at particular energies therefore indicates the presence of a specific element in the sample under study - furthermore, the intensity of the peaks is related to the concentration of the element within the sampled region.

4.4.3 Scanning electron microscopy (SEM) and energy dispersive X-ray spectroscopy (EDX)

SEM was used to observe the morphology of Ni-Zn-P catalyst and the dispersion on polyurethane foam. The sample must be conductive to prevent charging by coating with gold particle by ion sputtering device. Sample was analyzed by JEOL JSM-6400 scanning electron microscopy. Energy dispersive X-ray spectroscopy is an analytical technique used for the elemental analysis or chemical characterization of a sample which was analyzed by Link ISIS Series 300 program at Scientific and Technological Research Equipment Center (STREC), Chulalongkorn University.

4.4.4 Inductively Coupled Plasma-Optical Emission Spectroscopy (ICP-OES)

The percentage of metal loading of each catalyst prepared in this study was analyzed by inductively-coupled plasma optical emission spectroscopy (ICP-OES). The amount of Ni-Zn-P on the surface of polyurethane foam was measured with an inductively coupled plasma atomic emission spectrometer (ICP-AES) Perkin Elmer 20 model PLASMA-1000. About 0.005 g (weight to an exact amount) of catalyst was dissolved in 7 ml hydrofluoric acid 49% and 2 ml hydrochloric acid 37%, stir until all solid are solution then make volume up to 100 ml using de-ionized water by the volumetric flask which has the volume of 100 ml.

4.4.5 Surface area measurement

The specific surface area was determined by nitrogen adsorption method. The single point specific surface area of the catalysts was measured by Micromeritics ChemiSorb 2750 using nitrogen as the adsorbate with the sample weight 0.1 g and degas at 95^{o}C for as-synthesized sample.

CHAPTER V

RESULTS AND DISCUSSION

This chapter presents the results and discussion of Ni-Zn-P catalysts supported on polyurethane (PU) foam prepared by electroless deposition method with different amounts of Zn for the selective hydrogenation of acetylene in excess ethylene. The catalytic properties of Ni-Zn-P on PU foam were compared with Ni-Zn-P/γAl_2O_3 pellet, Ni-Zn-P/γ-Al_2O_3 powder, 0.82%Pd/PU foam, 1.37%Pd/PU foam, and Pd-Ag/γ-Al_2O_3 pellet (commercial). The results of various characterization techniques for describing the catalyst properties are also presented.

5.1 Characterization

5.1.1 The elemental compositions of the catalysts

The elemental compositions (Ni, Zn, and P) of the catalysts were analyzed by the inductively-coupled plasma optical emission spectroscopy (ICP-OES). The results are shown in Table 5.1.

Table 5.1 The elemental compositions of the Ni-Zn-P supported on PU foam catalysts prepared with different amounts of Zn in bath

Catalyst	Ni (%wt)	Zn (%wt)	P(%wt)
Ni-Zn-P/PU foam (Zn 6 g/l)	40.1	7.3	1.2
Ni-Zn-P/PU foam (Zn 12g/l)	36.0	18.2	1.3
Ni-Zn-P/PU foam (Zn 18g/l)	33.7	20.0	0.8
Ni-Zn-P/PU foam (Zn 24g/l)	31.5	17.7	0.9

The Ni-Zn-P catalysts were prepared from the electroless bath that contained 42 g/l nickel sulfate ($NiSO_4 \cdot 6H_2O$), 24 g/l sodium hypophosphite (NaH_2PO_2), and various amounts of zinc sulfate ($ZnSO_4 \cdot 7H_2O$) varying from 6, 12, 18, 24 g/l in bath. The results in Table 5.1 showed that the actual amounts of Ni, Zn, and P presented in the samples were lower than the initial amounts in bath. This is because some of the metals were remained dissolved in the electroless bath and were not deposited on the polyurethane foam. The Ni actual content in the catalysts significantly decreased from 40.1 to 31.5 wt% with increasing amount of Zn in bath from 6 to 24 g/l. The amount of Zn, however, increased from 7.3 to 20.0 wt% with increasing amount of Zn from 6 to 18 g/l. Further increase of the amount of Zn from 18 g/l to 24 g/l showed an opposite trend in which wt% of the Zn actual content was decreased to 17.7 wt%. The amounts of P in the catalysts were not significantly changed with increasing amounts of Zn in bath.

The elemental compositions of the Ni-Zn-P catalysts supported on γ-Al_2O_3 were also determined by the ICP-OES and the results are shown in Table 5.2. The catalysts were prepared by electroless deposition method using the same conditions as those supported on PU foam with the amount of Zn in bath 18 g/l. From Table 5.2, it is clearly shown that the shape of the supports strongly affected the amounts of metal deposition on the catalysts. The Ni-Zn-P/γ-Al_2O_3 powder contained significantly higher amount of Ni actual content than the pellet γ-Al_2O_3. The amount of Ni in the Ni-Zn-P/γ-Al_2O_3 powder was also slightly higher than the Ni-Zn-P/PU foam prepared with similar amount of Zn in bath.-. The amounts of Zn, however, were lower than those on the PU foam for both Ni-Zn-P/γ-Al_2O_3 powder and Ni-Zn-P/γ-Al_2O_3 pellet.

Table 5.2 The elemental compositions of the Ni-Zn-P catalysts supported on γ-Al_2O_3

Catalyst	Ni (%wt)	Zn (%wt)	P (%wt)
Ni-Zn-P/γ-Al_2O_3 powder	39.6	11.2	2.97
Ni-Zn-P/γ-Al_2O_3 pellet	13.4	15.0	1.016

For comparison, the Pd catalysts supported on PU foam were also prepared by electroless deposition method with different amounts of Pd 0.2 and 0.0009 g in bath. The actual amounts of Pd were determined by the ICP-OES and the results are shown in Table 5.3. Increasing amount of Pd in bath from 0.0009 to 0.2 g resulted in a slight increase of the amount of Pd deposited on the PU foam. It is suggested that the characteristics of metal deposition are limited by the electroless deposition method.

Table 5.3 The actual amount of Pd contained in the Pd catalysts supported on PU foam

Catalyst	Pd in electroless bath (g)	Pd (%wt)	
		Intended	Actual
Pd/PU-1	0.2	68.00	1.37
Pd/PU-2	0.0009	1.00	0.82

5.1.2 Deposition rate of Ni-Zn-P on PU foam

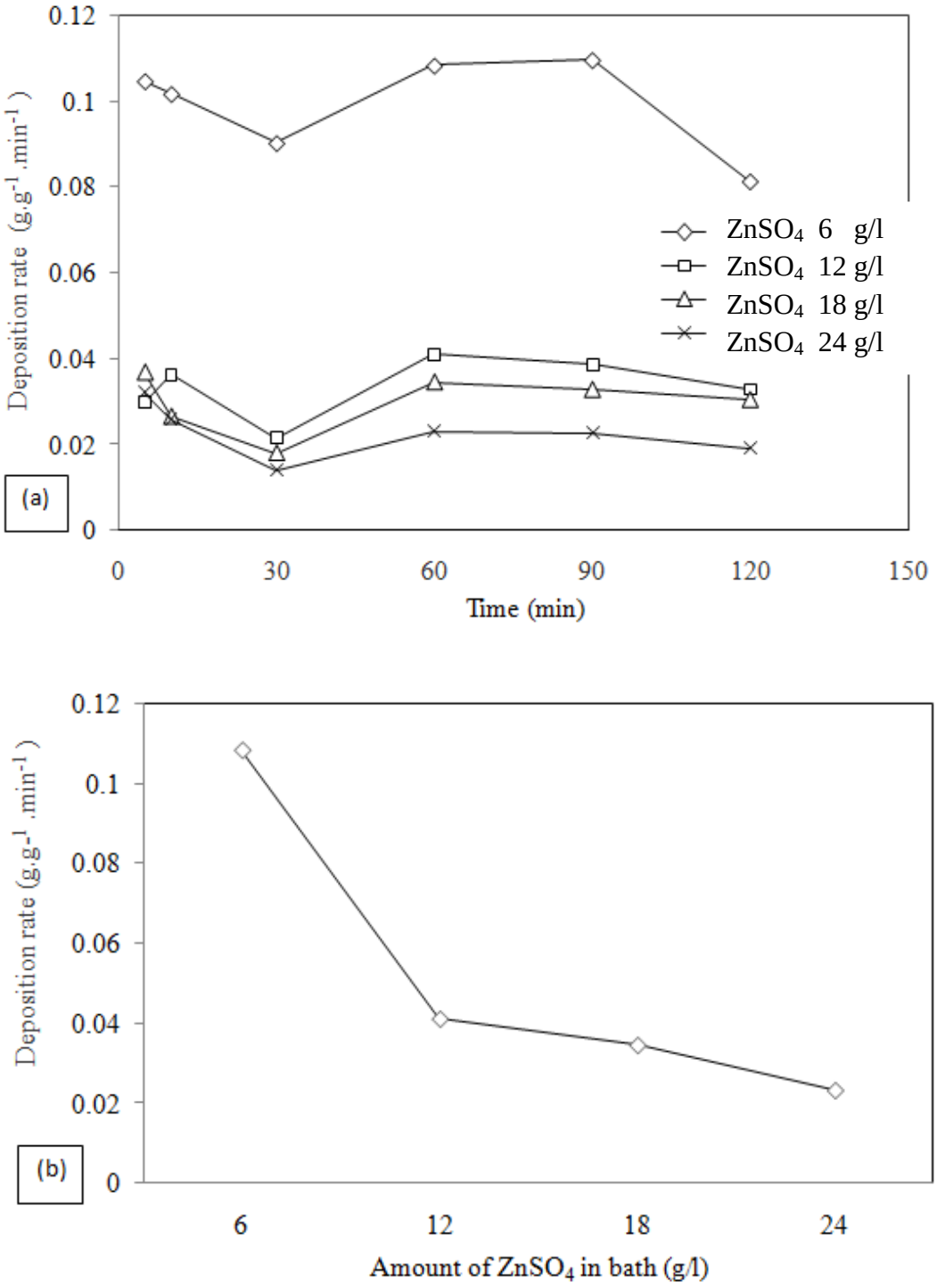

Figure 5.1 Deposition rate in electroless bath of Ni-Zn-P catalysts (a) Comparison of different amounts of $ZnSO_4$ as a function of deposition time. (b) With various amounts of $ZnSO_4$ in bath at deposition time 1 hr.

Deposition rate is defined as the amount of metal deposited of unit mass foam substrate per unit of time. The deposition rate of Ni-Zn-P catalysts on PU foam prepared with different amounts of $ZnSO_4$ as a function of deposition time is presented in Figure 5.1(a). The results indicated that in the first period, the rate of deposition decreased respectively with increasing time up to 30 min. After that, the deposition rateincreased and reached a plateau at amount 60 min. During the 60-120 min desposition time, the deposition rate of the samples containing $ZnSO_4$ in bath from 12 g/l to 24 g/l remained nearly constant. There was a significant drop of the deposition rate after 120 min for the sample containing the lowest amount of $ZnSO_4$ in bath (6 g/l). It was observed that during the initial deposition of the Ni-P-Zn catalyst with Zn 6 g/l in bath, the reaction occurred violently as seen from lots of bubbles in the electroless bath. This may cause the electroless solution to be deteriorated rapidly when the deposition time reached 90 min. The effect of $ZnSO_4$ content on the deposition rate of Ni-Zn-P catalysts on PU foam is shown in Figure 5.1(b). It can be seen that the deposition rate decreased obviously with increasing amount of $ZnSO_4$ in electroless bath. In this study, when the content of $ZnSO_4$ is 6 g/l the deposition rate is fastest with a maximum rate ca. 0.1 $g.g^{-1}\cdot min^{-1}$. When the content of $ZnSO_4$ 12 g/l the deposition rate rapidly decreased to ca. 0.04 $g.g^{-1}\cdot min^{-1}$.The addition of $ZnSO_4$ with concentration 18 and 24 g/l show the deposition rate of 0.03 and 0.01 $g.g^{-1}\cdot min^{-1}$., respectively. In other words, the presence of zinc retarded the overall deposition rate of the metals during the electroless deposition of Ni-Zn-P alloys. Much higher deposition rate was obtained when relatively low amounts of $ZnSO_4$ were employed in order of $ZnSO_4$ 6 g/l > 12 g/l > 18g/l > 24 g/l. Because the mixed potential became more positive and the plating current density decreased with increasing of the $ZnSO_4$ concentration in the electroless bath. The results in this study followed a well established trend in the literature about the effect of zinc ions on the Ni–Zn–P deposition process [78-79]. B.Veeraraghavan *et.al* (2004) [74] reported that Zn^{2+} ions acted as an inhibitor for the electroless depositionof Ni-Zn-P alloy.

The effect of different sizes of the polyurethane foam on the rate of metal deposition of the Ni-Zn-P catalysts was also investigated and the results are shown in Figure 5.2. It was found that the deposition rate of metal on PU foam17.2 ppi was higher than on the PU foam size 10.5 ppi. The deposition rate of the Ni-Zn-P

on PU foam with the smallest pore size 24.1 ppi was lowest. There may be some limitation of the metals depositing in the middle position of the polyurethane foam.

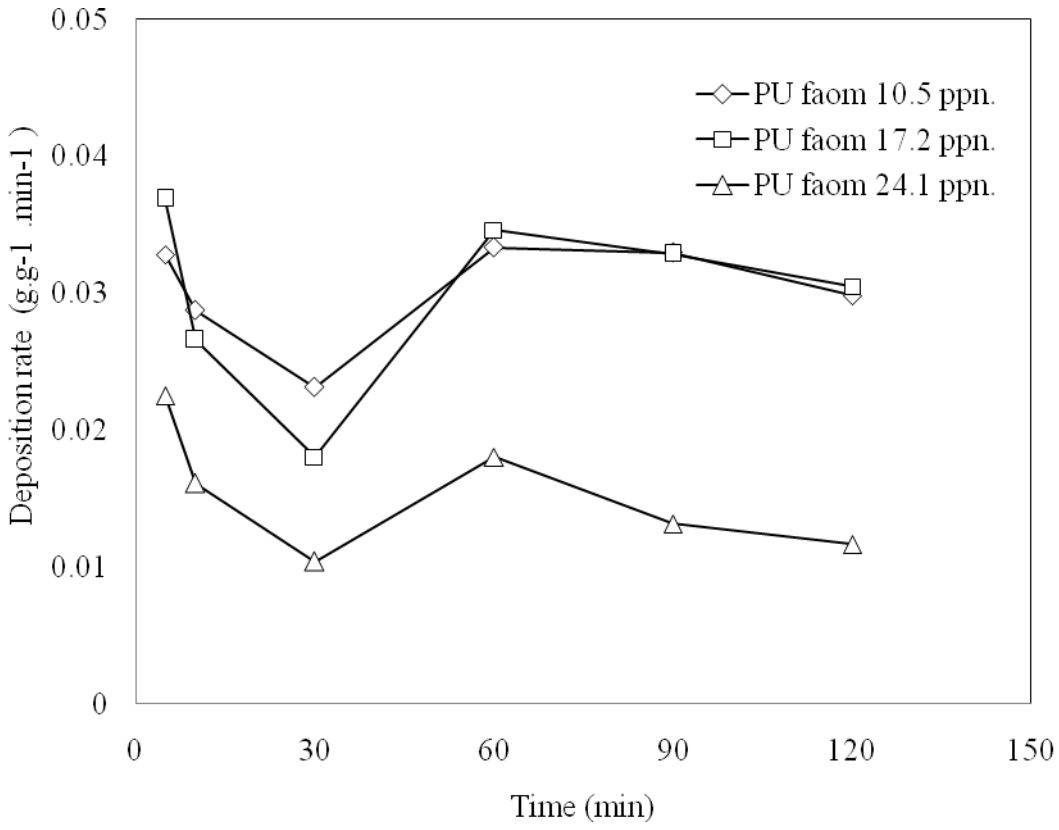

Figure 5.2 Deposition rate in electroless bath of Ni-Zn-P catalysts with amount of $ZnSO_4$ in bath 18 g/l with different size of 10.5, 17.2, 24.1 ppi PU foam as a function of deposition time.

*ppi = pore per inch

5.1.3 Surface area of the catalysts

Specific surface area of the catalyst was determined by nitrogen adsorption method. The BET (Brunauer Emmett Teller) isotherm was employed for calculation of the surface area. The BET surface areas of the catalysts are listed in Table 5.4. The results show that specific surface area of PU foam was very low, indicating that they were non-porous materials.. The γ-Al_2O_3 powder and γ-Al_2O_3 pellet had the BET surface areas of 41.9 and 123.1 m^2/g, respectively. After electroless deposition of Ni-Zn-P, the surface area decreased suggesting that some of the metals were located inside the pores of the γ- Al_2O_3 [43].

Table 5.4 Specific surface areas of the catalysts.

Catalyst	Specific surface area (m^2/g)
PU foam	0.003
Ni-Zn-P/PU foam (Zn 6 g/l)	0.005
Ni-Zn-P/PU foam (Zn 12 g/l)	0.004
Ni-Zn-P/PU foam (Zn 18 g/l)	0.008
Ni-Zn-P/PU foam (Zn 24 g/l)	0.007
γ-Al_2O_3 powder	41.9
Ni-Zn-P/γ-Al_2O_3 powder	22.5
γ-Al_2O_3 pellet	123.1
Ni-Zn-P/γ-Al_2O_3 pellet	100.6

5.1.4 Scanning electron microscopy (SEM) and energy dispersive X-ray spectroscopy (EDX)

Scanning electron microscopy (SEM) is a tool for observing the morphology and metal dispersion. The SEM micrographs of Ni-Zn-P catalysts prepared by electroless deposition with amount of $ZnSO_4$ in bath 18 g/l supported on different PU foam sizes 10.5 ppi, 17.2 ppi and 24.1 ppi are shown in Figure 5.3, 5.4 and 5.5, respectively. From the SEM results, there were no significant differences in the morphology of the Ni-Zn-P prepared on different PU foam sizes.

The three dimensional network of the PU foam microstructure was not much altered after electroless deposition of the metals. Some cracks were observed on all the PU foam samples due to the treatment with 30% NaOH. It is clearly seen that increasing the amount of $ZnSO_4$ concentration in the electroless bath decreased the amount of the metals deposited on the PU foams. The Ni-Zn-P with amount of Zn 18 g/l showed the good dispersion on support. However, smaller nodular structure appeared on the surface of the samples with higher amount of zinc [74,78,79].

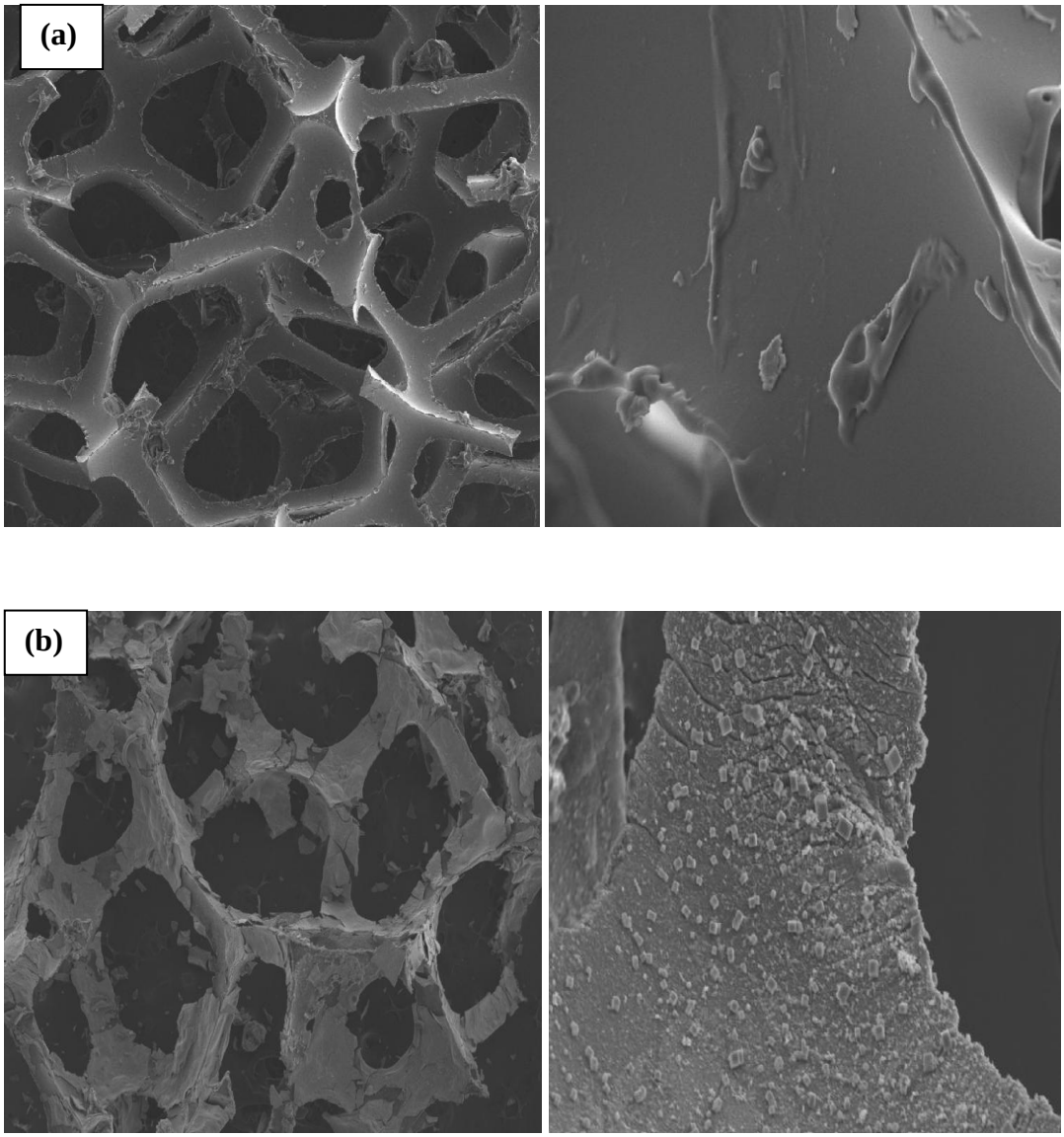

Figure 5.3 SEM micrographs of Ni-Zn-P catalysts prepared by electroless deposition with amount of $ZnSO_4$ in bath 18 g/l supported on PU foam size 10.5 ppi (×15 (left) and × 400 (right))

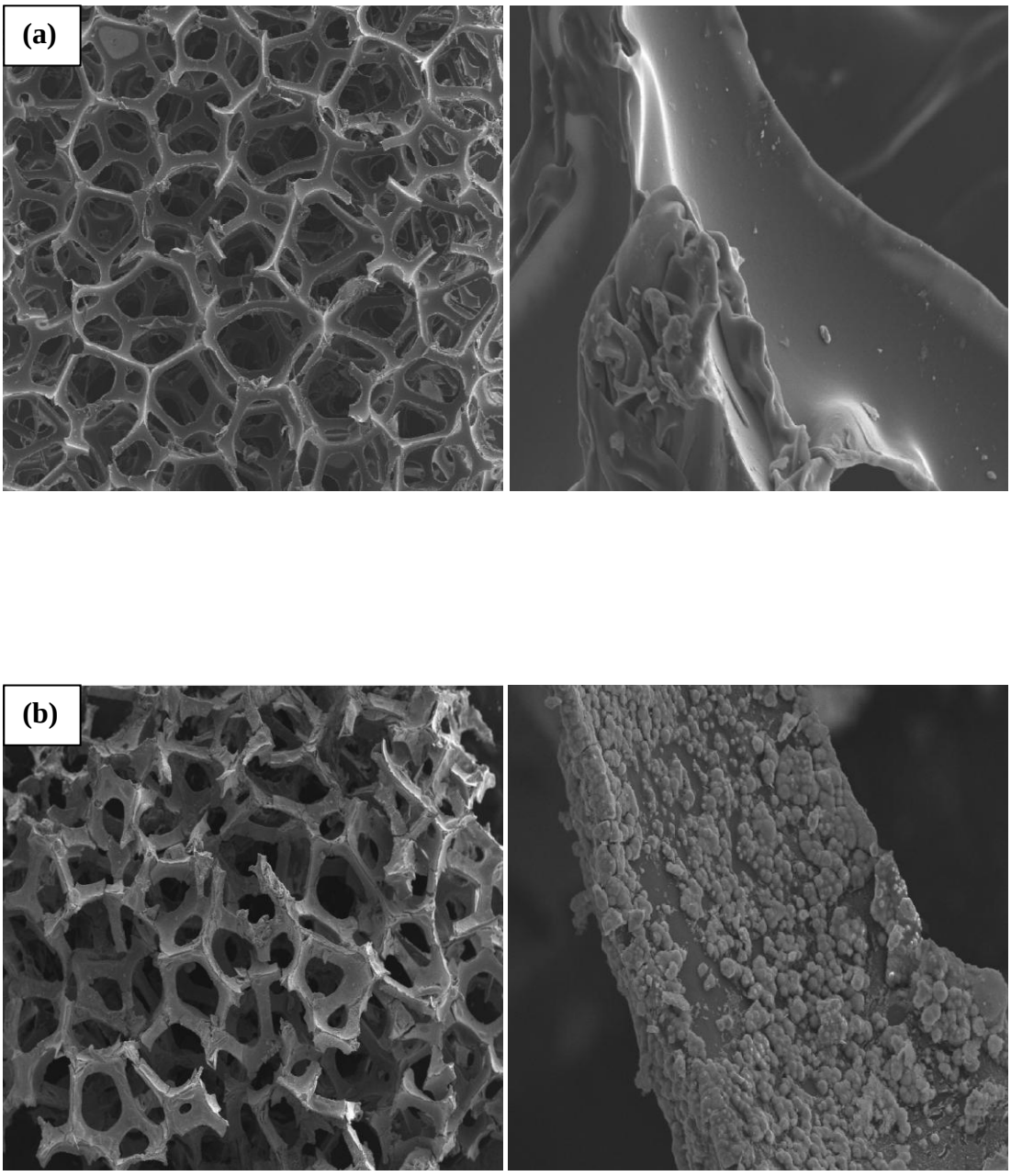

Figure 5.4 SEM micrographs of Ni-Zn-P catalysts prepared by electroless deposition with amount of $ZnSO_4$ in bath 18 g/l supported on PU foam size 24.1 ppi (×15 (left) and × 400 (right))

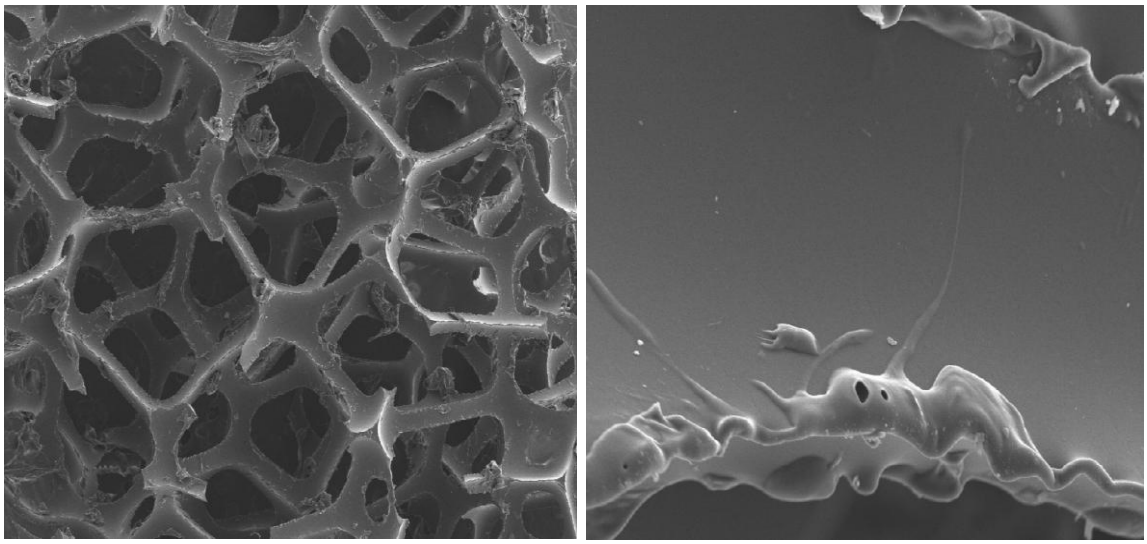

(a) PU foam before supported

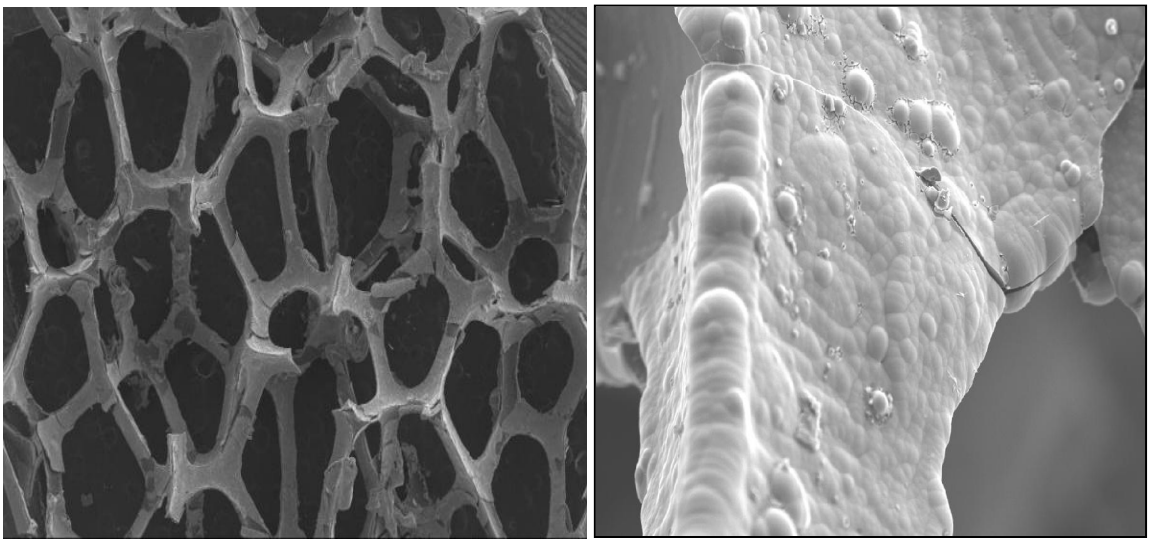

(b) Ni-Zn-P/PU foam ($ZnSO_4$ 6 g/l)

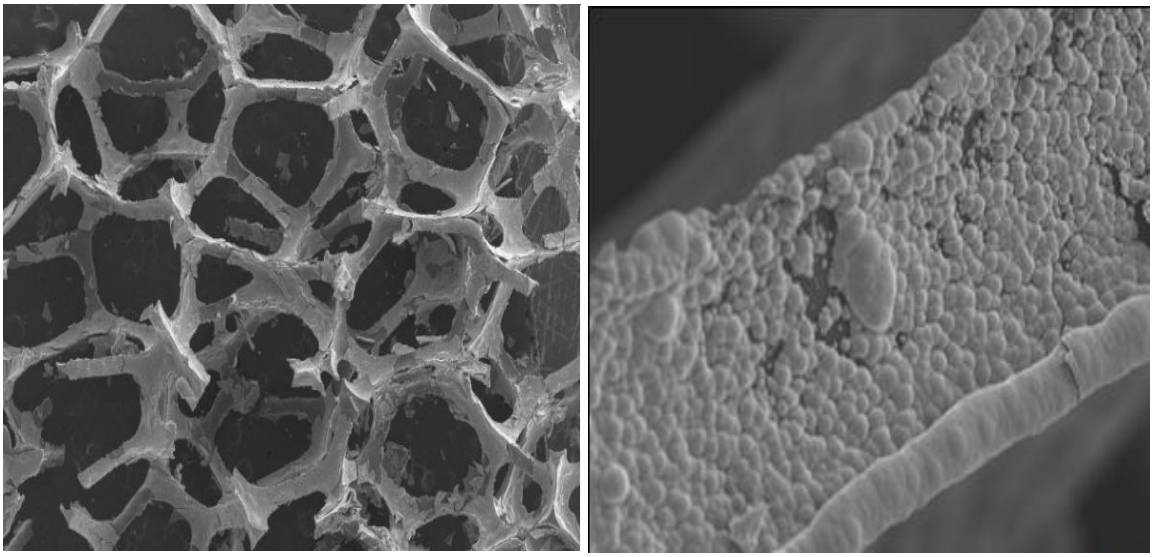

(c) Ni-Zn-P/PU foam ($ZnSO_4$ 12 g/l)

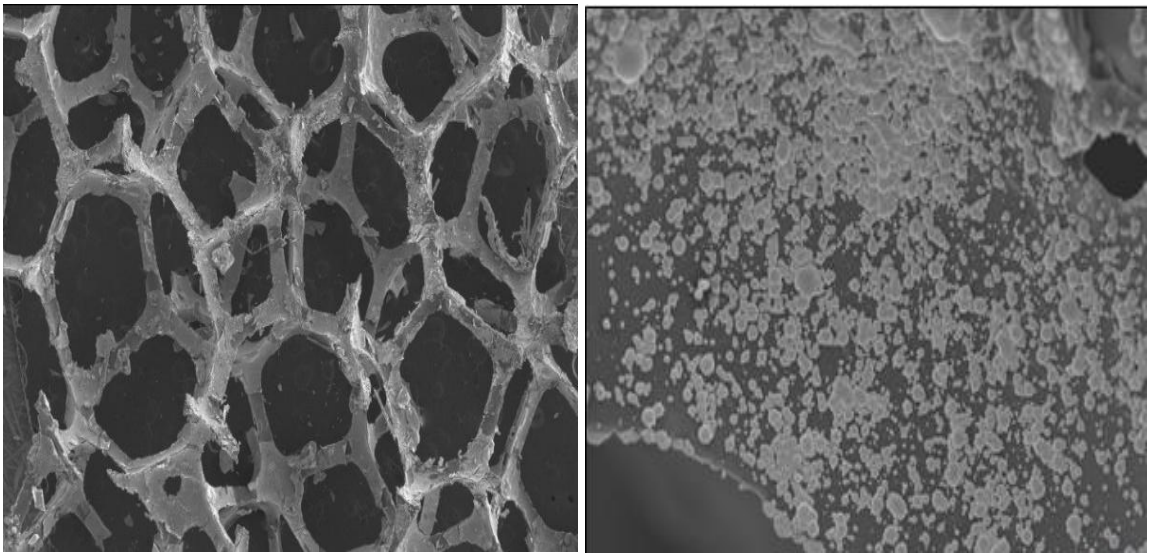

(d) Ni-Zn-P/PU foam ($ZnSO_4$ 18 g/l)

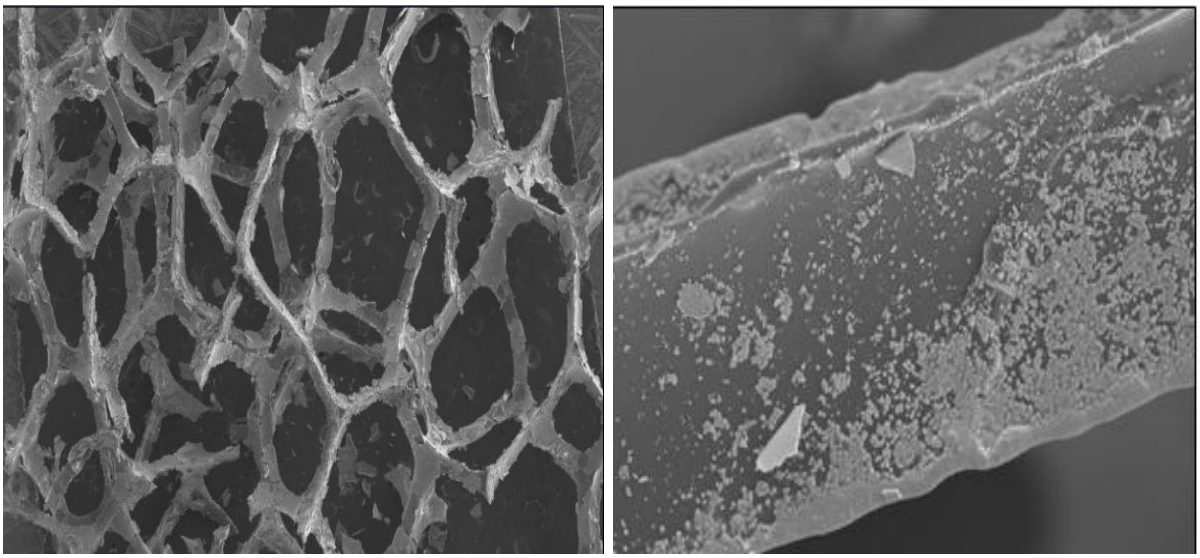

(e) Ni-Zn-P/PU foam ($ZnSO_4$ 24 g/l)

Figure 5.5 SEM micrographs of Ni-Zn-P catalysts prepared by electroless deposition method with different amounts of $ZnSO_4$ in bath: (a) before supported (b) 6 g/l (c) 12 g/l (d) 18 g/l (e) 24 g/l (×15 (left) and × 400 (right))

The Energy-dispersive X-ray spectroscopy (EDX) is an analytical technique used for the elemental analysis or chemical characterization of a sample. The EDX spectra of PU foam after electroless deposition of Ni-Zn-P catalysts with various amounts of zinc in bath are shown in Figure 5.6 and the EDX results are shown in Figure 5.7. The wt% of Ni on the Ni-Zn-P catalysts decreased from ca. 78% to ca. 65% with increasing amount of Zn in bath from 6 g/l to 18 g/l and wt% of Zn increased with increasing amount of Zn with a maximum ca. 21 %. Further increase Zn amount to 18 g/l and 24 g/l showed an opposite trend in which wt% of Ni increased to ca. 69% and Zn decreased to ca. 18%. The amount of P was ranging between 5.03 - 7.22 wt% and was not significantly changed with increasing amount of Zn in bath. Increasing the Zn ion concentration in the bath, the surface coverage of Ni ions decreased while the Zn ion surface coverage increased. Thus, it can be expected

that the Ni content in the deposit would decrease as a function of $ZnSO_4$ concentration in the bath [74,78,79].

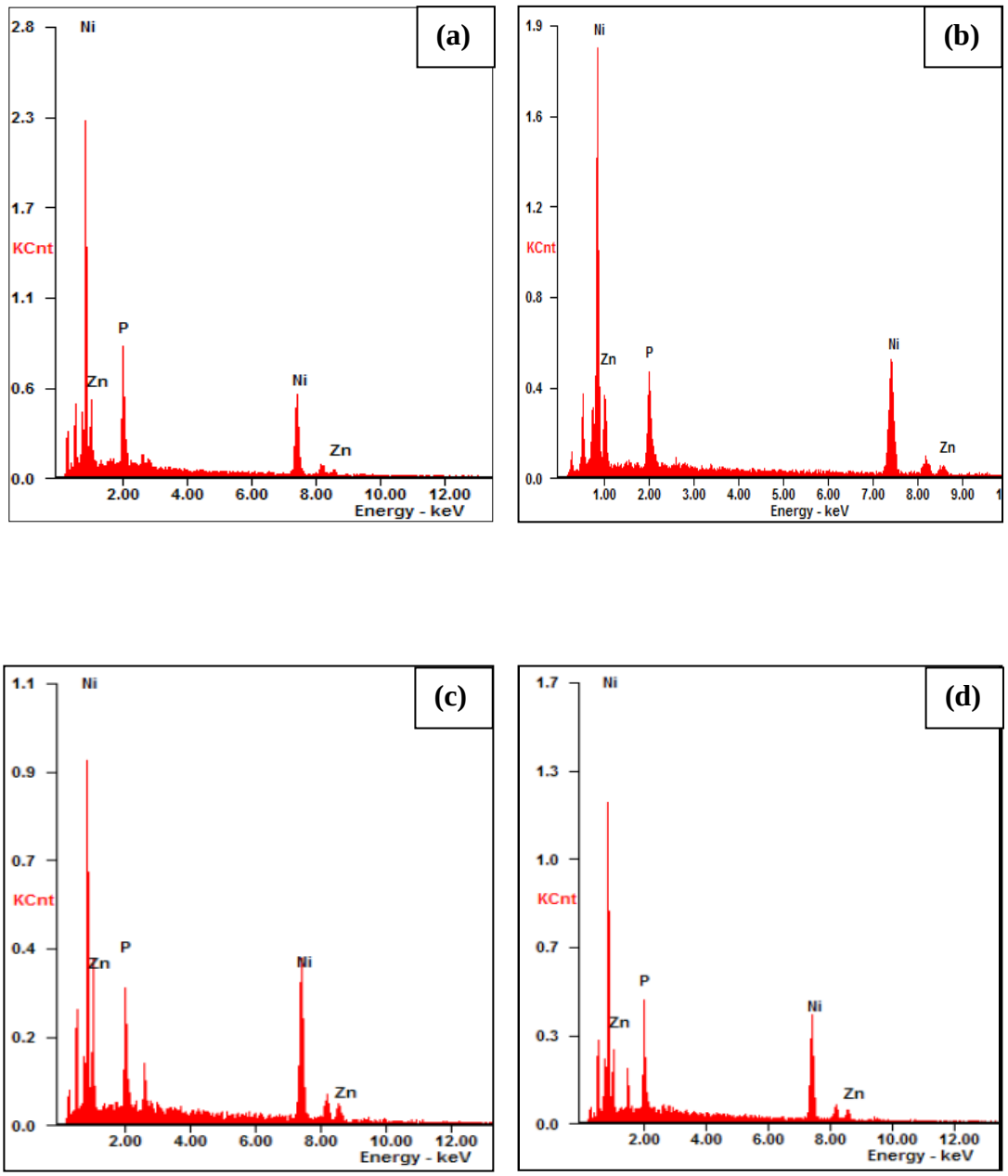

Figure 5.6 EDX spectra of Ni-Zn-P catalysts prepared by electroless deposition method with various amounts of $ZnSO_4$ in bath (a) 6 g/l (b) 12 g/l (c) 18 g/l (d) 24 g/l

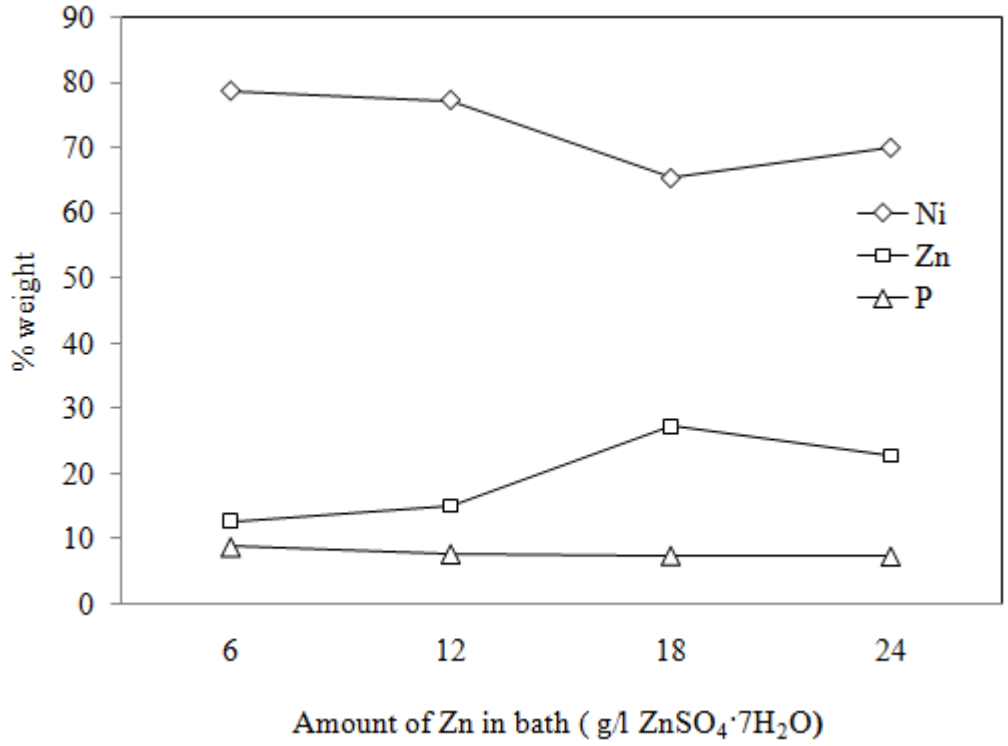

Figure 5.7 EDX results of PU foam after electroless deposition of the Ni-Zn-P sample with various amounts of $ZnSO_4$ in bath.

The amounts of Ni-Zn-P on PU foam were measured by EDX technique at different positions of foam and the results are shown in Figure 5.8 (a)-(d). The results revealed that the metals were less deposited at the middle than the edge for all the samples.

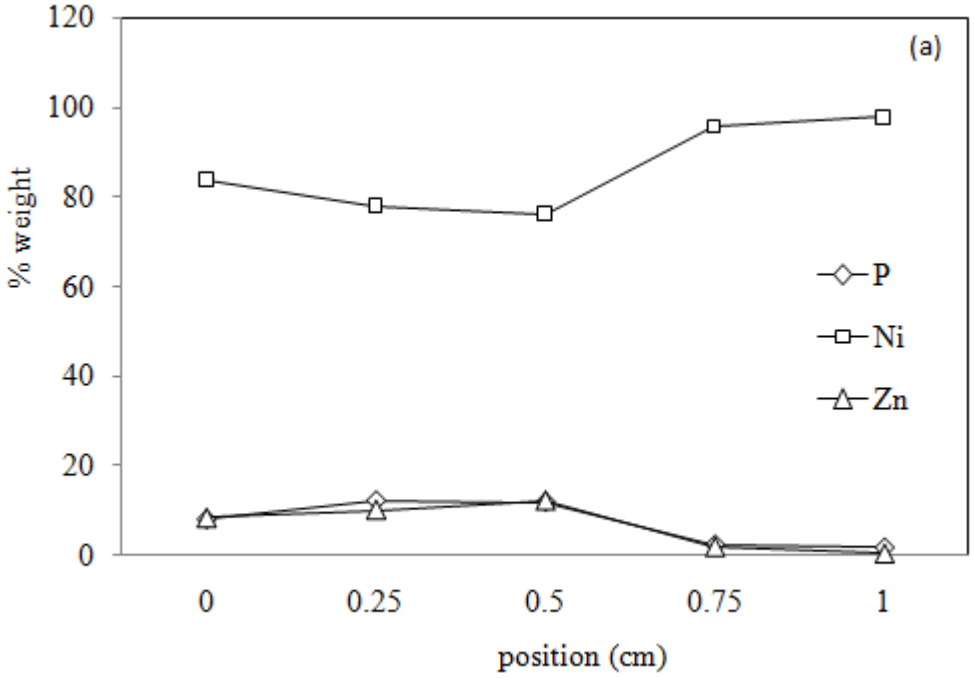
(a)
120
100
80
60
40
20
0
% weight
P
Ni
Zn
0
0.25
0.5
0.75
1
position (cm)

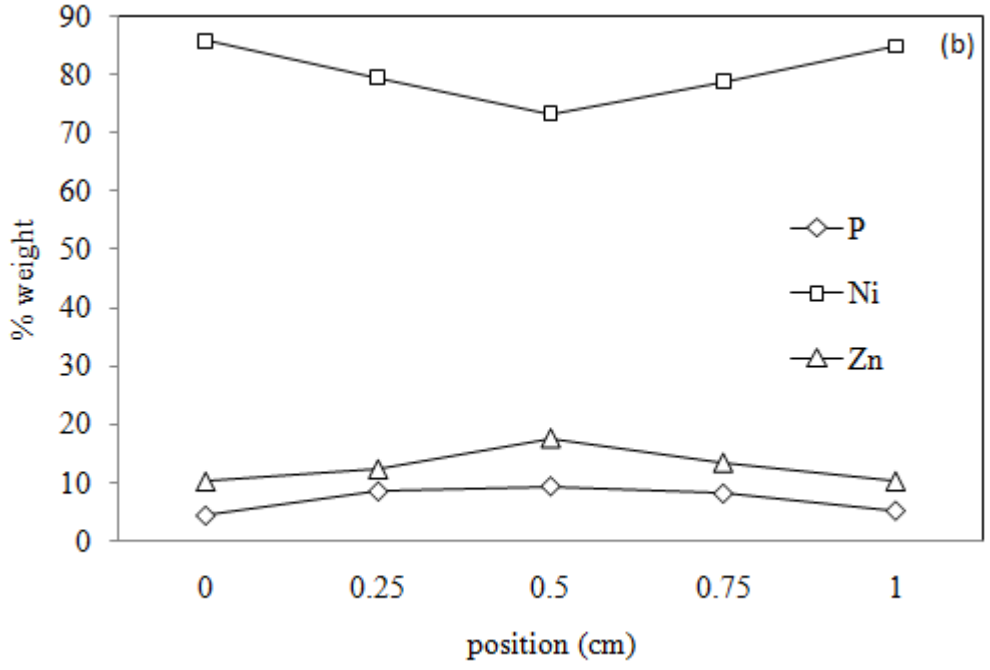
(b)
90
80
70
60
50
40
30
20
10
0
% weight
P
Ni
Zn
0
0.25
0.5
0.75
1
position (cm)

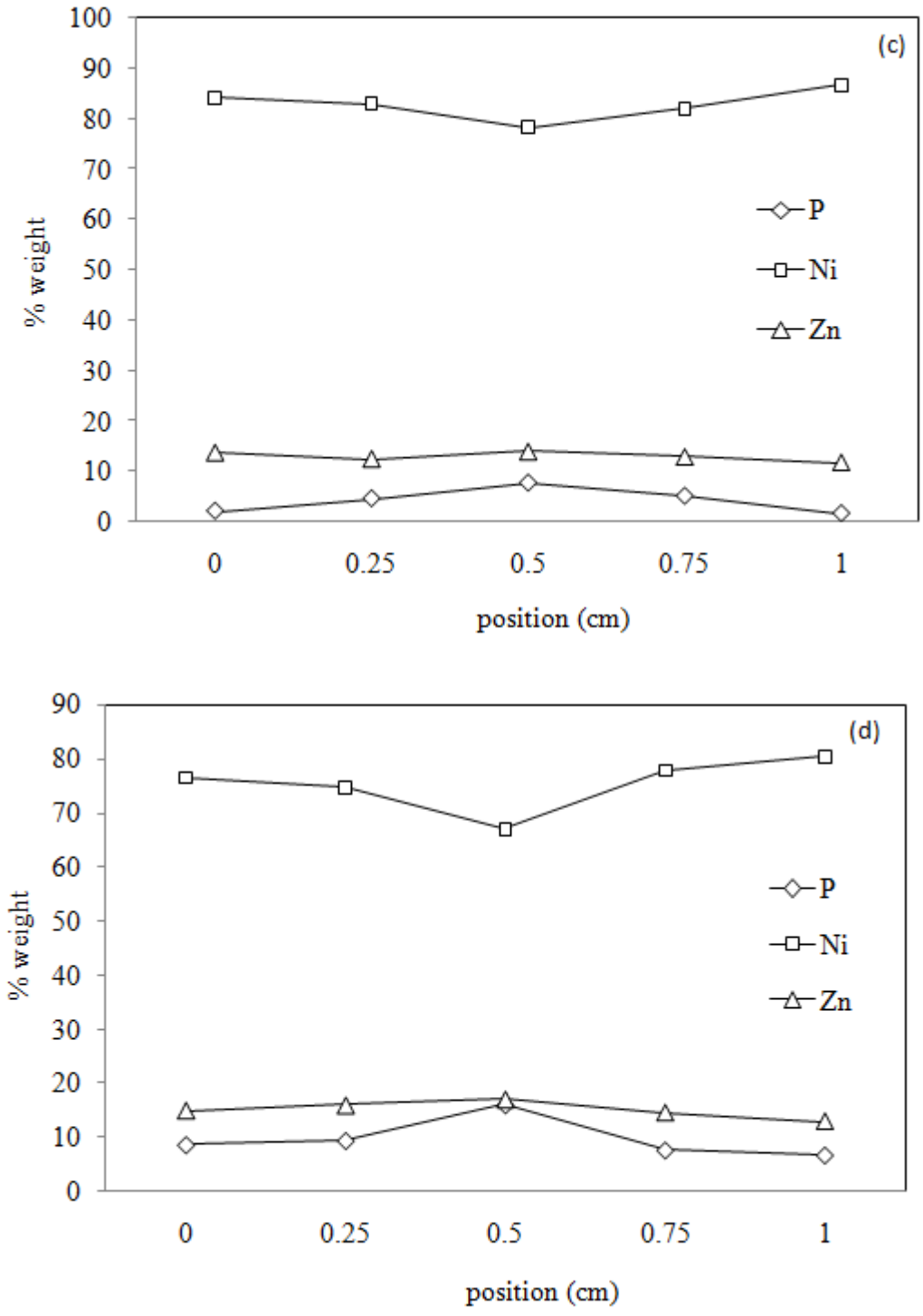

Figure 5.8 EDX results of PU foam in the different positions after electroless deposition of the Ni-Zn-P sample with varied amount of $ZnSO_4$ in bath a) 6 g/l, b) 12 g/l, c) 18 g/l, d) 24 g/l

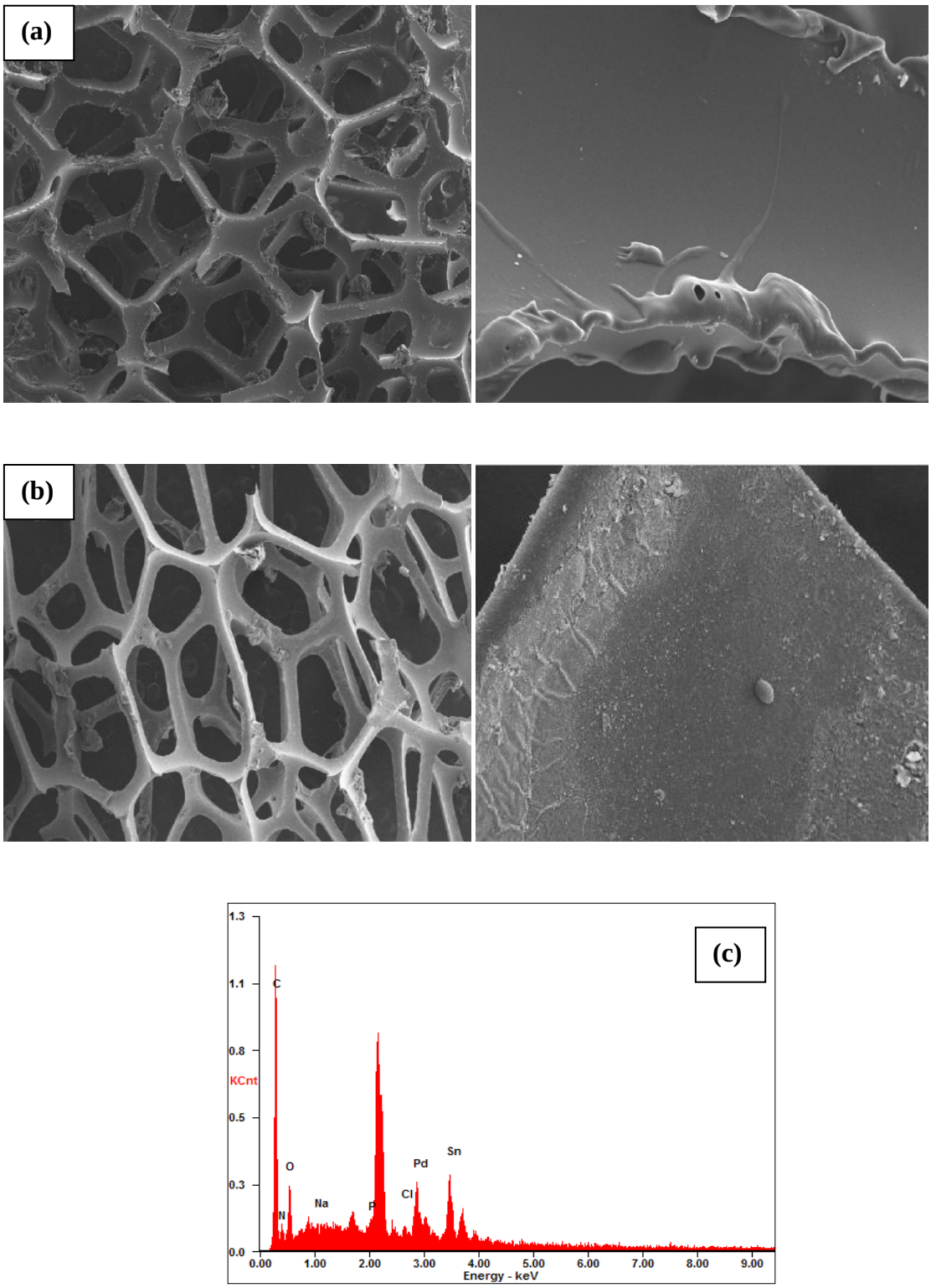

Figure 5.9 SEM micrographs of PU foam (a) before supported Pd (b) 0.82%Pd/PU foam (×15 (left) and × 400 (right)) (c) EDX spectra of 1%Pd/PU foam

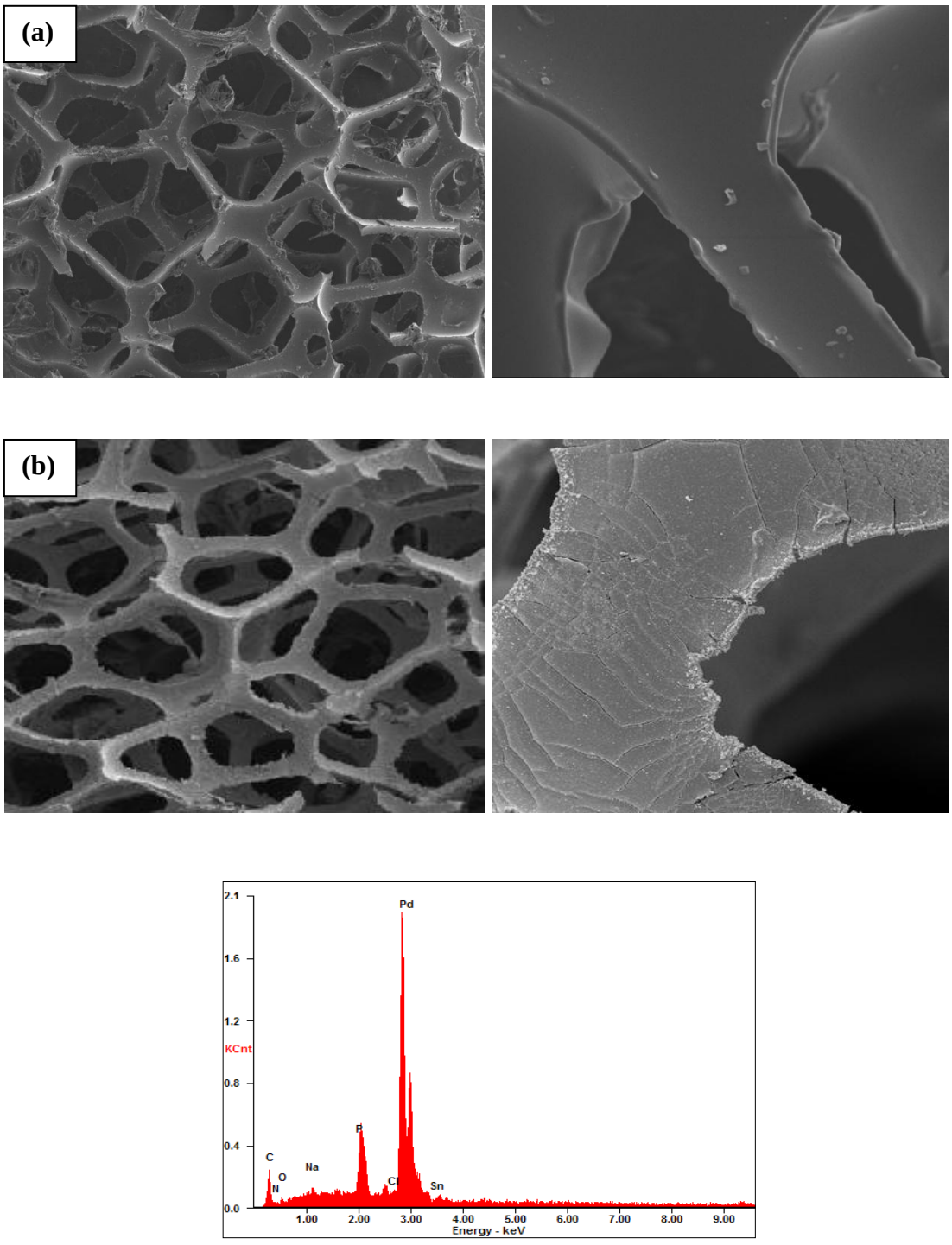

Figure 5.10 SEM micrographs of PU foam (a) before supported Pd (b) 1.37% Pd/PU foam (×15 (left) and × 400 (right)) (c) EDX spectra of Pd/PU foam

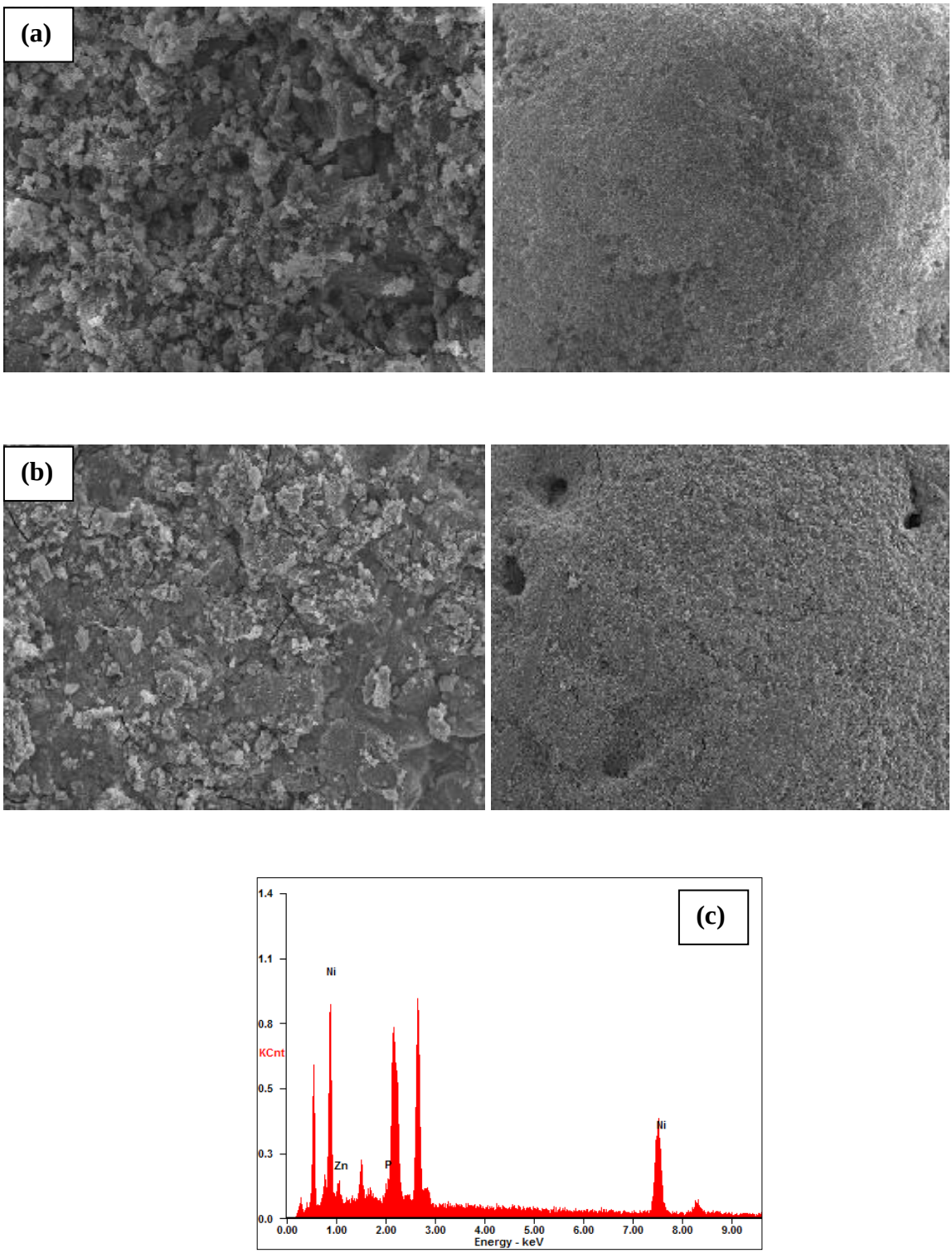

Figure 5.11 SEM micrographs of γ-Al_2O_3 pellet (a) before supported (b) Ni-Zn-P/γ-Al_2O_3 pellet ($ZnSO_4$ 18 g/l)(×100 (left) and × 1000 (right)) (c) EDX spectra of Ni-Zn-P/γ-Al_2O_3 pellet ($ZnSO_4$ 18 g/l)

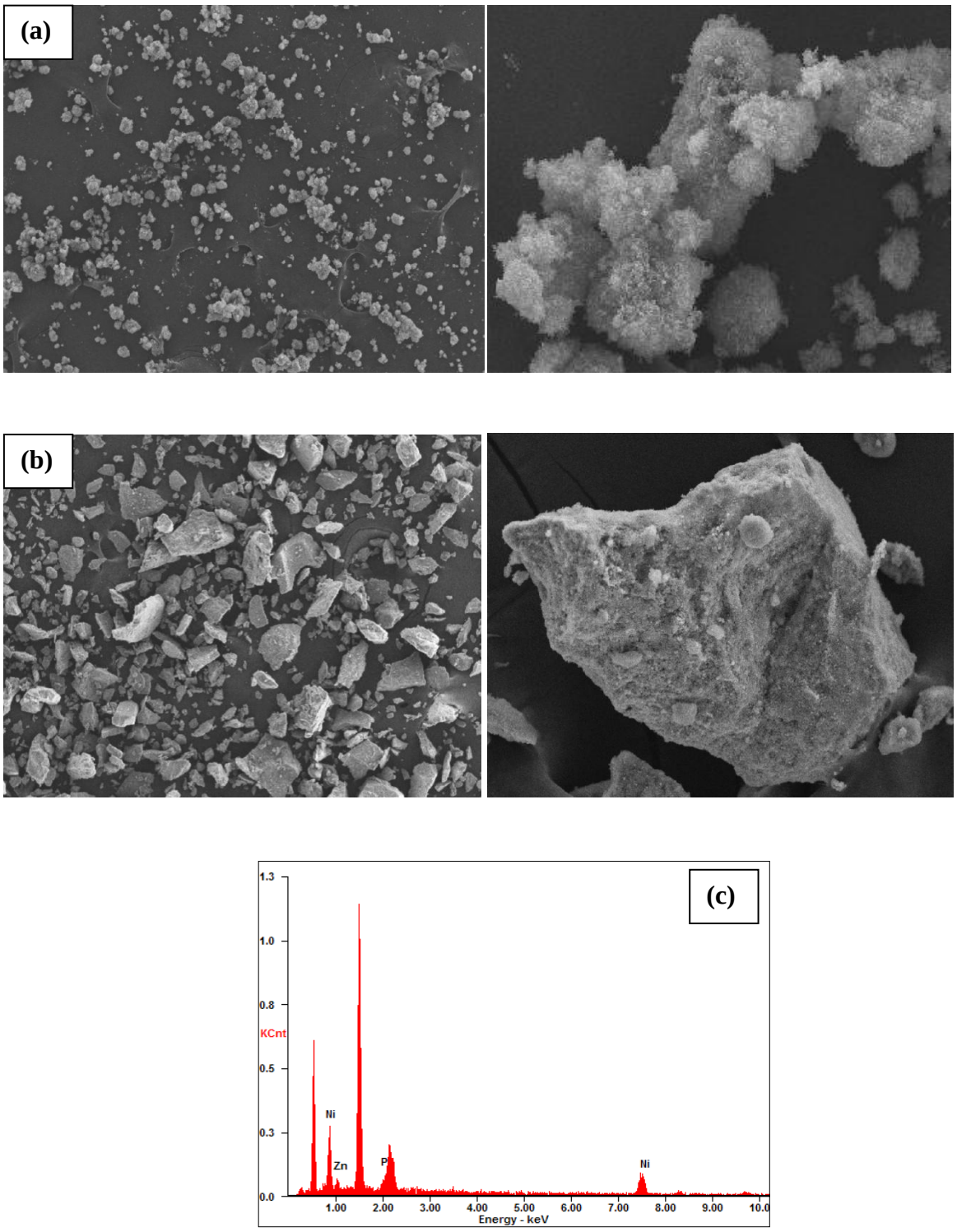

Figure 5.12 SEM micrographs of γ-Al_2O_3 powder (a) before supported (b) Ni-Zn-P/γ-Al_2O_3 powder ($ZnSO_4$ 18 g/l) (×100 (left) and × 1000 (right)) (c) EDX spectra of Ni-Zn-P/γ-Al_2O_3 powder ($ZnSO_4$ 18 g/l)

The SEM micrographs of the catalysts before and after plating for 1 hr of 0.82% Pd on the polyurethane foam are shown in Figure 5.9 (a) and (b) respectively. The 0.82%Pd catalyst after plating was smooth and showed good dispersion on the surface of PU foam. The EDX results are shown in Figure 5.9 (c). The wt% of Pd on catalysts is ca. 19%. Besides Pd, the deposition of Sn on the polyurethane foam surface ca. was 17%. It is suggested that washing was not completed during the pretreatment of PU foam. The amount of P was also found at ca. 2%wt. The $H_2PO_2^-$ oxidation and the reduction of P are shown in the following reactions [74]:

Oxidation of hypophosphite:

$$H_2PO_2^- + H_2O \xrightarrow{\text{Catalytic surface}} H_2PO_3^- + 2H^+ + 2e^-$$

Reduction reaction for P:

$$2H_2PO_2^- + H^+ + e^- \longrightarrow P + H_2PO_3^{2-} + H_2O + H_2$$

From the SEM micrograph of polyurethane foam before and after coating with 0.2 g in bath are shown in Figure 5.10 (a) and (b). Figure 5.10 (c) shows the EDX spectra of the elements on the 1.37% Pd/PU foam. It is clearly seen that the main component was Pd ca. 78 wt%. P and Sn were also found on the surface of PU at ca. 6% and 3%, respectively.

Figure 5.11 (a) and (b) show the SEM micrographs of γ-Al_2O_3 pellet before and after coating with Ni-Zn-P catalysts. The morphology of catalysts was slightly changed because of the layer Ni-Zn-P platingon the surface of γ-Al_2O_3 pellet. The surface layer after plating was smoother than the γ-Al_2O_3 support [58]. Figure 5.11 (c) is the EDX spectrum of Ni-Zn-P/γ-Al_2O_3 pellet. It indicates that the coating was composed of Ni, Zn, and P at ca. 87, 9, 3 wt% respectively.

The SEM micrographs of γ-Al_2O_3 powder is shown in Figure 5.12 (a). The SEM micrograph of Ni-Zn-P supported on γ-Al_2O_3 powder is shown in Figure 5.12 (b). The γ-Al_2O_3 powder became more agglomerated (or more crystalline) after deposition of Ni-Zn-P by electroless deposition method. . Figure 5.12 (c) is the EDX

spectrum of Ni-Zn-P/γ-Al_2O_3 powder. The wt% of Ni, Zn and P were ca. 72, 19 ,8 wt% respectively.

5.1.5 Compression test

The stress-strain curves of Ni-Zn-P catalysts supported on polyurethane foam with various amounts of $ZnSO_4$ 6 g/l, 12 g/l, 18 g/l, and 24 g/l in bath by electroless deposition method were performed by using an Instron universal testing machine and the results are shown in Figure 5.13. The results showed that % strain increased as a function of stress for all the samples. The stress value decreased with increasing amount of Zn in the catalysts in the same trend as the deposition rate results in the order: $ZnSO_4$ 6 g/l >12 g/l >18 g/l > 24 g/l.

For industrial application, the catalyst may be operated under high pressure conditions. The mechanical properties of materials are important for industrial use. The effect of coating efficiency on the mechanical properties of the Ni-Zn-P on PU foam catalysts are shown in Table 5.5. It was found that increasing Zn in electroless bath caused a decrease in the density and modulus. These results are also consistent to the deposition rate results. The highest density and modulus of catalysts were obtained on the catalyst with the lowest amount of Zn in bath (6 g/l) at $8.98x10^{-2}$ g•cm^{-3} and $8.76x10^{-2}$ Mpa, respectively.

A comparison of stress-strain curves of the samples prepared with $ZnSO_4$ 18 g/l on different sizes of polyurethane foam are shown in Figure 5.14. The results showed that 10.5 ppi PU foam gave slightly higher stress value than 24.1 ppi and the 17.2 ppi PU foam gave the lowest stress value.

Table 5.6 shows the coating efficiency of 3 sizes of polyurethane foam supported Ni-Zn-P catalysts prepared with Zn in bath 18 g/l. The density and modulus were found to be in the order 17.2 ppi > 24.1 ppi > 10.4 ppi PU foam. Hence, the17.2 ppi polyurethane foam was selected for the other studies in this research.

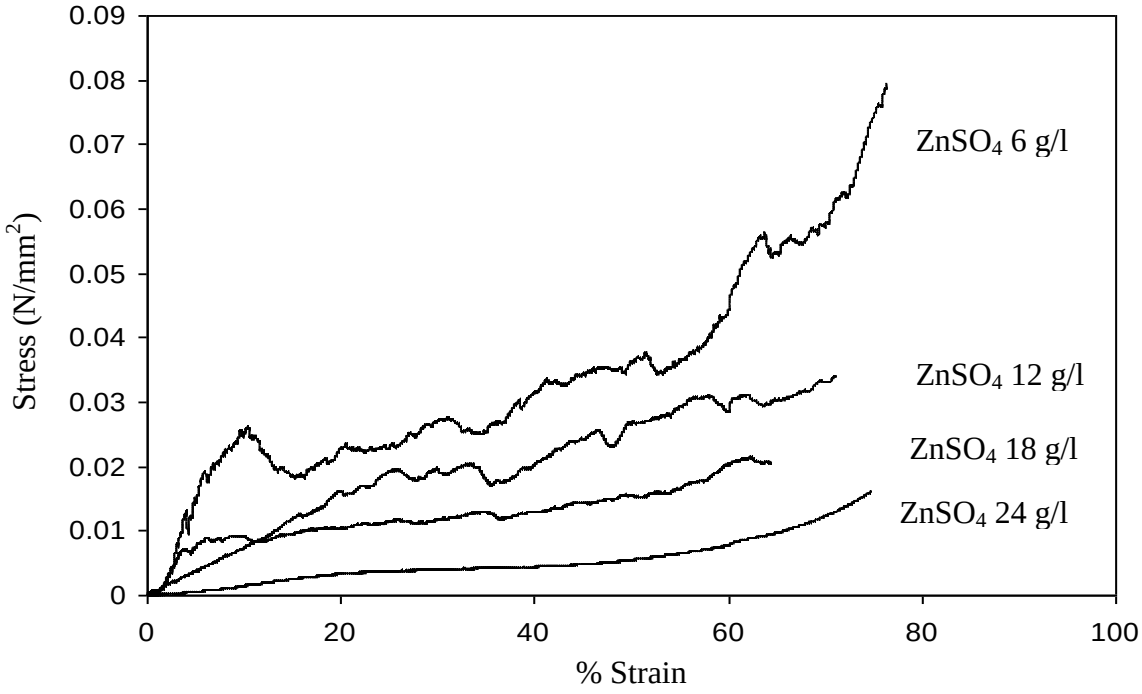

Figure 5.13 Stress-Strain curves for Ni-Zn-P/PU foam with different amount of $ZnSO_4$ in bath

Table 5.5 Material properties of Ni-Zn-P supported on Polyurethane foam with various amount of $ZnSO_4$

Sample	Density (g •cm^{-3})	Modulus (Mpa)
Ni-Zn-P/PU foam (Zn 6 g/l)	$8.98x10^{-2}$	$8.76x10^{-4}$
Ni-Zn-P/PU foam (Zn 12 g/l)	$7.29x10^{-2}$	$7.80x10^{-4}$
Ni-Zn-P/PU foam (Zn 18 g/l)	$6.95x10^{-2}$	$3.93x10^{-4}$
Ni-Zn-P/PU foam (Zn 24 g/l)	$3.32x10^{-2}$	$1.83x10^{-4}$

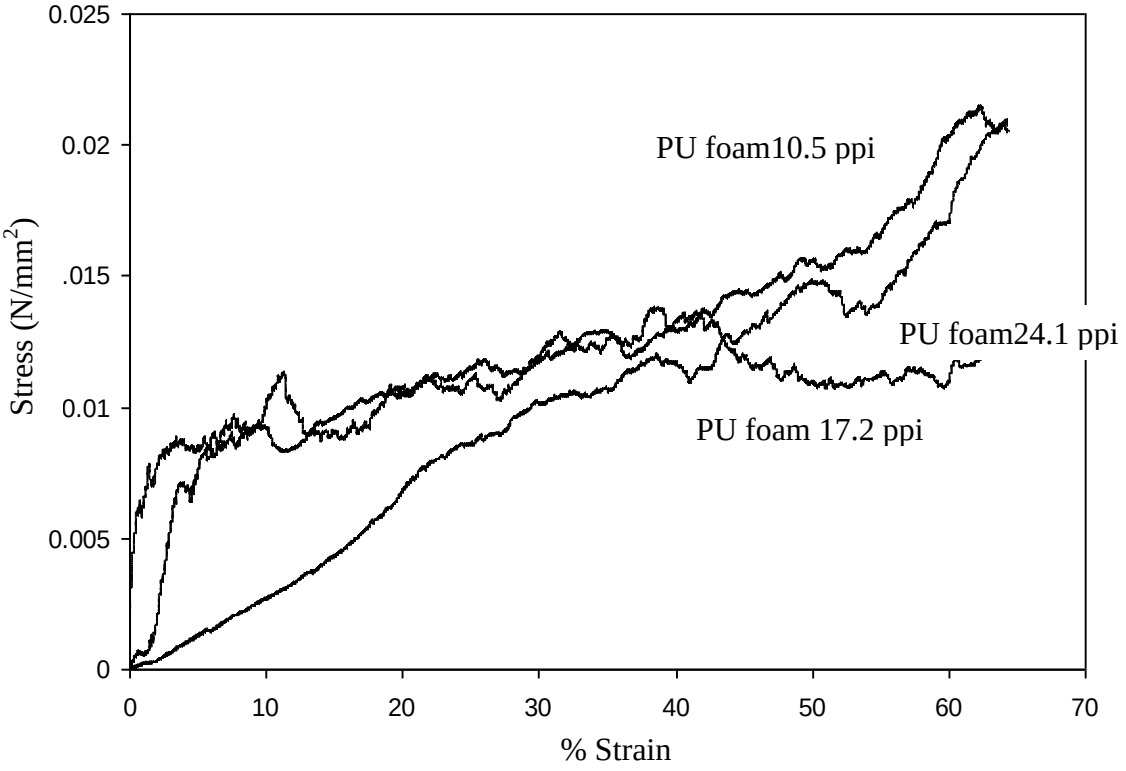

Figure 5.14 Stress-Strain curves for Ni-Zn-P/PU foam ($ZnSO_4$ 18 g/l) with different size of PU foam

Table 5.6 Material properties of the different sizes polyurethane foam supported Ni-Zn-P prepared with Zn 18 g/l in bath.

Sample	Density (g •cm^{-3})	Modulus (Mpa)
PU foam 10.5 ppi	$1.03x10^{-2}$	$1.44x10^{-4}$
PU foam 17.2 ppi	$1.04x10^{-2}$	$3.94x10^{-4}$
PU foam 24.1 ppi	$0.28x10^{-2}$	$3.25x10^{-4}$

5.1.6 X-ray Photoelectron Spectra (XPS) analysis

Table 5.7 The XPS results of Ni-Zn-P supported on PU foam with various amount of $ZnSO_4$ in electroless bath

Sample	Binding Energy (eV)					
	Ni 2p(3/2)	Ni 2p(3/2)	Ni 2p(1/2)	Zn 2p(3/2)	Zn 2p(3/2)	P 2p
Ni-Zn(6 g/l)-P/PU	856.9	-	874.4	1022.8	1045.7	134.1
Ni-Zn(12 g/l)-P/PU	856.5	-	-	-	-	132.9
Ni-Zn(18 g/l)-P/PU	856.6	862.8	874.7	1022.4	1045.2	133.4
Ni-Zn(24 g/l)-P/PU	856.3	861	874.1	1022.3	1045.9	133.2

XPS is a very useful tool to study the chemical states of the element on a solid surface. The XPS results of Ni-Zn-P catalysts on PU foam prepared with the various amount of $ZnSO_4$ are shown in Table 5.7 and Figure 5.15. The elemental scan was carried out for Ni 2p, Zn 2p, and P 2p. . The peak at binding energy 856.3-874.7 eV was observed and was attributed to Ni^{2+} ion [43,80,81]. Similar results were obtained for the other samples prepared with 6, 12, and 24 g/l $ZnSO_4$. It is thus suggested that nickel on the surface of Ni-Zn-P catalysts was presented mostly in the form of nickel oxide. The XPS peaks corresponding to Zn 2p and P 2p also suggest the oxide forms of these metals [82].

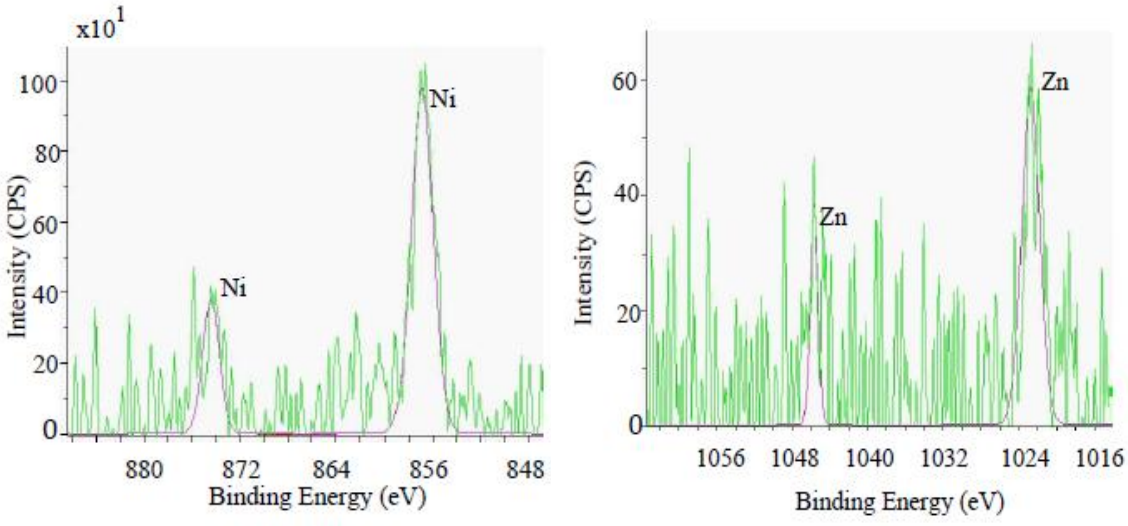

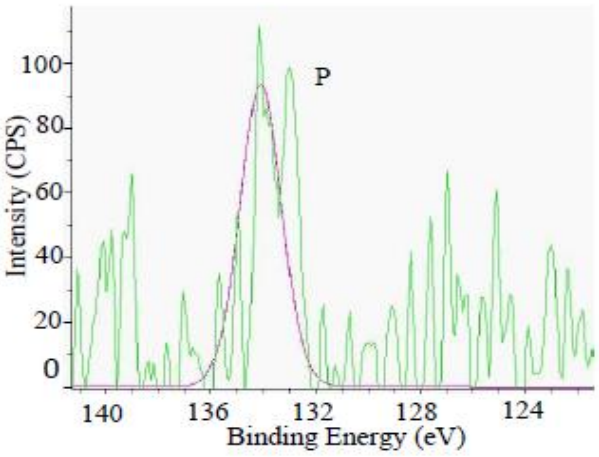

(a) $ZnSO_4$ 6 g/l

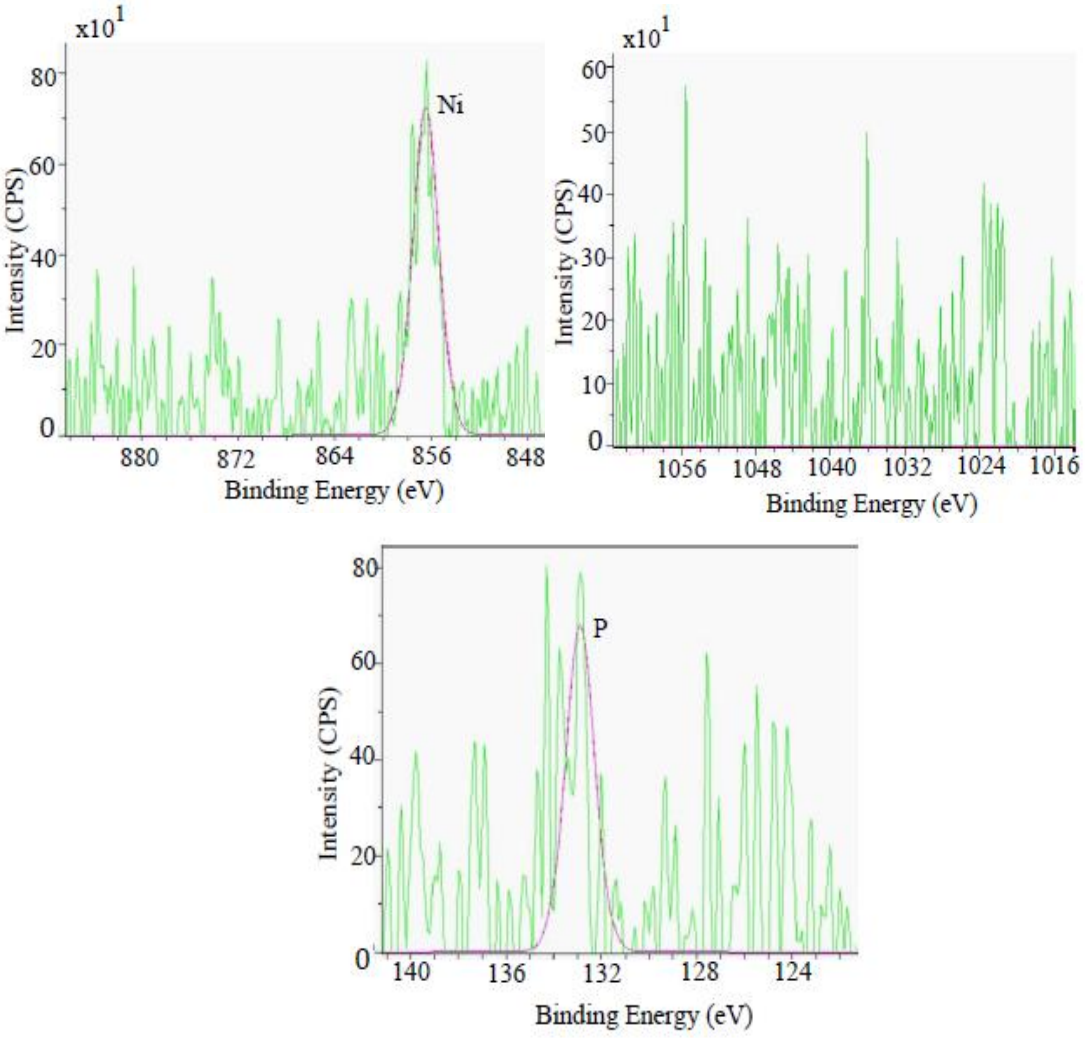

(b) $ZnSO_4$ 12 g/l

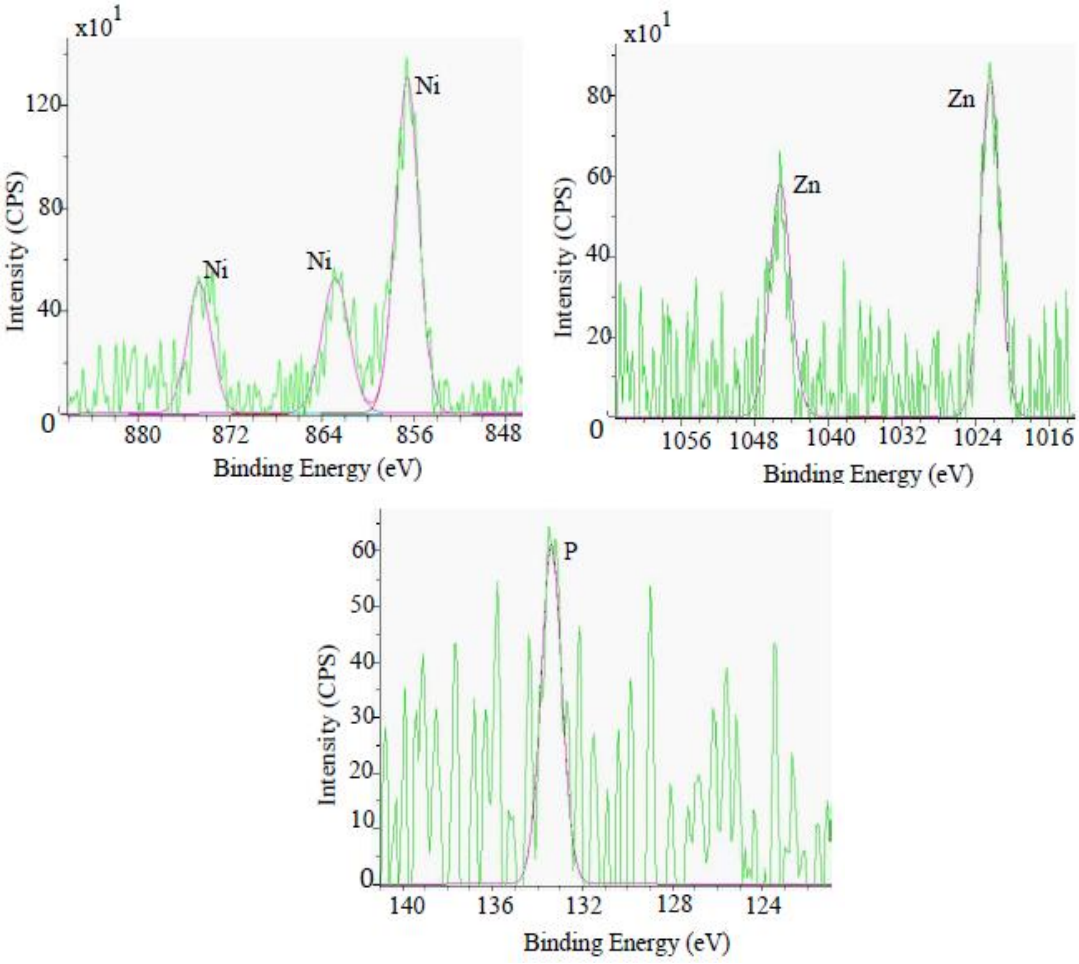
x10^1
Intensity (CPS)
Ni
Ni
Ni
Binding Energy (eV)
x10^1
Intensity (CPS)
Zn
Zn
Binding Energy (eV)
Intensity (CPS)
P
Binding Energy (eV)

(c) $ZnSO_4$ 18 g/l

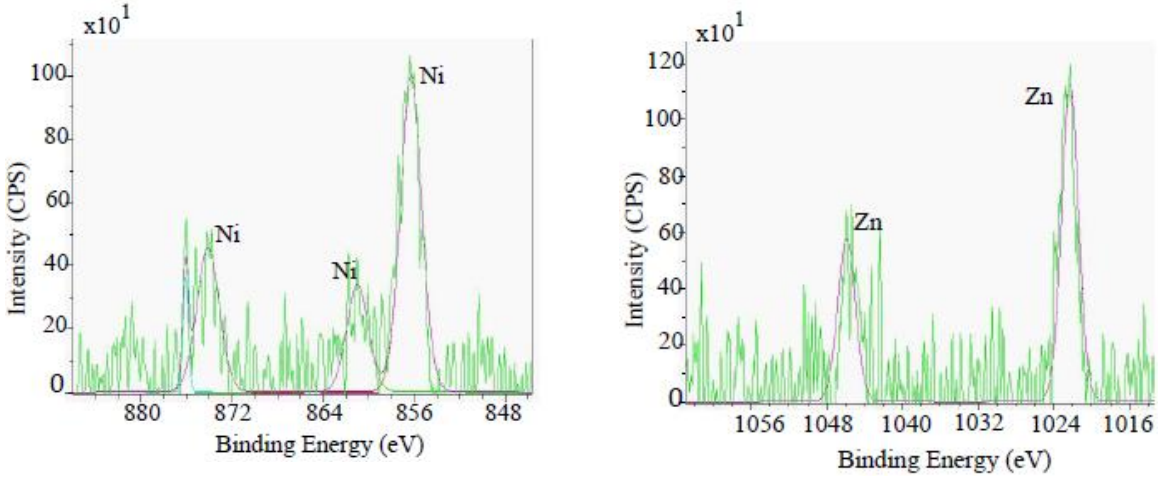
x10^1
Intensity (CPS)
Ni
Ni
Ni
Binding Energy (eV)
x10^1
Intensity (CPS)
Zn
Zn
Binding Energy (eV)

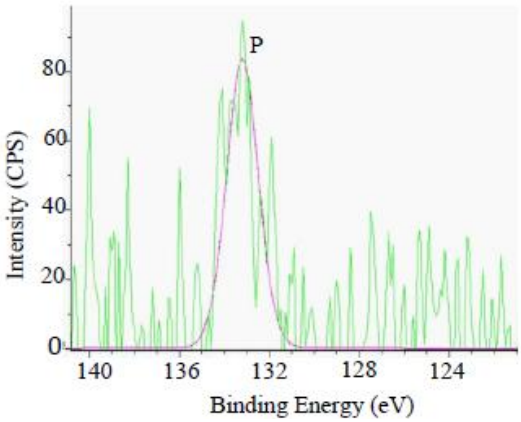

(d) $ZnSO_4$ 24 g/l

Figure 5.15 The XPS spectra of the Ni-Zn-P/PU foam with various amounts of $ZnSO_4$ in bath (a) 6 g/l (b) 12 g/l (c) 18 g/l (d) 24 g/l

5.1.7 X-ray diffraction (XRD) analysis

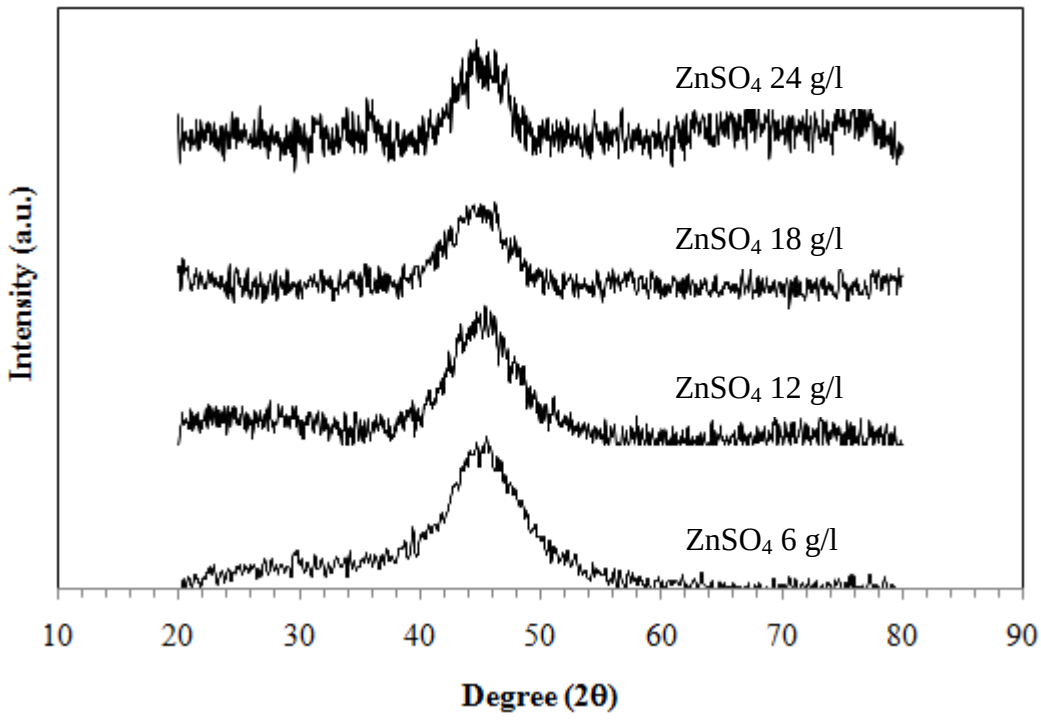

Figure 5.16 The XRD patterns of the Ni-Zn-P/PU foam with various amounts of $ZnSO_4$ in bath 6, 12, 18, 24 g/l.

The X-ray diffraction patterns of Ni–Zn–P catalysts on PU foam are shown in Figure 5.16. The XRD peaks displayed at 2θ degree = 45.6, 45.48, 45.12, 44.92 were observed for the samples with $ZnSO_4$ in bath 6, 12, 18, 24 g/l, respectively and were attributed to the Ni (1 1 1) phase of the polycrystalline Ni–Zn–P [58,77] The XRD characteristic peaks of Zn and P were not found for all the catalyst samples.

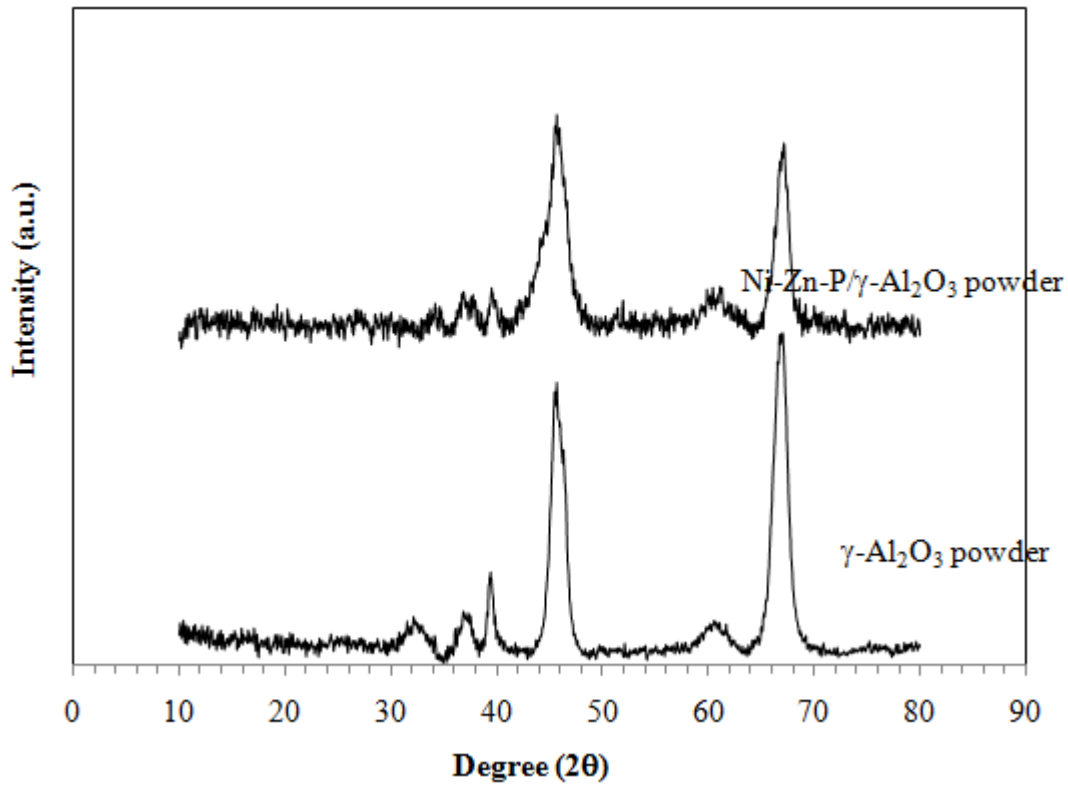

Figure 5.17 XRD patterns of Ni-Zn-P/γ-Al_2O_3 powder ($ZnSO_4$ 18 g/l) and γ-Al_2O_3 powder

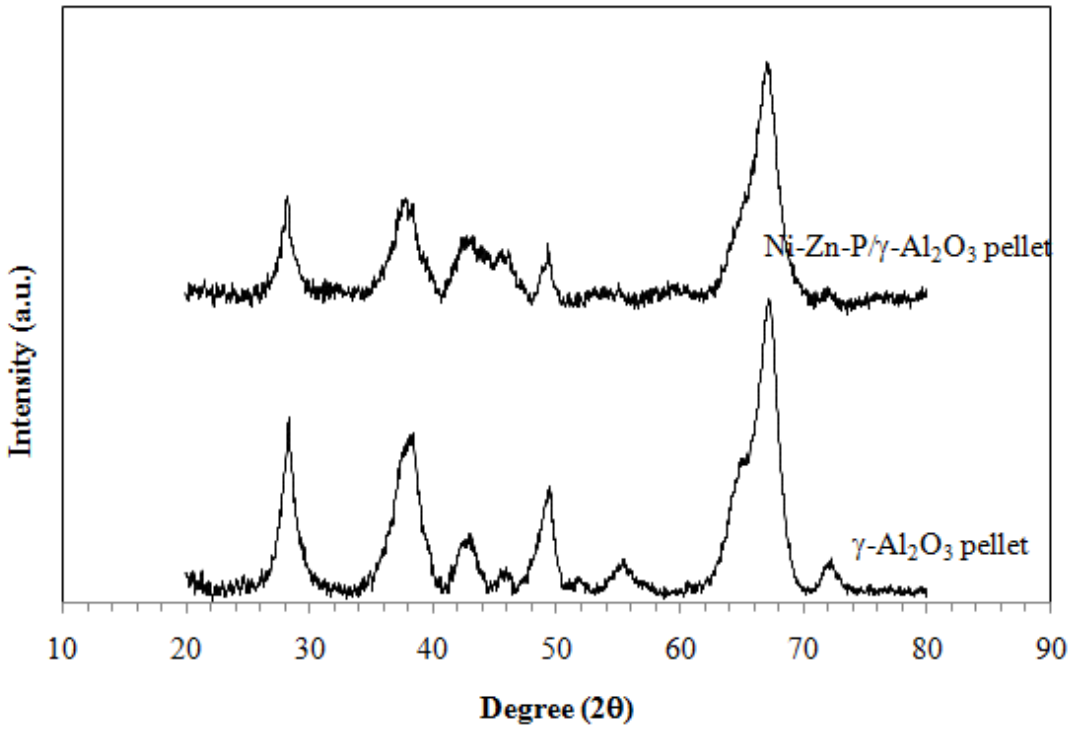

Figure 5.18 XRD pattern of Ni-Zn-P/γ-Al_2O_3 pellet ($ZnSO_4$ 18 g/l) and γ-Al_2O_3 pellet

The XRD patterns of the alumina powder support and the Ni-Zn-P/γ-Al_2O_3 powder with amount of $ZnSO_4$ 18 are shown in Figure 5.17. For the pure gamma phase, the XRD peaks at 2θ degrees 32.1°, 37.3°, 39.4°, 45.6°, 61° and 66.7° were evident.[83] The XRD peak of nickel was found at 45.6° and the positions assigned to Zn were not found in this sample.

Figure 5.18 shows the XRD patterns of γ-Al_2O_3 pellet support and Ni-Zn-P supported on γ-Al_2O_3 pellet by electroless deposition method with amount of $ZnSO_4$ 18 g/l. The XRD patterns of commercial γ-Al_2O_3 pellet were observed at 38.1°, 46.1°, 67.22° similar to the pure γ- phase. The other peaks which are shown in the XRD pattern may belong to the impurities in the γ-Al_2O_3 pellet [83]. The Ni-Zn-P/γ-Al_2O_3 pellet showed the XRD peak of Ni at 46.15^o and the positions assigned to Zn were not detected in this sample.

5.1.8 The catalytic performances in the selective acetylene hydrogenation

The catalyst performances in the gas-phase selective hydrogenation of acetylene were evaluated in terms of acetylene conversion and ethylene gain. Ideally, all of acetylene converted into ethylene because of one molecule of acetylene converted for molecule of hydrogen. But in actual cases, some hydrogen will be consumed in side reaction to ethane.

The performance of catalysts in this study are reported in terms of acetylene conversion and ethylene gain observed from the following reaction:

$$C_2H_2 + H_2 \longrightarrow C_2H_4$$
$$C_2H_4 + H_2 \longrightarrow C_2H_6$$

Activity of the catalyst for acetylene conversion is defined as mole of acetylene converted with respect to acetylene in the feed:

$$C_2H_2\text{conversion (\%)} = \frac{100 \text{ x [mole of } C_2H_2 \text{ in feed} - \text{mole of } C_2H_2 \text{ in product]}}{\text{mole of } C_2H_2 \text{ in feed}}$$

Ethylene gain was calculated from moles of hydrogen and acetylene:

$$C_2H_4 \text{ gain (\%)} = \frac{100 \text{ x } [dC_2H_2 - (dH_2 - dC_2H_2)]}{dC_2H_2}$$

Where dC_2H_2 is the different moles of acetylene in feed and product and dH_2 is the different mole of hydrogen in feed and product.

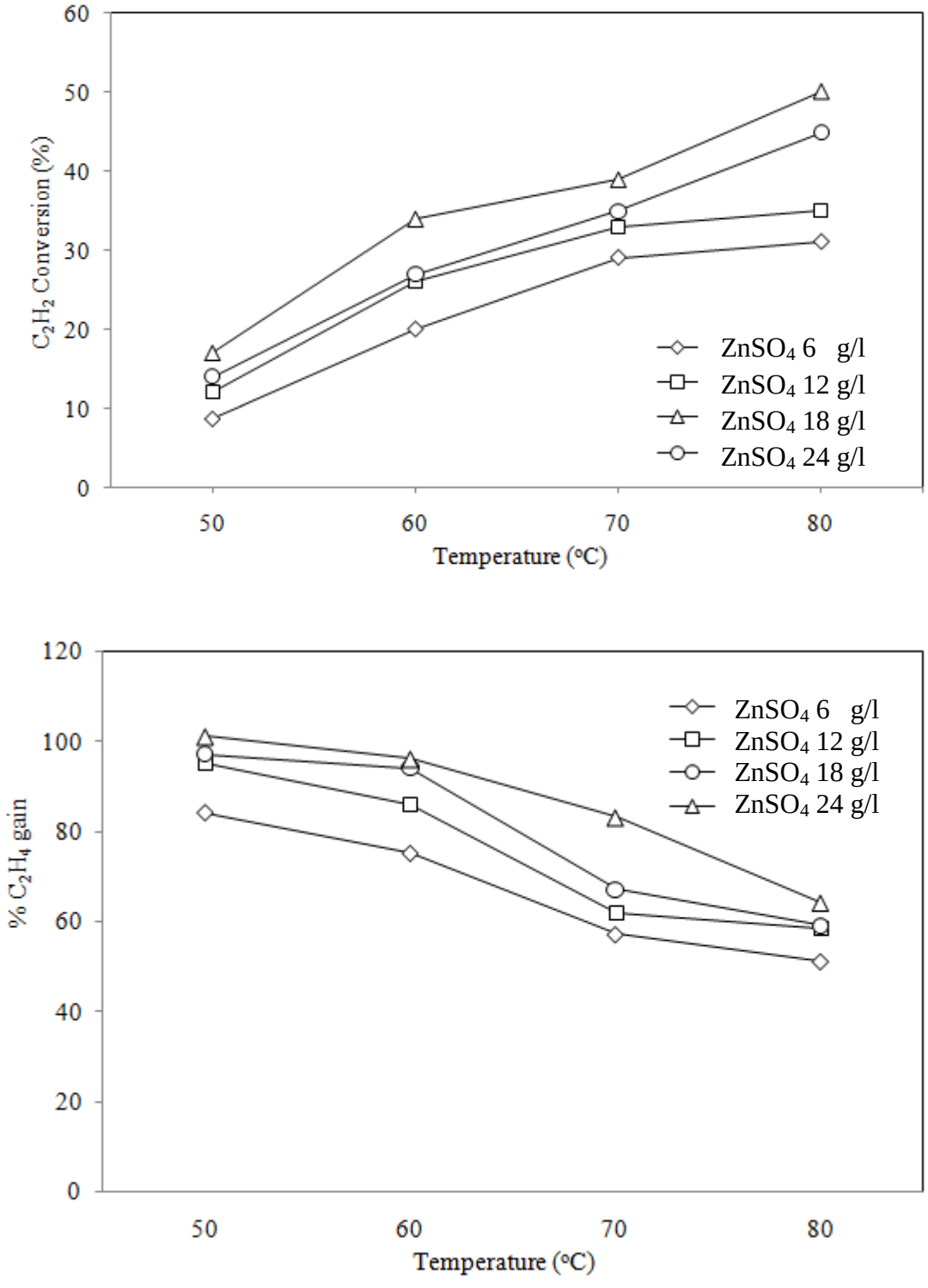

Figure 5.19 Performances of Ni-Zn-P/PU foam catalysts prepared with various amounts of Zn in bath in the selective acetylene hydrogenation at different reaction temperatures.

The selective hydrogenation of acetylene to form ethylene was carried out over Ni-Zn-P supported on polyurethane foam prepared with various amount of Zn 6, 12, 18, 24 g/l at reaction temperatures 50-80^{o}C as shown in Figure 5.19. The conversion of acetylene increased with the reaction temperature. The acetylene conversion at 80^{o}C of the catalysts prepared with $ZnSO_4$ in bath 6, 12, 18, 24 g/l were 31 %, 34 %, 47 %, and 44 %, respectively. The ethylene gain over all of the samples was decreased with increasing the temperature because of ethylene is produced as an intermediate in acetylene hydrogenation reaction[84] The catalysts with higher amount of $ZnSO_4$ in bath also showed higher ethylene gain. According to the ICP-OES results, the amount of Zn in bath 18 g/l resulted in the highest amount of Zn in the Ni-Zn-P catalysts on the polyurethane support. Much higher acetylene conversion and ethylene gain was obtained when relatively high amounts of $ZnSO_4$ were employed in the order: $ZnSO_4$ 18 g/l >24 g/l > 12g/l > 6 g/l. These results are also in good agreement with the SEM micrographs results which showed that $ZnSO_4$ 18 g/l provided the best dispersion of Ni-Zn-P on the PU foam.

According to the literature, the Ni-based catalysts usually generate coke that deactivates the catalyst in the selective acetylene hydrogenation. Both coking rate and amount of coke increase with increasing Ni concentration. The negative effect of the sintering coke on the catalyst stability caused the decrease of conversion level over reaction time. It has been suggested that the addition of Zn affected the reduction of sintering on the Ni-based catalysts [42,43,69]

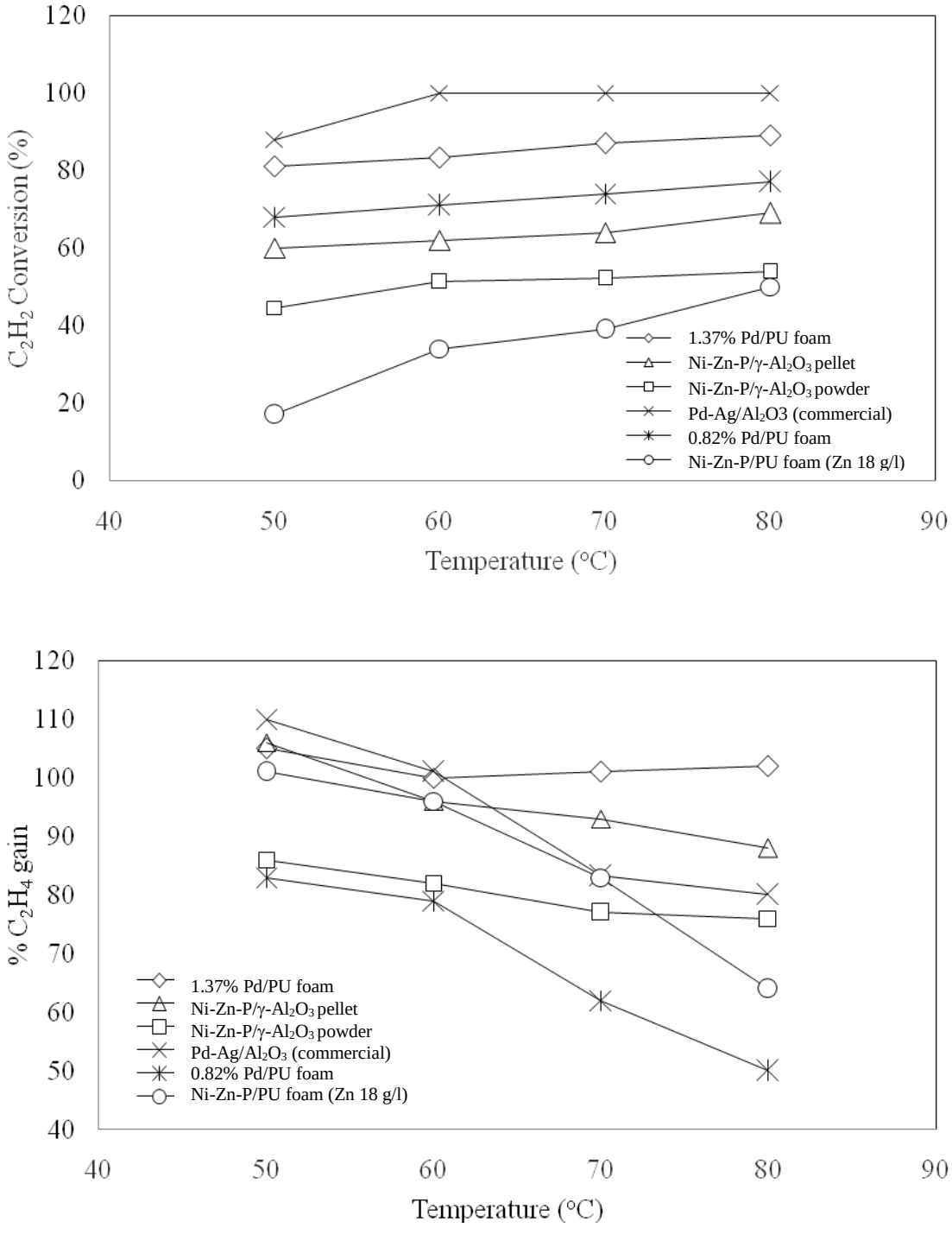

Figure 5.20 Performance of 0.82%Pd/PU foam, 1.37%Pd/PU foam, Ni-Zn-P/γ-Al_2O_3(Zn 18g/l) pellet, Ni-Zn-P/γ-Al_2O_3 (Zn 18g/l) powder, Pd-Ag/Al_2O_3 and Ni-Zn-P/PU foam(Zn 18 g/l) in the selective acetylene hydrogenation with various temperatures.

The catalytic performances of the other catalysts in the selective acetylene hydrogenation comparing to the Ni-Zn-P/PU foam are shown in Figure 5.20. The acetylene conversion of all catalysts directly increased with increasing temperature as the kinetic energy of the system increases with temperature. Opposite trend was found for ethylene gain which was declined when the reaction temperature was increased [84] The Ni-Zn-P catalysts on PU foam were compared with the Ni-Zn-P on different supports such as the, Ni-Zn-P/γ-Al_2O_3 pellet and the Ni-Zn-P/γ-Al_2O_3 powder catalysts prepared by electroless deposition method with amount of $ZnSO_4$ in bath 18 g/l. In the catalytic reaction tests, the samples were compared using the same density as that of Ni-Zn-P/PU foam. The Ni-Zn-P/γ-Al_2O_3 pellet catalyst exhibited higher acetylene conversion and ethylene selectivity than that supported on γ-Al_2O_3 powder. Although the conversion of acetylene over the Ni-Zn-P/PU foam was lowest among the various Ni-Zn-P catalysts, the ethylene gain was higher than that of Ni-Zn-P/γ-Al_2O_3 powder. The activity was improved in the order: Ni-Zn-P/γ-Al_2O_3 pellet > Ni-Zn-P/PU foam > Ni-Zn-P/γ-Al_2O_3 powder. The catalytic reaction results were correlated to the dispersion of Ni-Zn-P on the support, the Zn/Ni ratio, as well as the BET surface area of the catalysts.

Commercially, supported Pd-based catalysts are employed in the selective acetylene hydrogenation in industrial application. In this research, 0.82% and 1.37% Pd supported on polyurethane foam were prepared by electroless deposition method and compared with the Ni-Zn-P/PU foam with amount of Zn 18 g/l. From Figure 5.20, it was found that 1.37% Pd/PU foam exhibited the highest conversion and ethylene gain and the activity improved in the order: 1.37% Pd/PU foam > Ni-Zn-P/PU foam > 0.82% Pd/PU foam.

Pd-Ag/γ-Al_2O_3 is a commercial catalyst that been used in acetylene hydrogenation reaction**.** The acetylene conversion over the commercial Pd-Ag/γ-Al_2O_3 catalyst was higher than the other catalysts at 50-80 ^oC. However, the ethylene gain of this catalyst was significantly dropped when the reaction temperature was increased to 70°C and 80°C. This may be due to the formation of coke deposition on the Pd particles during the reaction on the commercial Pd-Ag/γ-Al_2O_3 catalyst.

CHAPTER VI

CONCLUSIONS AND RECOMMENDATIONS

6.1 Conclusions

The presence of zinc retarded the overall deposition rate of the metals during the electroless deposition of Ni-Zn-P alloys. The rate of deposition during the electroless deposition of Ni-Zn-P on PU foam was decreased with increasing amount of $ZnSO_4$ in the electroless bath in the order of $ZnSO_4$ 6 g/l >12 g/l > 18g/l > 24 g/l. The optimum deposition time was determined to be 60 min. The maximum amount of Zn being able to deposit on the PU foam was 20 wt% using 18 g/l $ZnSO_4$. The highest Zn/Ni wt/wt% ratio being able to produce by this method was 0.42. The Ni-Zn-P/PU foam catalysts prepared with 18 g/l $ZnSO_4$ also exhibited more refined surface morphology and better catalyst performances in the selective acetylene hydrogenation.

Comparing to the Ni-Zn-P/PU foam, the use of Al_2O_3 supports for electroless deposition of Ni-Zn-P catalysts showed improvement in the acetylene conversion and ethylene selectivity in the order: Ni-Zn-P/Al_2O_3 pellet (surface area 100.6 m^2/g) > Ni-Zn-P/Al_2O_3 powder (surface area 22.5 m^2/g) > Ni-Zn-P/PU foam (surface area < 1 m^2/g.

6.2 Reccommendations

1.The effect of interaction between Ni-Zn-P and the support on the catalyst performance should be studied using more sophisticated.

2.The effect of Ni-Zn-P/Al_2O_3 for selective hydrogenation of acetylene in excess ethylene should be study for other phase such α-Al_2O_3.

REFERENCES

[1] H. Wei, J.R. Mccormick, R.F. Lobo, J.G. Chen, Journal of Catalysis, 246 (2007): 40-51.

[2] S.H.Lee, Dept. of Chemical & Biomolecular Engineering [online]. 2011. Available from: http://www.klmtechgroup.com/PDF/Articles/edm64a.pdf [2012, Jan 1]

[3] J.H. Kang, E.W. Shin, W.J. Kim, J.D. Park, S.H. Moon, Catalyst Today, 63 (2000): 183-188.

[4] Y. Azizi, C. Petit,V. Pitchon, Journal of Catalysis, 256 (2008): 338–344.

[5] A. Sárkány, Zs. Révay, Applied Catalysis A: General, 243 (2003): 347–355.

[6] Z. Guilin, W. Puguang, J. Zongxuan, Y. Pinliang, L. Can, Chinese Journal of Catalysis, 32 (2011): 27–30.

[7] J. Rebelli, M. Detwiler, S. Ma, C.T. Williams, J.R. Monnier, Journal of Catalysis, 270 (2010): 224–233.

[8] M.T. Schaal, A.Y. Metcalf, J.H. Montoya, J. P. Wilkinson, C.C. Stork, C.T. Williams, J.R. Monnier, Catalysis Today, 123 (2007): 142–150.

[9] B. Darin,California Transparency in supply Chains Act Disclosure [online]. 2000. Available from : http://www.cpchem. com [2011, Dec 22]

[10] W.J. Kim, J.H. Kang, I.Y. Ahn, S.H. Moon, Journal of Catalysis, 226 (2004): 226–229.

[11] I.Y. Ahn, J.H. Lee, S.K. Kim, S.H. Moon, Applied Catalysis A: General, 360 (2009): 38–42.

[12] S.K. Kima, J.H. Lee, I.Y. Ahn, W.J. Kimb, S.H. Moo, Applied Catalysis A: General, 401 (2011): 12–19.

[13] M.J. Vincent**,** R.D. Gonzalez , Applied Catalysis A: General, 217 (2001): 143-156.

[14] S,Chinayon, O. Mekasuwandumrong, P. Praserthdama, J. Panpranot, Catalysis Communications, 9 (2008): 297–2302.

[15] J.H. Kang, E.W. Shin,W.J. Kim, J.D. Park, S.H. Moon, Journal of Catalysis, 208 (2002): 310–320.

[16] J. Panpranot, K. Kontapakdee, P. Praserthdam, Applied Catalysis A: General, 314 (2006): 128–133.

[17] A. Sárkány, A. Horváth, A. Beck, Applied Catalysis A: General, 229 (2002): 117-125.

[18] A. Sárkány, O. Geszti, G. Sáfrán, Applied Catalysis A: General, 350 (2008): 157-163.

[19] A. Sárkány, A. Becka, A. Horváth, Z. Révay, L. Guczi, Applied Catalysis A: General, 253 (2003): 283–292.

[20] S. Komhoma, O. Mekasuwandumrong, P. Praserthdam, J. Panpranot, Catalysis Communications, 10 (2008): 86–91.

[21] E.W. Shin, J.H. Kang, W.J. Kim, J.D. Park, S.H. Moon, Applied Catalysis A: General, 223 (2002): 161–172.

[22] W.J. Kim, E.W. Shin, J.H. Kang, S.H. Moon, Applied Catalysis A: General, 251 (2003): 305–313.

[23] L. Zhao, Z. Wei, M. Zhu, B. Dai, Journal of Industrial and Engineering Chemistry, (2011).

[24] P. Praserthdam, B. Ngamsoma, N. Bogdanchikova, S. Phatanasri, M. Pramotthana, Applied Catalysis A: General, 230 (2002): 41–51.

[25] A. Pachulski, R. Schödel, P. Claus, Applied Catalysis A: General, 440 (2011): 14-24.

[26] R.N. Lamb, B. Ngamsom, D.L. Trimm, B. Gong, P.L Silveston, P. Praserthdam Applied Catalysis A : General, 268 (2004): 43-50.

[27] Q. Zhang, J. Li, X. Liu, Q. Zhu, Applied Catalysis A: General, 197 (2000): 221-228.

[28] W.Huang[a], J.R. McCormick[b], R.F. Lobo[a], J.G. Chen, Journal of Catalysis, 15 (2007): 40-51

[29] B. Ngamsom, N. Bogdanchikova, M.A. Borja, P. Praserthdam, Catalyst Communications, 5 (2004): 243-248.

[30] M.J. Vincent, R.D. Gonzalez, Applied Catalysis A: General, 217 (2001): 143-156.

[31] P. Albers, K. Seibold, G. Prescher, H. Müller, Applied Catalysis A: General, 176 (1999): 135-146.

[32] C. Lambert, M. Vincent, J. Hinestroza, N. Sun, R. Gonzalez, Studies in Surface Science and Catalysis, 130 (2000): 2687-2692.

[33] M. Larsson, J. Jansson, S. Asplund, Journal of Catalysis, 178 (1998): 49-57.

[34] B.M. Choudary, M.L. Kantam, N.M. Reddy, K.K Rao, Y. Haritha, V. Bhaskar, F. Figueras,A Tuel, Applied Catalysis A: General, 181 (1999): 139-144.

[35] C.E. Gigola, H.R. Aduriz, P. Bodnariuk, Applied Catalysis, 27 (1986): 133-144.

[36] A. Sárkány, A.H. Weiss, L. Guczi, Journal of Catalysis, 98 (1986): 550-553.

[37] S.O. Aydınoglu, A.E. Aksoyl, International Journal of Hydrogen energy, 36 (2011): 2950-2959.

[38] S. Yolcular, O. Olgu, Catalysis Today, 138 (2008): 198–202.

[39] J.T. Wehrli, D.J. Thomas, M.S. Wainwright, D.L. Trimm, N.W. Cant, Applied Catalysis, 66 (1990): 199-208.

[40] I.Y. Ahn, W.J. Kim, S.H. Moon, Applied Catalysis A: General, 308 (2006): 75–81.

[41] D.L. Trimm, I.O.Y. Liu, N.W. Cant, Applied Catalysis A: General, 374 (2010), 58–64.

[42] V. Rives, F.M. Labajos, R. Trujillano, E. Romeo, C. Royo, A. Monzo´n, Applied Clay Science, 13 (1998): 363–379.

[43] J. C. Rodr´ıguez, A. J. Marchi, A. Borgna, A. Monz´on, Journal of Catalyst, 171 (1997): 268–278.

[44] Q.H. Tian, X.Y. Guo, Metals Society of China, 20 (2010): 283-287.

[45] S. Narayanan, S. Selvakumarb, A. Stephenb, Surface and Coatings Technology, 172 (2003): 298–307.

[46] W.A. Kaplan, R.L. Tabor, Cellular Polymers, 12 (1993): 102.

[47] M. Thirumal, D. Khastgir, N.K. Singha, B.S. Manjunath, Journal Apply Polymer Science, 108 (2008): 1810.

[48] T. Wang, L. Zhang, D. Li, J. Yin, S. Wu, Z. Mao, Bioresource Technology, 99 (2008): 2265-2268.

[49] M.L. Derrien, Study Surface Science Catalyst, 27 (1986): 613-666.

[50] W.K.Lam, L.Lloyd, Oil Gas Journal, (1972): 66-70.

[51]J.J. Bergmeister, E-Series Catalyst.doc [online]. 2011. Available from: http://www.cpchem.com/specialtychem/library/CatalystPoisons pdf. [2012, Jan 1]

[52] H. Cutman, H. Lindlar, New York: Marcel Dekker, (1969): 355-362.

[53] S.A. Miller, London: Ernest Benn Ltd. 2, (1996).

[54] C. DeBoer,Plating, Wilimedia Foundation. Inc [online]. 2011. Available from: http://en.wikipedia.org/wiki/Plating.html. [2011, Dec 22]

[55] E. J. O'Sullivan, IBM T.J. Watson Research Center [online]. 2011. Available from: http://www.electrochem.cwru.edu/ encycl/art-d02-eless-dep.html. [2011, Dec 22]

[56] C.Shreepathy, Organic Chemistry [online]. 2011. Available from: http://wiki.answers.com/ Q/ What are the advantages and disadvantages of electroless plating.html. [2011, Dec 22]

[57] W. Milwaukee, Artistic Plating Company, Inc. [online]. 2011. Available from: http://www.balseal.com/docs / techlibrary /tr16_020707131158.pdf.html. [2011, Dec 22]

[58] W. Yang, S. Luo, B. Zhang , Z. Huang, X. Tang, Applied Surface Science, 254 (2008): 7427–7430.

[59] N. Thomas, Thomas Publishing Company [online]. 2011. Available from: http://www.thomasnet .com/articles/custom-manufacturing-fabricating/electroless-Nickle plating-pretreatment.html. [2011, Dec 23]

[60] M. Charbonnier, M. Romand, International Journal of Adhesion & Adhesives, 23 (2003): 277-285.

[61] O. Bayer, Wilimedia Foundation. Inc [online]. 2011. Available from: http://en.wikipedia.org/wiki/Polyurethane [2011, Dec 23]

[62] N. Sarier, E. Onder, Thermochimica Acta, 454 (2007): 90–98.

[63] H. Seyanagi, I. Kaoru, K. Ogawa, T. Masui, K. Ono, U.S. Patent, 777 (2006): 455.

[64] Christian Ligoure, Michel Cloitre, Polymer Blends, Composites and Hybrid Polymeric Materials, 46 (2005): 6402–6410.

[65] S.B. Zdonik, L.P. Hallee, E.J. Green, Petroleum Publishing Co.,(1970).

[66] R.N. Lamb, B. Ngamsom, D.L. Trimm, B. Gong, P.L. Silveston, P. Praserthdam, Applied Catalysis A: General, (2004)

[67] B. Ngamsom, N. Bogdanchikova, M.A. Borja, P. Praserthdam, Catalysis Communications, 5 (2004): 243–248.

[68] P. Praserthdam, S. Phatanasri, J. Meksikarin, Catalysis Today, 63 (2000): 209–213.

[69] Claude Guimon, Aline Auroux, Enrique Romero, Antonio Monzon, Applied Catalysis A, 251 (2003): 199–214.

[70] J. A. Pe na, J. Herguido, C. Guimon, A. Monz ´on, J. Santamar´ıa**,** Journal of catalysis, 159 (1996): 313–322.

[71] F. Studt, F.A. Pedersen, T. Bligaard, R.Z. Sørensen, C.H. Christensen, J.K. Nørskov, Science, 320 (2008): 1320-1322.

[72] J.T.Wehrli**,** D.J. Thomas**,** M.S. Wainwright**,** D.L. Trimm, N.W. Cant**,** Applied Catalysis, 70 (1991): 253-262.

[73] J.T. Wehrli **,** D.J. Thomas**,** M.S. Wainwright**,** D.L. Trimm**,** N.W. Cant**,** Studies in Surface Science and Catalysis, 68 (1991): 203-210.

[74] B. Veeraraghavan, H. Kim, B. Popov, Electrochimica Acta, 49 (2004): 3143–3154.

[75] A. Sharif, Y.C. Chan, Journal of Alloys and Compounds, 440 (2007): 117–121.

[76] D. Takács, L. Sziráki, T.I. Török, J. Sólyom, Z. Gácsi, K. Gál-Solymos, Surface & Coatings Technology, 201 (2007): 4526–4535.

[77] S. Ranganatha, T.V. Venkatesha, K. Vathsala, Applied Surface Science, 256 (2010): 7377–7383.

[78] B. Veeraraghavan , D.Slavkov , S. Prabhu , M. Nicholson , B. Haran ,B. Popov , B.Heimann, Surface and Coatings Technology, 167 (2003): 41–51.

[79] H. Kim, N.P. Branko , S. Ken, Chen Corrosion Science, 45 (2003): 1505–1521.

[80] I. Mikami, Y. Yoshinaga, T. Okuhara, Applied Catalysis B: Environmental, 49 (2004): 173–179.

[81] I.Mikami, R.Kitayama, T. Okuhara, Applied Catalysis A: General, 297 (2006): 24–30.

[82] P.Q. Yuan, B.Q. Wang, Y.M. Ma, H.M. He, Z.M. Cheng, W.K. Yuan, Journal of Molecular Catalysis A: Chemical, 309 (2009): 124–130.

[83] C. Meephoka, C.Chaisuk, P. Samparnpiboon, P. Praserthdam, Catalysis Communications, 9 (2008): 546–550.

[84] B. Ngamson, N. Bogdanchicova, M.A. Borja, P. Praserthdam, Catalyst communication, 5 (2004): 243-248.

APPENDICES

APPENDIX A

CALCULATION FOR CATALYST PREPARATION

The calculation shown below is for 1% of Pd which dissolved in electroless solution of 0.82%Pd/PU foam.

The polyurethane support weight used in preparation is 0.06 g.

Based on 100 g of catalyst used, the composition of the catalyst will be as follows:

Palladium = 1 g

Polyurethane foam = 100-1 = 99 g

For 0.06 g of polyurethane foam

Palladium required = (0.06x1)/99 = 0.0006 g

The molecular weight of palladium is 106.42

The molecular weight of palladium is 177.33

Then the Palladium (II) chloride is required:

$$\text{Palladium (II) chloride required} = \frac{\text{Mw of } PdCl_2 \text{ x palladium required}}{\text{Mw of Palladium}}$$

$$= \frac{(177.33) \text{ x } (0.0006)}{106.42}$$

$$= 0.0009 \text{ g}$$

The Palladium (II) chloride required 0.0009 g in electroless bath.

APPENDIX B

CALCULATION FOR ACTUAL COMPOSITION OF METAL CONTAINED IN CATALYSTS

The actual compositions of metal contained in the catalysts were analyzed by Inductively-coupled plasma optical emission spectroscopy (ICP-OES).

The 0.01 g of Pd/PU foam was dissolved in a solution containing 49% HF and 37% HCl with volume ratio 7:2 and heat at 40 ºC over night

The calculation for actual amounts of Pd in Pd/PU foam

The 0.01 g of Pd was dissolved in a electroless bath

The result form ICP-OES analysis was 0.82 mg/l

$$\%\,Wt = \frac{concentration(ppm)}{weight(g) \times 100}$$

The actual % wt Pd = $\frac{0.82 \text{ mg/l}}{0.01 \text{ g x100}}$ = 0.82 %

The actual amount of Pd/PU foam was 0.82 %

APPENDIX C

CALCULATION OF DEPOSITION RATE

The deposition rate was calculated by the following equation:

$$\text{Deposition rate} = \frac{(m_2 - m_1)}{(m_1 t)}$$

Where m_1 = masses of the specimen before electroless plating

m_2 = masses of the specimen after electroless plating

t = The time of electroless plating bath.

APPENDIX D

CALCULATION FOR METERIAL PROPERTIES

Calculation for modulus value of the Ni-Zn-P/PU foam with amount of $ZnSO_4$ 18 g/l in bath

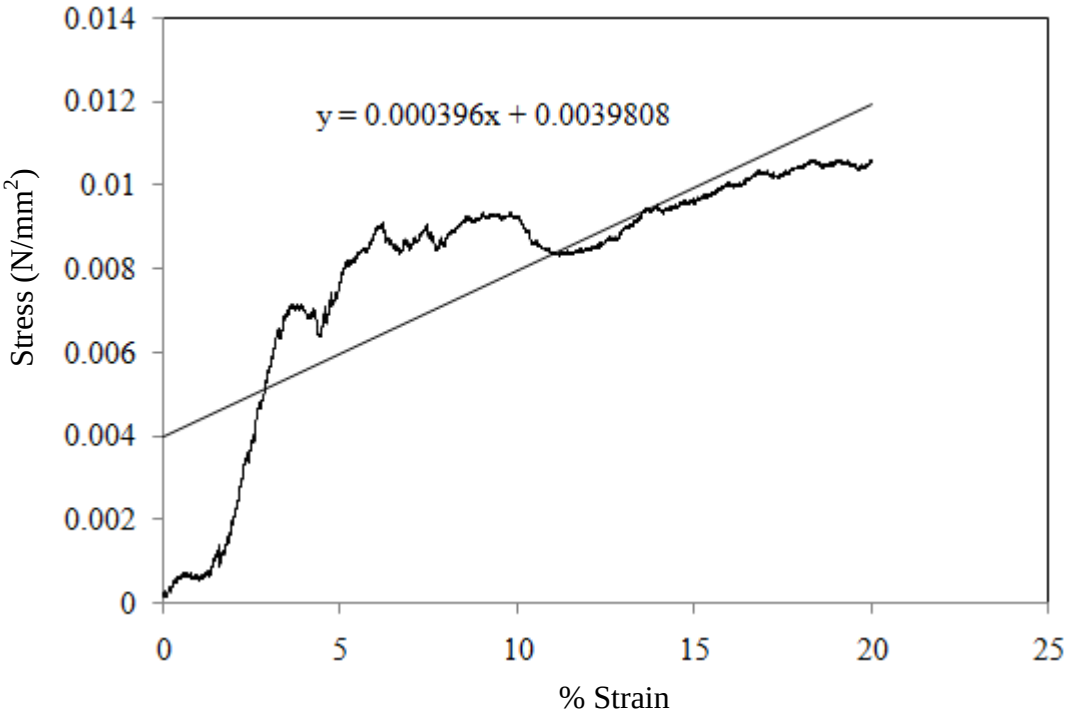

Figure D.1 Stress-Strain curves for Ni-Zn-P/PU foam with amount of $ZnSO_4$ 18 g/l in bath.

Stress value in y-axis and % Strain in x-axis are exhibited in the hraph, which the slope is a modulus (Mpa) value was $3.96x10^{-4}$ Mpa.

APPENDIX E

CALCULATION CURVES

This appendix showed about the calibration curves for calculation of composition of the reactant and products in selective acetylene hydrogenation reaction. The reactant is 1.5% C_2H_2 , 1.7% H_2, and balanced C_2H_4 (TIG Co., Ltd) and the desired product is ethylene. The other product is ethane.

Gas chromatograph equipped with a TCD detector (SHIMADZU TCD GC 8APT, molecular sieve 5A) was used to analyzed the H2 concentration.

Gas chromatograph equipped with a FID detector (SHIMADZU FID GC 8APF, carbosieve column S-II) for separating CH_4, C_2H_2, C_2H_4 and C_2H_6.

The calibration curves of hydrogen and acetylene are shown in the following figures.

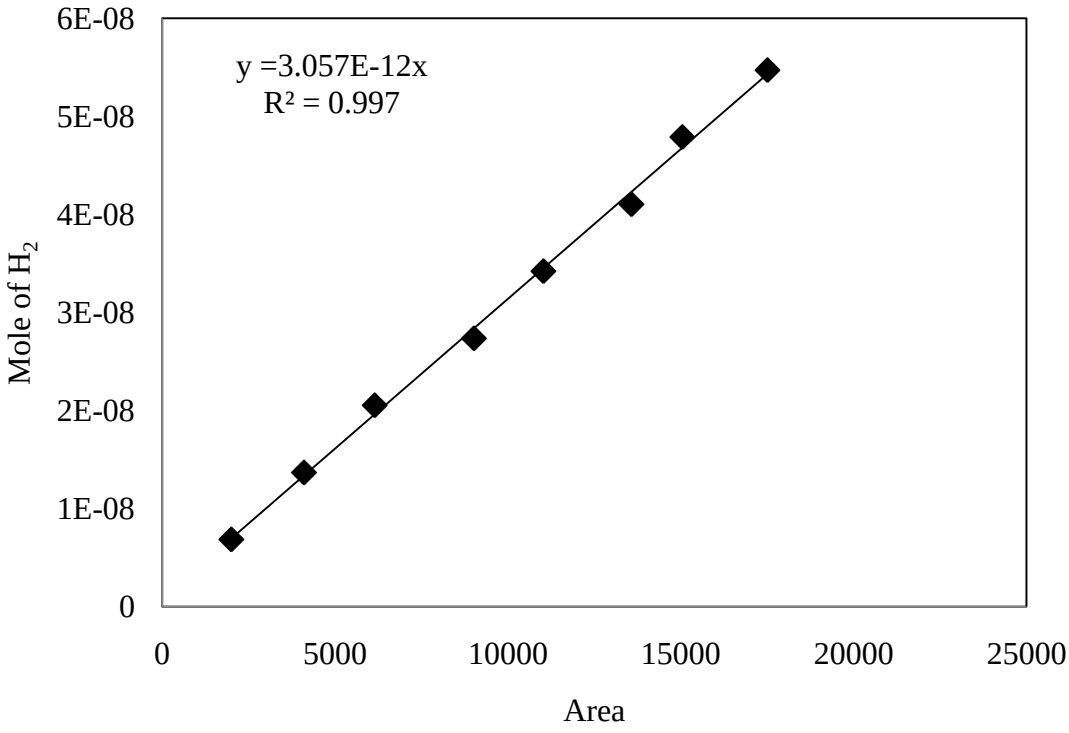

Figure E.1 The calibration curve of hydrogen from TCD of GC-8APT.

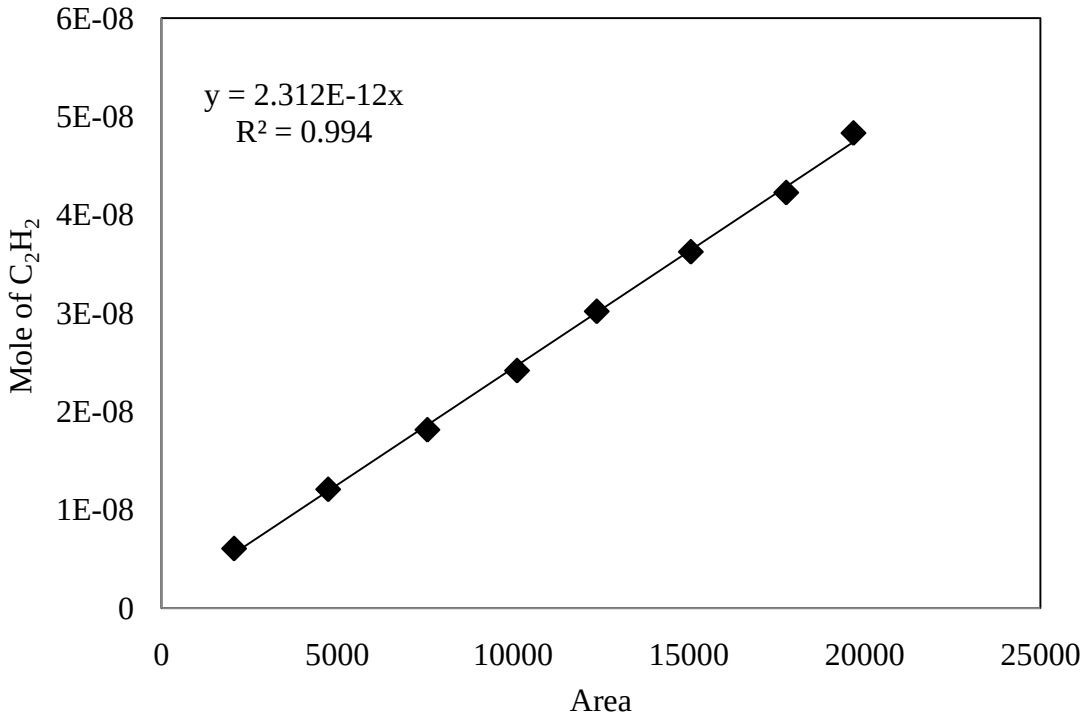

Figure E.2 The calibration curve of acetylene from FID of GC-8APF.

APPENDIX F

CALCULATION OF C_2H_2 CONVERSION AND C_2H_4 GAIN

The catalyst performance for the selective hydrogenation of acetylene was evaluated in terms of activity for acetylene conversion and ethylene gain based on the following equation:

$$C_2H_2 + H_2 \longrightarrow C_2H_4 \quad (1)$$
$$C_2H_4 + H_2 \longrightarrow C_2H_6 \quad (2)$$

Activity of the catalyst for acetylene conversion is defined as mole of acetylene converted with respect to acetylene in the feed:

$$C_2H_2\text{conversion (\%)} = \frac{100 \text{ x [mole of } C_2H_2 \text{ in feed} - \text{mole of } C_2H_2 \text{ in product]}}{\text{mole of } C_2H_2 \text{ in feed}}$$

where mole of C_2H_2 can be measured employing the calibration curve of C_2H_2 in Figure E.2, APPENDIX E., i.e.,

mole of C_2H_2 = (area of C_2H_2 peak from integrator plot on GC-8APF) $\cdot$ 2.312 $\cdot 10^{-12}$

Ethylene gain was calculated from moles of hydrogen and acetylene:

$$C_2H_4 \text{ gain (\%)} = 100x\frac{[dC_2H_2 - (dH_2 - dC_2H_2)]}{dC_2H_2}$$

Where dC_2H_2 = mole of acetylene in feed – mole of acetylene in product

dH_2 = mole of hydrogen in feed – mole of hydrogen in product

mole of H_2 can be measured employing the calibration curve of H_2 in Figure E.1, APPENDIX E., i.e.,

mole of H_2 = (area of H_2 peak from integrator plot on GC-8APT) $\cdot$3.057 $\cdot 10^{-12}$

VITA

Miss Sara Ahmadi Pirshahid was born in December 2nd, 1987 in Bangkok, Thailand. She finished high school from Satriwittaya 2 School, Bangkok and received Bachelor's Degree in Chemical Technology from the Faculty of Science, Chulalongkorn University in 2009. She subsequently completed the requirements for a Master's Degree in Chemical Engineering at the Department of Chemical Engineering, Faculty of Engineering, Chulalongkorn University in 2011.